Genome editing to reveal peptidergic heterogeneity of POMC neurons regulating energy and glucose balance

A thesis submitted by

Cho Shing Low

in partial fulfillment of the requirements for the degree of

PhD

In

Cell, Molecular, and Developmental Biology

Tufts University

Sackler School of Graduate Biomedical Sciences

May 2018

Adviser: Dong Kong, Ph.D.

Abstract

Diabetes is a global health concern that has dire consequences if left unchecked. However, the pathogenesis of diabetes is still not completely understood and so effective treatments are lacking. Growing evidence has shown that neurons in the brain, particularly those in the hypothalamus, play an important role in regulating whole body blood glucose, and that their dysfunctions contribute to the development of diabetes. Nevertheless, the complexity of the neural system, and difficulties in probing neuronal functions *in vivo,* have left us with an incomplete understanding of both the molecular mechanism and neuro-circuitry of centralized blood glucose regulation. In our recent study, we have perturbed a major group of glucose-sensing neurons in the hypothalamus, Pro-opiomelancortin (POMC) neurons in the arcuate nucleus (ARC). We observed that these groups of neurons play a significant role in regulating whole body glucose homeostasis. Here we utilize a battery of genetic approaches to scrutinized the machinery operating within them. Briefly, using a chemogenetic approach with both cell-type and spatial specificity to acutely manipulate the firing of these neurons, we observed that these neurons directly regulate energy expenditure, locomotion and blood glucose levels. Utilizing novel CRISPR technology in vivo, we specifically ablated POMC in the ARC. We found that POMC is necessary for energy and locomotor homeostasis, but has only a secondary effect on glucose levels. Thus, we hypothesize that another key neuropeptide found in POMC neurons, cocaine amphetamine regulated transcript (CART) may control glucose homeostasis. Using a similar approach, we show that CART is necessary to maintain blood glucose levels and that its depletion in Type 1 diabetes (T1D) and Type 2 diabetes (T2D) mouse models contribute to the development of hyperglycemia. Finally, using an unbiased approach and terminal inhibition we conclude that the paraventricular nucleus of the hypothalamus (PVH) is the main downstream glucoregulatory target. Collectively, these findings provide direct evidence

to the underlying molecular mechanisms of POMC neuronal activity and the neural circuits used to employ them. Our study has provided novel insight into brain-regulated glucose homeostasis and has identified potential targets for treating and preventing diabetes.

Table of Content

List of Figures

List of Tables

List of Abbreviations

2-DG, 2-deoxyglucose
α-MSH, alpha-melanocyte-stimulated hormone
β-endorphin, beta endorphin
AAV, adeno-associated virus
ARC, arcuate nucleus
Agrp, agouti-related protein
BAT, brown adipose tissue
BG, blood glucose
BIC, bicuculline
BW, body weight
CART, cocaine amphetamine regulated transcript
CNO, clozapine N-oxide
CNS, central nervous system
DIO, diet-induced obesity
DMH, dorsomedial hypothalamus
DSD, double stranded break
FI, food intake
G-6-Pase, glucose-6-phosphatase
GABA, γ-amino-butyric acid
GPCR, G-protein coupled receptor
GE and GI, glucose-excited and glucose-inhibited
GT, glucose tolerance
GTT, glucose tolerance test
HFD, high fat diet
HGP, hepatic glucose production
ICV, intracerebroventricular
ITT, insulin tolerance test
IS, insulin sensitivity
LH, lateral hypothalamus
MC4R, melanocortin receptor 4
Mstn, myostatin
Npy, neuropeptide Y
PCK1, phosphoenolpyruvate carboxykinase
POMC, pro-opiomelanocortin
PTT, pyruvate tolerance test
PVH, paraventricular nucleus of the hypothalamus
sgRNA, specific guide RNA
STZ, streptozotoxin
T1D and T2D, Type 1 and 2 diabetes
WAT, white adipose tissue.

Chapter 1: Introduction

The integration of peripheral inputs into the central nervous system (CNS) has long been studied for its role in maintaining energy and glucose homeostasis. The ability of neurons within the brain to detect a variety of circulating nutrients and hormones and in turn tune the system to the current metabolic state is essential for survival. Alterations or setting of a new threshold in this system leads to the development of obesity and diabetes. Evidence for CNS-based glucose control has primarily been established by the identification of key neural circuits underlying glucose homeostasis. Due to the variety of inputs and difficulty in deciphering this neural network, much of the underlying molecular mechanisms and neural circuits are largely unknown. Correlations between cause and effect may be drawn, but many of the conclusions are in conflict. However, certain models have consistently provided evidence to support CNS-based glucose control. This introduction will highlight these key findings objectively and focus on potential novel therapies which may be physiologically relevant for the treatment of obesity and diabetes. The introduction will conclude with unknowns in the field, which were the driving force behind this research.

1.1 Regulation of energy and glucose homeostasis by the hypothalamus

Bidirectional communication between the hypothalamus and the periphery is vital for proper physiological function. Classical lesion experiments and more modern cell-specific genetic approaches have led to the identification of key nuclei within the hypothalamus that are responsible for the maintenance of whole body homeostasis. These include the arcuate nucleus (ARC), dorsomedial hypothalamus (DMH), ventromedial nucleus (VMH), paraventricular nucleus (PVH) and the lateral hypothalamus (LH). Furthermore, the hindbrain and midbrain regions have been shown to interpret synaptic input from the hypothalamus and various brain regions to modulate the sympathetic nervous system (SNS) and parasympathetic nervous systems (PNS),

and as a result, maintain feeding, energy expenditure and basal glucose levels in the periphery via the PNS or SNS (Geerling et al., 2014; Thorens, 2014).

1.1.1 Arcuate Nucleus

The ARC is located along the third ventricle and is bridged by the median eminence, which lacks a complete blood brain barrier. As a result, neurons within this region are able to sense circulating hormones and metabolites from the periphery (Garfield et al., 2009; Gautron et al., 2015) and determine the energy state of the system. In addition, this region has been shown to receive significant synaptic inputs from the hypothalamus and forebrain nucleus (Wang et al., 2015), suggesting that they integrate both peripheral and brain based inputs. As one of the first sensors of peripheral signals, the ARC is postulated to be the key mediator of energy balance and glucose homeostasis (Cone et al., 2002) through two molecularly distinct populations of neurons residing in the ARC: the anorexigenic pro-opiomelanocortin (POMC) neurons and orexigenic agouti-related peptide/ neuropeptide Y (AgRP/NPY) neurons.

Activated by a state of energy deficit, AgRP neurons are necessary for food seeking and consumption and have been recently shown to modulate whole body glucose homeostasis (Aponte et al., 2011; Krashes et al., 2011; Takahashi and Cone, 2004) . Classical experiments utilizing monosodium glutamate lesions identified the ARC as a key region for the maintenance of energy homeostasis and the prevention of obesity. Even though NPY/AgRP neurons within the ARC have been well established for their orexigenic role in the CNS, earlier studies reported conflicting results. Transgenic mice deficient in NPY and/or AgRP displayed unaltered food intake and body weight compared to control mice (Qian et al., 2002). Similarly, using a diphtheria toxin approach to specifically ablate NPY/AgRP expressing cells during the neonatal phase resulted in

no significant change in body weight or food intake (Luquet et al., 2005). It was not until these experiments were replicated in adult mice that the orexigenic role of these neurons became evident. Shortly after diphtheria toxin injection, the adult mice developed acute anorexia, reduced body weight and reduced basal blood glucose (Gropp et al., 2005). Finally, with the development of methods for acute and cell-type specific activation through the use of optogenetic and chemogenetic techniques, dramatic and robust feeding was observed following stimulation of the NPY and AgRP neuronal populations in the ARC (Aponte et al., 2011; Krashes et al., 2011). These experiments confirmed the role of CNS NPY and AgRP neurons in regulating feeding behavior.

AgRP neurons project not only to their counterpart POMC neurons in the ARC, but also other regions in the hypothalamus such as the LHA and PVH as well as extra hypothalamic regions such as the bed nucleus of stria terminals (BNST) and the paraventricular thalamus (PVT) (Wang et al., 2015). Interestingly, channelrhodopsin assisted circuit mapping (CRACM) studies have shown that AgRP neurons project to downstream neurons in a one to one ratio (Betley et al., 2013). Only specific projection sites (i.e. the AgRP to PVH, LHA, anterior BNST and PVT) elicit voracious feeding upon optogenetic stimulation, while other projections (i.e. AgRP to the aBNST) are responsible for mediating glucose homeostasis (Steculorum et al., 2016). Recent work has shown that activation of the AgRP to ventrolateral aBNST projections, but not the dorsal medial aBNST projections, acutely modify insulin stimulated glucose uptake in brown adipose tissue (BAT) as well as increase myostatin levels, a signature for muscle related products and insulin sensitivity (Steculorum et al., 2016).

POMC neurons in the hypothalamus have long been postulated to be the counterbalance to AgRP neuron's orexigenic effects. A considerable amount of evidence has implicated POMC-derived peptides in the regulation of bodyweight, energy balance

and glucose homeostasis. The first genetic evidence that demonstrated the consequence of POMC impairment in humans was described in the late 1990s following the realization that the melanocortin system is crucial for normal body weight maintenance in mice (Ollmann et al., 1997). A genetic screen in obese patients identified a child that contained a heterozygous mutation in the coding region of POMC, resulting in a truncated form of not only the POMC protein, but also its biologically active fragments adrenocorticotropic hormone (ACTH), α melanocyte stimulating hormone (α-MSH) and β-endorphin. They concluded that the patient's early onset obesity and red hair pigmentation was due to POMC-deficiency syndrome (Krude et al., 1998). A later study identified three more cases of children with either homozygous or heterozygous POMC mutations that resulted in severe hyperphagia and obesity (Krude et al., 2003). Recently, a more comprehensive study was performed on a large Turkish family which had a high prevalence of obesity. They contained a single nucleotide deletion at the 5' coding region of the POMC gene that resulted in the loss of all POMC-derived peptides. The study found that 11 of the 12 relatives with the heterozygous mutation in the POMC gene had early onset obesity compared to just one of the seven wild-type relatives. Consistent with previous findings, another study described a single child with the homozygous mutation who developed hyperphagia and obesity postnatally (Farooqi et al., 2006). To study POMC-deficiency, a POMC-null mutant mouse line was developed. Early characterization of its phenotype was similar to observations made in human patients and a novel agonist for α-MSH showed therapeutic potential in reducing body weight in the mutant animals (Yaswen et al., 1999). Unfortunately, due to major obstacles that will be described in the following sections, no viable therapy has emerged from these studies.

Apart from the ARC, POMC is also expressed in the nucleus tractus solitaries (NTS) of the caudal medulla and the pituitary gland (Balthasar et al., 2004). Following translation, proprotein POMC is cleaved to produce a wide range of biologically active fragments including adrenocorticotrophin (ACTH), β-endorphin, α-melanocyte stimulating hormone (α-MSH), β-MSH and γ-MSH (Castro and Morrison, 1997). Once the 32 kilo Dalton (KDa) POMC propeptide is made, it is passed through the golgi stacks and is specifically targeted to secretory granules via a signaling peptide sequence (Cool et al., 1997). POMC is post-translationally processed within these granules primarily by serine proteases, prohormone convertases 1 (PC1) and 2 (PC2). PC1 cleaves the POMC proprotein into proACTH and β-liptrophin (β-LPH). ProACTH is then further cleaved by PC1 into N-POC, joining peptide and ACTH. PC2 cleaves β-LPH into γ-LPH and β-endorphin. In humans, the pituitary gland does not produce PC2. Thus, the only POMC derived products are N-POC, ACTH and β-LPH (White and Gibson, 1998). To produce a mature α-MSH requires more than just prohormone convertases. ACTH is first trimmed of its carboxy-terminal basic amino acids by carboxypeptidase E (CPE) and then it is amidated by peptidyl α-amidating mono-oxygenase (PAM) to yield desacetyl-αMSH. Finally, n-acetyltranferace converts desacetyl-αMSH into a mature α-MSH (Pritchard et al., 2002). The peptides derived from POMC are diverse in their biological roles, but the central mechanism of action is mainly mediated by melanocortin receptors. There are five known melanocortin receptors, but only the MC3R and MC4R are relevant to POMC's role in regulating homeostasis (Figure 1.1).

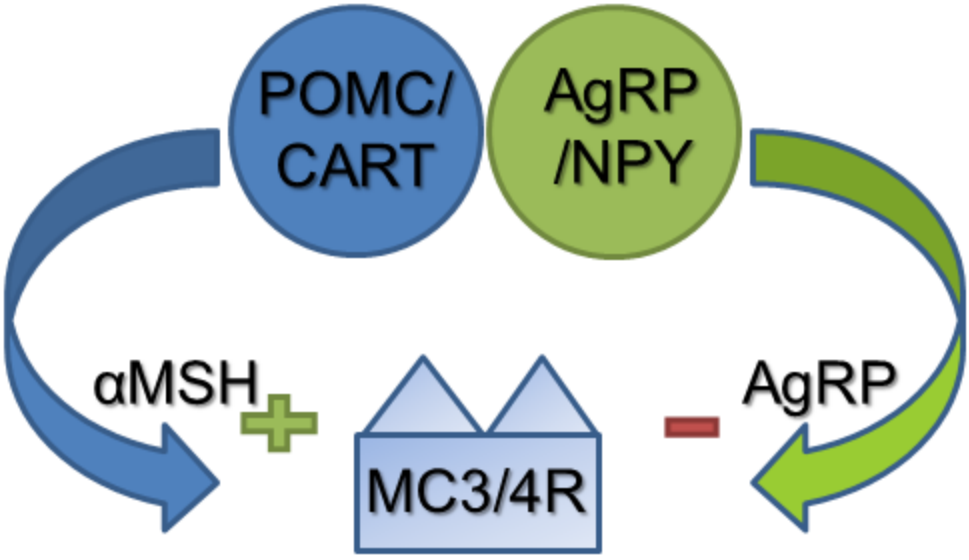

Figure 1.1: The central melanocortin system. The central melanocortin system. Agouti-related peptide (AgRP) and proopiomelanocortin (POMC) neurons in the arcuate neurons project to melanocortin receptor (MCR) expressing neurons. The MCR is then activated by αMSH, a classical satiety signal or inhibited by the antagonist AGRP which stimulates food intake

MC4R is highly expressed in the hypothalamus in particular regions that are known to be important for homeostatic regulation, such as the LH, DMH, and most importantly the paraventricular nucleus (PVH) (Mountjoy et al., 1994). Early knock-out (KO) experiments of MC4R in mice clearly showed the development of obesity through hyperphagia and hyperglycemia (Huszar et al., 1997). In addition, a patient with a heterozygous mutation in the coding region of MC4R was shown to be predisposed to develop obesity shortly after birth, but surprisingly no hyperglycemia was observed (Vaisse et al., 1998). In mouse models that recapitulate the heterozygous MC4R mutation, a moderate gain in body weight was observed (Cone, 1999; Huszar et al., 1997). Finally, pharmacological agonists of MC4R have been shown to reduce food intake, body weight and increase energy expenditure (Fani et al., 2014). Unfortunately, translating this agonist into a viable therapy has been a challenge. A number of

preclinical therapies had to be administered directly into the CNS to avoid the blood-brain barrier and poor bioavailability when consumed orally. Side effects including increased blood pressure, heart rate and taste aversion have been reported (Kievit et al., 2013). As a result, no MC4R agonist has been shown to be an effective treatment for obesity in humans.

The role of MC3R in metabolic homeostasis is not as clearly demonstrated as in the case of MC4R. In screens looking for mutations in the MC3R coding region of obese and average weight individuals, no correlation between sequence variants and obesity were reported (Li et al., 2000) . These results were later supported by a larger study focusing on obese individuals in North America, which also showed no association between mutations in the MC3R gene and sever obesity (Calton et al., 2009). Despite these findings, a recent study in Europe identified three mutations in the MC3R gene that led to the development of human obesity. Unfortunately, these results were not confirmed by previous work in North America (Mencarelli et al., 2011). In MC3R KO mice, there was weight gain through accumulation of adipose tissue, however when compared to MC4R KO mice, the obesity would only be considered mild (Butler et al., 2000; Sutton et al., 2006). When challenged with a high fat diet (HFD) on the other hand, the weight gain and impaired glucose tolerance were comparable between the two KO lines (Trevaskis et al., 2007). This suggests an alternative pathway in which metabolic dysregulation leading to obesity and diabetes is independent of hyperphagia. The underlying mechanisms differentiating MC3R and MC4R need to be further investigated before a clear explanation can be drawn.

The upstream regulation of POMC neurons in the hypothalamus plays a key role in the control of the melanocortin pathway. Many groups have observed that POMC neuronal activation and transcription levels depend directly on the energy state,

suggesting early on that these neurons expressing the POMC gene may play an important role in regulating homeostasis. POMC neurons are known as glucose-excited neurons, which increase their firing rate in response to elevated levels of extracellular glucose (Parton et al., 2007). One of the most well supported explanations for how glucose increases the electrical activity of glucose-excited neurons is based on the mechanism pancreatic β-cells use to secret insulin into the circulation. In this model, glucose enters into the cytoplasm through the aid of transmembrane glucose transporters (Kang et al., 2001). During basal physiological levels of glucose, it does not bind due to low affinity. However, when it reaches saturation following a meal, then the binding of glucose occurs and transport is initiated. Once within the cell, glucose undergoes glycolysis and phosphorylation to create products, which can then be used to generate ATP (Matschinsky, 1996). As a result of the shift in the ATP:ADP ratio, ATP-inhibited K^+ (KATP) channels in the plasma membrane close, causing depolarization (Aguilar-Bryan et al., 1998). The increase in action potential frequency comes from the opening of voltage-dependent calcium channels and the influx of extracellular calcium. Key genetic manipulation in POMC neurons has provided evidence supporting this mechanism and its importance in glucose homeostasis. Transgenic expression of a mutant Kir6.2, a major subunit of the KATP channel makes it 250 times less sensitive to ATP closure. In POMC neurons, this almost completely impaired response to extracellular glucose change, resulting in whole body glucose tolerance impairment (Parton et al., 2007). Another potential contributor to the regulation of activity within these neurons comes from astrocytes. These cells have been shown to take up glucose, convert it into lactate and then release it into the extracellular space (Pellerin and Magistretti, 1994). The lactate is then transported by monocarboxylate (MCT) into the cell where it is incorporated into the mechanism described previously to produce ATP (Kang et al., 2004). Evidence supporting this has shown that certain neurons respond to

varying extracellular levels of lactate (Yang et al., 1999). But even without lactate, neurons can still sense and respond to glucose, suggesting that astrocytes may provide a parallel mechanism for glucose sensing (Dunn-Meynell et al., 2002).

In support of the idea that these neurons are finely tuned to respond to metabolic changes, rodents subjected to acute fasting showed suppressed expression of POMC mRNA in the hypothalamus (Brady et al., 1990). Inversely, in overfed rats POMC expression in the ARC was upregulated by 180% relative to controls (Hagan et al., 1999). Transcription is also in part controlled by circulating hormone levels. In mouse models of type 2 diabetes and obesity in which they are either leptin deficient (ob/ob) or leptin receptor deficient (db/db), mRNA levels of POMC were markedly decreased (Mizuno et al., 1998). In more neuronal specific experiments in which the leptin receptor is depleted from POMC neurons, mice became obese and a trend in mRNA reduction was evident (Balthasar et al., 2004). Moreover, chronic intraperitoneal injections of leptin were able to partially rescue POMC expression in 48 hour fasted mice and ob/ob mice, but not in leptin receptor deficient mice (Schwartz et al., 1997). Early work pointed to the ARC as the primary starting point for leptin signaling in the control of glucose homeostasis. In leptin receptor depleted mice, re-expression of the receptor in the ARC using viral techniques decreased body weight and hyperphagia modestly, but remarkably normalized blood glucose levels and dark cycle activity (Coppari et al., 2005). Of note, re-expression of leptin receptor solely in POMC neurons almost identically mimicked the rescue of glycemic control as described in the previous experiment. In addition, by crossing POMC-Cre mice with a LoxP-flanked transcriptional blocker line to prevent leptin receptor transcription, they reported partial rescue of energy balance and a mild reduction in overall body weight compared to leptin deficient controls (Berglund et al., 2012). In insulin-deficient type 1 diabetes (T1D) induced by

streptozotocin (STZ), chronic intracerebroventricular (ICV) infusion of leptin was sufficient to prevent lethality and dramatically reduced hyperglycemia. This beneficial effect dissipated within 48 hours following interruption in leptin treatment (Fujikawa et al., 2010). The potential for leptin as a therapy for T1D was supported by experiments on non-obese diabetic (NOD) mice. With implantation and administration of leptin through an alzet osmotic pump, all diabetic mice showed reduction in plasma glucose levels (Wang et al., 2010). In STZ induced T1D mice lacking leptin receptors in POMC neurons, the hyperglycemia-lowering effect of ICV leptin administration was significantly blunted with no observable change in body weight or food intake compared to controls. Unsurprisingly, in the same diabetic model but with leptin receptor expression in POMC neurons, expression of the receptor contributed to the glucose lowering effect in leptin treated mice (Fujikawa et al., 2013). On the other hand, insulin receptor deletion in the CNS did not elicit the same magnitude of homeostatic impairment as leptin or leptin receptor depletion. Insulin receptor deletion in mice did produce diet-sensitive obesity and elevations in body weight, however (Bruning et al., 2000). Since then, many have tried to unravel the main neuronal population and mechanism by which insulin acts in the brain. A logical starting point would be POMC neurons in the ARC due to their well-established role in regulating energy and glucose metabolism. Recent findings have produced conflicting results, however. Specific deletion of the insulin receptor in POMC neurons failed to alter food intake, body weight or basal blood glucose levels (Konner et al., 2007). Curiously, both leptin and insulin activate intracellular phosphatidylinositol-3 kinase (PI3K), but deletion of the leptin receptor as stated previously caused obesity while deletion of the insulin receptor does not. Expression of the insulin receptor in only POMC neurons was sufficient to promote hepatic glucose production as measured by glucose clamp studies (Lin et al., 2010). Double deletion of both the insulin and leptin receptors did not alter body weight, but did significantly raise basal blood glucose levels

(Hill et al., 2010). This compilation of evidence supports the hypothesis that POMC neurons are able to sense and integrate peripherally derived hormones in the blood and it suggest a divergent system in the regulation of energy balance and glucose homeostasis (Figure 1.2). The functional mechanism of leptin and its potential as a therapy will be discussed further, along with caveats and issues with experimental design from earlier studies.

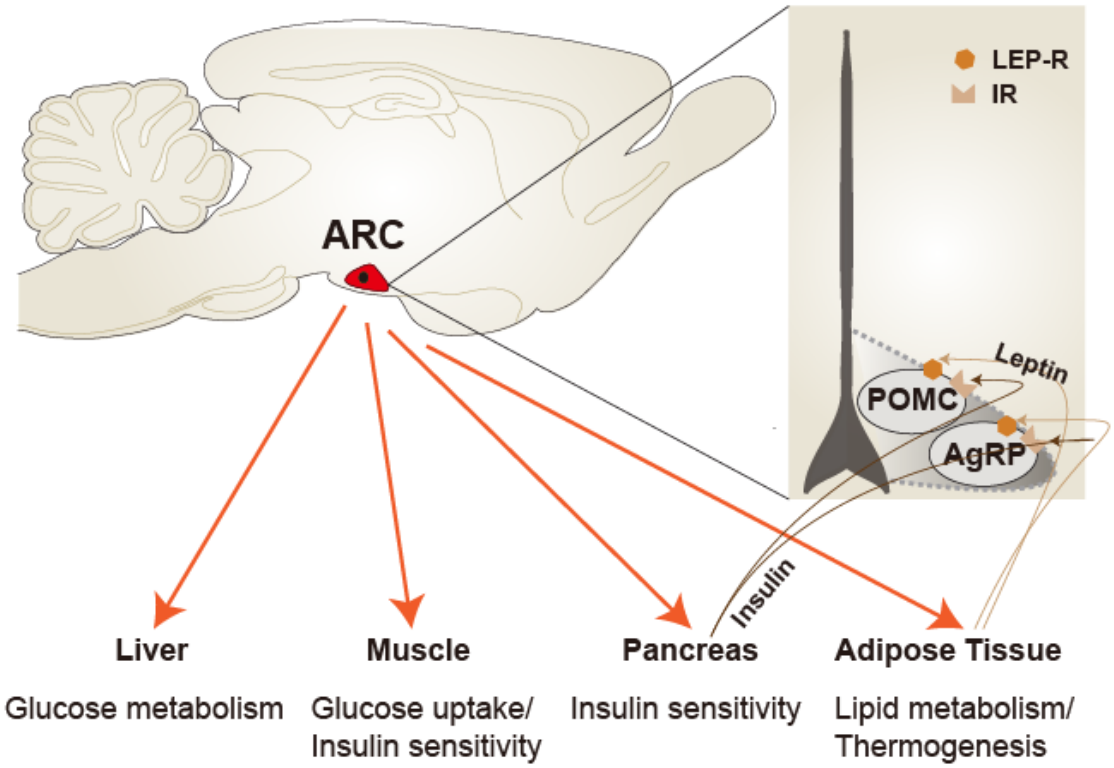

Figure 1.2: Arcuate regulation of peripheral functions. Leptin and insulin secreted by adipose tissue and the pancreas, respectively, travel through the circulation until it is degraded cleared or binds to its corresponding receptor. In the ARC AgRP and POMC containing neurons, express both leptin receptor (LEP-R) and insulin receptor (IR). Activation of these receptors causes changes in neuropeptide expression, which modulates peripheral function to maintain energy balance, glucose metabolism and feeding. Figure .

1.1.2 Paraventricular nucleus

The PVH integrates afferent inputs from many regions of the brain, which are able to sense nutrient and hormone levels, most of which originate from the hypothalamus. Retrograde-tracing experiments have also shown strong connectivity with the hindbrain region, which not only integrates circulating signals from the periphery, but also vagal afferents from the gastrointestinal tract (Larsen et al., 1994). These signals converge in the PVH where they are interpreted and efferent signals are sent to the parasympathetic and sympathetic preganglionic cells, which connect with peripheral tissues including white adipose tissue, the pancreas, liver and brown adipose tissue (Bamshad et al., 1998; Jansen et al., 1997; Song et al., 2008; Stanley et al., 2010). Through these connections, the PVH is able to modulate these tissues to alter insulin secretion, adipose deposition, thermogenesis, glucose uptake and hepatic gluconeogenesis (Geerling et al., 2010; Marino et al., 2011; Stanley et al., 2010). The PVH is also known as the primary hub for endocrine control in the CNS. It contains neurons which release corticotrophin-releasing hormone (CRH) and thyrotropin-releasing hormone into the median eminence to regulate the hypothalamic-pituitary-adrenal (HPA) and hypothalamic-pituitary-thyroid (HPT) axes respectively. In addition, the ventrolateral region of the PVH releases vasopressin or oxytocin (OXT) into the circulation to control food intake, energy balance, fluid balance and reproductive functions. As a whole, the PVH uses these afferent inputs to determine the energy state of the system and elicits an appropriate response to maintain homeostasis and ensure survival.

CRH neurons are credited as the principal effectors in the HPA axis in conjunction with the pituitary and adrenal gland to mediate stress responses. Following an input that elicits a stress response, CRH is released into the hypophysial portal

vessels, which provide direct access to the pituitary gland. Binding of CRH to the CRH type 1 receptor (CRH1R) in humans and rodents initiates the production and release of ACTH into the circulation. Once released, the main objective is to bind to the melanocortin 2 receptor (MC2R) located on the adrenal cortex. This stimulates the synthesis and secretion of glucocorticoids (GC), a class of steroid hormones whose main action is to maintain adequate levels of glucose in times of stress. It is able to perform this function by promoting gluconeogenesis in the liver (Exton, 1979; Kraus-Friedmann, 1984) and reducing glucose uptake in skeletal muscle and white adipose tissue (Di Dalmazi et al., 2012; Kuo et al., 2013). This is demonstrated through very simple experiments in which GC injected into humans has been shown to increase gluconeogenesis (Tounian et al., 1997). In adrenalectomized mice, administration of GC is sufficient to restore the impairment in glucose production in the liver (Exton et al., 1976; Sistare and Haynes, 1985). In contrast, surgical removal of the adrenal gland leads to increases in insulin induced glucose disposal by skeletal muscle (Haluzik et al., 2002). Mechanistically, this has been attributed to GC's ability to attenuate insulin-induced GLUT4 transport of glucose through the cell membrane (Dimitriadis et al., 1997; Weinstein et al., 1998). To prevent chronic exposure to GC, a negative feedback mechanism is in place to inhibit hypothalamic release of CRH. In the hypothalamus, GC receptors are highly concentrated in the PVH. Due to the low affinity of GC to their receptors, binding does not occur until circulating levels are elevated following stress (Reul and de Kloet, 1985). Local administration of GC in this region has been shown to reduce neuronal activity and inhibit ACTH secretion (Sawchenko, 1987; Watts, 2005). As a result, CRH neurons provide acute elevations in circulating glucose to ensure proper brain function in times of need. In addition, there is a well-established counter regulatory mechanism to ensure the system returns to baseline levels following stress induced hyperglycemia.

TRH neurons located in the PVH are known to be the key regulators of the HPT axis. Following afferent input or activation by circulating hormones or neuropeptides, TRH is released into the pituitary portal through the median eminence (Ishikawa et al., 1988). It is then carried by the capillaries that form the veins to the pituitary gland. This stimulates the synthesis and release of thyrotropin (TSH) from the anterior pituitary (Steinfelder et al., 1991). TSH then acts on the thyroid to initiate thyroid hormone (TH) biosynthesis and secretion. The two main THs which exert the bulk of the biological functions are triiodothyronine (T3) and thyroxine (T4). T3 is characterized as the most biologically active due to its increased affinity for thyroid hormone receptors (THR) compared to T4 (Galton et al., 2007). Normal thyroid concentrations in the circulation are essential for growth and development during early life and for the maintenance of metabolic and energy homeostasis later in life (Yen, 2001). Hypothyroidism is a debilitating disease in which patients have low circulating levels of T4 due to the inability of TSH to stimulate hormone release. Symptoms routinely include slow heart rate, impaired cold tolerance, and various metabolic dysfunctions (Beck-Peccoz et al., 2017). On the other hand, patients with hyperthyroidism have an overactive thyroid gland and experience increased metabolism which leads to weight loss, rapid heart rate, and heat intolerance (Blackwell, 2004). Under normal conditions, TRH gene expression is directly regulated by the energy status of the organism. In rats deprived of food for 48 hour, T3 levels in the periphery were significantly reduced along with pro-TRH mRNA levels in the PVH (Blake et al., 1991). These neurons also receive robust input from first order sensory neurons within the ARC. NPY release and binding to TRH neurons has been shown to suppress expression and release, while leptin and α-MSH has been linked to increases in expression (Ghamari-Langroudi et al., 2010; Vella et al., 2011). ICV administration of α-MSH is sufficient to maintain TRH release during fasting (Fekete et al., 2000). Unsurprisingly, 50-60% of TRH neurons in the PVH have been shown to

express MC4R mRNA (Liu et al., 2003). Similar to CRH neurons, there is a negative feedback mechanism. Once levels of T3 are elevated, binding to THR in the PVH and pituitary represses transcription of TRH and TSH (Hoermann et al., 2015). Once again balance within a system is essential for normal physiological function and the ability to adapt to external stresses.

The classic belief has been that the main role of OXT neurons is to control the reproductive processes including birth, lactation, and maternal behavior (Insel, 2010). These neurons have also been implicated in the regulation of body weight, food intake, and energy expenditure. In pharmacological studies where OXT is administered systemically or centrally, rats fed a chow diet developed hypophagia (Arletti et al., 1990; Olson et al., 1991). Furthermore, ICV injection of OXT induced energy expenditure and weight loss (Zhang et al., 2011). Genetic models of OXT receptor deficiency exhibited late onset obesity compared to controls (Takayanagi et al., 2008). Mice deficient in OXT have lower total body temperatures compare to controls and when subjected to cold, OXT neurons were activated, suggesting that these neurons may play a role in thermoregulation (Kasahara et al., 2007). Pseudorabies viral tracing from the BAT has shown clear connectivity to OXT neurons within the PVH, further supporting their role in body temperature regulation (Oldfield et al., 2002). This subset of neurons highlights another subpopulation within the PVH that provides descending signals to the periphery to maintain homeostasis.

1.1.3 Ventromedial Hypothalamus

Similar to other key hypothalamic regions, early lesion studies identified the VMH as an important center for maintaining normal feeding and body weight. It has been reported that bilateral lesion to the ventromedial nuclei produced the most pronounced

body weight gain in rats (Brooks and Lambert, 1946) compared to lesions made posteriorly to the VMH, which potentially terminated connection to downstream neurons (Graff and Stellar, 1962; Hennessy and Grossman, 1976). The dramatic body weight gain was first attributed to the severe hyperphagia that developed shortly following surgery (Balagura and Devenport, 1970; Becker and Kissileff, 1974; Brobeck et al., 1943). Remarkably, during the first four to five weeks following surgery it was not uncommon to observe adult female rats consuming double their normal daily intake, resulting in 10g of body weight gain per day (King and Gaston, 1977). Consistent with this evidence, electrical stimulation of the VMH suppressed feeding in ad libitum fed rats during the dark phase (Ruffin and Nicolaidis, 1999).

One of the first hypotheses explaining how the VMH might sense and regulate satiety was through the monitoring of specific metabolites carried to the brain through the circulatory system (Kennedy, 1950, 1953). This was supported by an interesting experiment where two age matched litter mate rats were joined by creating an opening in the peritoneal cavities, uniting them together. It was confirmed that they exchanged plasma by injecting evans blue dye into one rat and observing transfer. Of note, when one rat received surgical lesions to the VMH it behaved as previously discussed and became hyperphagic. However, the conjoined rat which was free of the lesion died unless it also received a VMH lesion (Hervey, 1959). Recently, it has been observed that a subpopulation of neurons within the VMH are highly sensitive to changes in central glucose levels (Song and Routh, 2005). A microinjection of glucose into the VMH has been shown to increase the firing rate of the sympathetic nerves to the BAT in a dose dependent manner (Sakaguchi and Bray, 1987a). Glucopenia induced by local perfusion of a non metabolizable form of glucose, 2-deoxyglucose, resulted in a two-fold increase in plasma glucose levels (Borg et al., 1995). Within the VMH it has been shown that GI

neurons are hyperpolarized through the AMPK-dependent pathway, which leads to nitric oxide production and in turn the closure of chloride channels (Murphy et al., 2009). However, neurons within the VMH can either be excited or inhibited by glucose, through mechanisms described previously (Miki et al., 2001; Murphy et al., 2009)(Figure 1.3). In summary, it is evident that the VMH is essential for the maintenance of whole body homeostasis through the monitoring of energy states, however the ability of neurons within the VMH to either be excited or inhibited by glucose further adds complexity to the system.

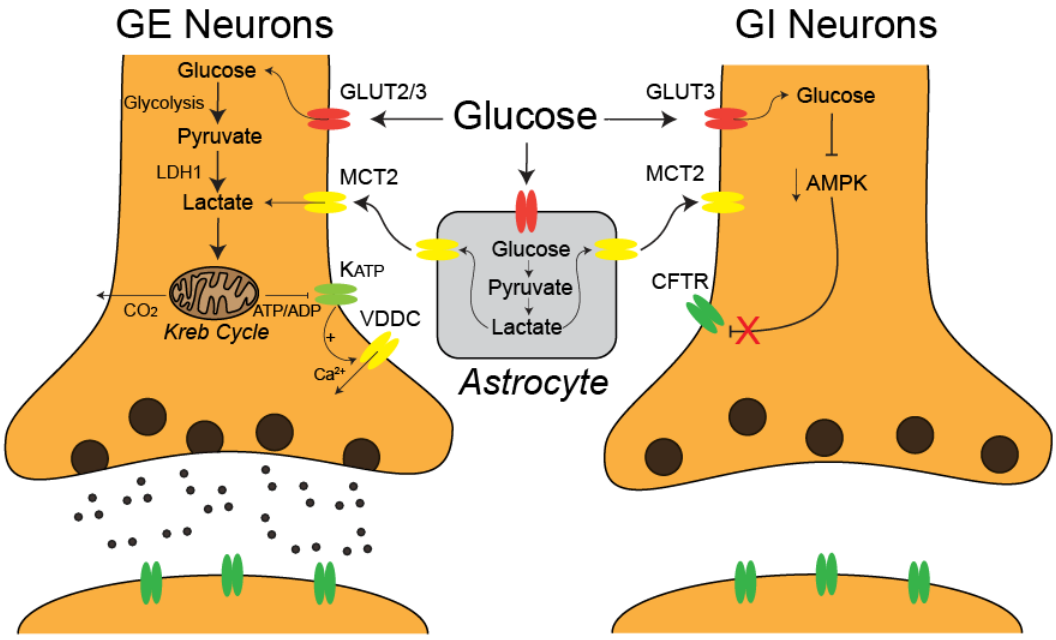

Figure 1.3: Glucose-sensing mechanisms. In glucose excited (GE) neurons it is postulated that during states of hyperglycemia glucose enters the neuron which leads to an increase in the ATP/ADP ratio. This causes ATP-sensitive potassium channels (K_{ATP}) to close, depolarizing the neuron and allowing voltage dependent calcium channels (VDDC) to open. The influx of calcium causes vesicle fusion and release of neurotransmitters and neuropeptides.On the other hand, glucose inhibited (GI) neurons take up glucose which inhibits activation of AMP-activated protein kinase (AMPK). This in turn does not allow AMPK to inactivate cystic fibrosis transmembrane conductance regulator (CFTR) chloride channel, resulting in a hyperpolarized state. In astrocytes, glucose uptake leads to lactate production, which is exported through monocarboxylic acid transporter (MCT) and enters into nearby neurons through MCT2. Once in the neuron the lactate is incorporated into the kreb cycle to produce ATP.

Apart from glucose, VMH neurons also express receptors for leptin and insulin. Impairments in either pathway has been shown to effect energy regulation and glucose homeostasis (Elmquist et al., 1998; Paranjape et al., 2011; Scott et al., 2009). Briefly, a microinjection of leptin into the VMH increases glucose uptake in the BAT, skeletal muscle, heart, and spleen (Minokoshi et al., 1999). Leptin receptor depletion in steroidogenic factor 1 (SF1) neurons specific to the VMH induced obesity, energy dysregulation and severe glucose tolerance impairment (Bingham et al., 2008). Injection of insulin into the VMH reduces SNS signaling (Sakaguchi and Bray, 1987b). Insulin knock-down with a lentiviral antisense sequence for the insulin receptor causes glucose intolerance independent of body weight gain assessed using glucose clamp techniques (Paranjape et al., 2011). Collectively, these data suggest that glucose, leptin and insulin sensing in the VMH are able to mediate peripheral changes to maintain energy balance and glucose homeostasis. However, not all phenotypical changes are observed in each case, suggesting a complicated divergent network which needs to be further investigated.

Due to the vast array of physiological functions controlled by the VMH, it is unsurprising that this region contains a heterogeneous population of different gene expressing neurons (McClellan et al., 2006). A few subtypes that have been individually studied include, cannabinoid receptor 1, pituitary adenylate cyclase activating polypeptide, cerebellin 1, brain-derived neurotrophic factor (BDNF), estrogen receptor α and progesterone receptor (Kim et al., 2008; Kim et al., 2010; Musatov et al., 2007; Segal et al., 2005; Xu et al., 2003). Of all the various neuronal groups found in the VMH, only SF-1 is exclusively restricted to this region (Bingham et al., 2006). Importantly, SF-1 expressing neurons have emerged as a sub-population which is vital for metabolic regulation. Early generation of SF-1 KO mice resulted in neonatal lethality due to the

failure of the adrenal gland to develop correctly. However, adrenal gland transplants from wild type (WT) mice were able to rescue these pups. A key observation was the increased body weight, which was significant starting at eight weeks of age and reached double the weight of control mice by the end of the monitoring period. Interestingly, they concluded that the weight gain was predominantly due to reduced activity rather than elevated food intake (Majdic et al., 2002). Along with impairments with adrenal gland development, SF-1 KO mice have also been shown to cause structural abnormalities and altered gene expression in the VMH. The contribution of other VMH neurons in SF-1 KO induced obesity cannot be ruled out (Davis et al., 2004; Majdic et al., 2002).

Another important mile stone in the field was the generation of SF-1-Cre transgenic mice by a few independent groups (Bingham et al., 2006; Dhillon et al., 2006). This allowed for the Cre/lox gene KO technique to be used to not only reinforce the importance of SF-1 neurons, but also investigate the contributions of key metabolic hormones. When crossed with leptin receptor *Lepr*$^{flox/flox}$ mice, there was significant weight gain that the authors primarily contributed to increased fat mass accumulation. When stressed with a HFD, the body weight difference became more pronounced resulting from increased food intake and decreased energy expenditure (Dhillon et al., 2006). Acute activation of SF-1 neurons with chemogenics supports the previously discussed findings regarding leptin's action in the VMH. Following intraperitoneal (IP) injection of clozapine N-oxide (CNO) in mice expressing hM3Dq in SF-1 neurons, they observed reduced food intake accompanied with increased energy expenditure. In addition, through hyperinsulinemic-euglycemic clamp studies, they also reported elevated levels of insulin induced glucose uptake in peripheral tissues (Coutinho et al., 2017). Contrary to leptin, insulin directly inhibits SF-1 neurons. Insulin receptor deletion in SF-1 neurons did not culminate in changes to body weight or glucose homeostasis,

but did protect against body weight gain, leptin resistance and glucose impairment when placed on a HFD (Klockener et al., 2011). Further studies using similar techniques have been used to decipher the downstream molecular pathway of leptin and insulin signaling within SF-1 neurons (Kim et al., 2012; Xu et al., 2010). While an interesting framework has emerged, much more work is required to fully understand this complicated network. Nonetheless, it is well established that SF-1 neurons in the VMH are important contributors to the regulation of metabolic homeostasis.

While investigating the protective effect of BDNF on adult cholinergic neurons in the hippocampus, minimal benefits were reported. However, ICV administration did alter feeding behavior, suggesting an alternative role of BDNF(Lapchak and Hefti, 1992). Follow up studies in rats detailed central administration of BDNF in appetite suppression and body weight reduction in a dose dependent manner. Interestingly, they also suggest the ability of BDNF to modify the set point for basal body weight independent of food intake and blood glucose (Pelleymounter et al., 1995b). This accidental discovery expanded the study of BDNF from promoting neuronal survival to the regulation of energy balance.

BDNF is a member of the neurotrophin family which consists of nerve growth factor, neurotrophin-3 and neurotrophin-4. BDNF acts through the binding of four known receptors, $p75^{NTR}$ tropomyosin-related kinase (TrK) A, TrKB and TrKC which activates a few downstream signaling pathways (Radziejewski et al., 1992). In terms of physiological relevance to mediating energy, glucose and lipid balance, BDNF signaling through TrkB and $p75^{NTR}$ is the most applicable. Ligand binding to TrkB initiates an intracellular signaling cascade which starts with activation of phospholipase C gamma (PLC-γ), motigen-activating protein kinase (MAPK) and phosphatidylinositol-3 kinase (PI3-K) (Patapoutian and Reichardt, 2001; Reichardt, 2006).

BDNF null mice generated to study its endogenous role were initially unsuccessful due to the high rate of postnatal lethality. To overcome these obstacles heterozygous BDNF $^{+/-}$ mice were used. They developed hyperphagia and gained significant amounts of body weight compared to controls (Lyons et al., 1999). A pivotal advancements was the ability to ablate BDNF at P21 by crossing *Bdnf* $^{Flox/Flox}$ with the CamK-cre93 transgenic mouse line. This allowed for the selective depletion of central BDNF and the postnatal survival of the experimental animals. Not unexpectedly, the mice developed more severe hyperphagia and body weight gain when compared to BDNF $^{+/-}$ mice (Lyons et al., 1999; Rios et al., 2001). Pair feed experiments concluded that body weight gain and metabolic complications were predominantly due to increased feeding. When food was restricted to basal WT mouse levels, they were able to prevent body weight gain, hyperglycemia, dyslipidaema, and resistance to leptin and insulin (Coppola and Tessarollo, 2004). This supports the hypothesis that the metabolic impairments were caused by the stresses applied to the system from hyperphagia-induced obesity. Further evidence in humans has only strengthened the link between BDNF and energy balance regulation. A genome-wide association study looked at 250,000 patients of European decent and identified BDNF as one of the loci linked to high BMI (Speliotes et al., 2010). In addition, patients suffering from Wilm's tumor, aniridia, genitourinary anomalies, and mental retardation (WAGR) with truncations in chromosome 11 (which includes the BDNF gene) had a 100% rate of developing early onset obesity compared to patients with active BDNF expression (Han et al., 2008). Within the hypothalamus, BDNF expression is the most prevalent in the VMH (Xu et al., 2003). Direct injection of BDNF into the VMH of food deprived rats was able to decrease feeding and body weight gain (Wang et al., 2007). Injection of an adeno-associated virus encoding cre recombinase into the VMH of *Bdnf* $^{Flox/Flox}$ mice to specifically delete BDNF resulted in hyperpagia-induced obesity, hyperglycemia and elevated levels of leptin

(Unger et al., 2007). These combined results show that not only is BDNF essential for appetite control, but that the VMH is one of the primary sources of BDNF in the brain.

1.1.4 Dorsomedial Hypothalamus

The DMH has been well established for its role in the control of food intake, drinking and body weight regulation (Bellinger and Bernardis, 2002). Starting in the 1940s, electrical stimulation in the region we know today as the DMH caused voracious feeding in cats (Hess and Akert, 1955). This led to large lesions being made in the hypothalamus, which included the DMH, in rats that caused reduced feeding, drinking and body length growth (Bernardis et al., 1963). As the lesion size became smaller and more specific it was confirmed that these phenotypes were also observed in DMH only lesions (Bernardis, 1970). When stressed with a HFD, rats with lesions solely in the DMH showed resistance to the development of obesity. Observations in mice susceptible to diet induced obesity (DIO) indicated increased neuronal activity in the DMH as observed by c-fos immunoreactivity (Xin et al., 2000). This correlated to observations made in DIO C57BL/6 mice, which showed dramatically elevated levels of NPY (Guan et al., 1998). In turn, it has been postulated that DMH neurons may us NPY to maintain body weight and energy homeostasis either directly or indirectly. Of note, knock-down of NPY in the DMH using AAV-mediated RNAi increased energy expenditure and improved glucose homeostasis through enhancements in insulin sensitivity. Reminiscent of earlier lesion studies, these mice were also resistant to DIO (Chao et al., 2011). Viral over expression of NPY in the DMH lead to increased food intake and body weight in lean rats (Yang et al., 2009). Even though overall less emphasis has been placed on the DMH compared to other hypothalamic regions, the body of evidence has undoubtedly shown the importance of this region in maintain energy and glucose homeostasis.

1.1.5 Lateral Hypothalamus

The LH is a heterogeneous structure, which contains distinct cell types that are both functionally and genetically distinct from one another. Sub-populations of these neurons have been shown to express abundant levels of both vesicular glutamate transporter (Vglut2) a marker for glutamatergic neurons or the inhibitory neurotransmitter GABA (Collin et al., 2003; Laque et al., 2013; Rosin et al., 2003). In addition, some cell groups also produce important neuropeptides, including orexin/hypocretin (Orx) and melanin-concentrating hormone (MCH). In combination with classical studies and modern techniques, an understanding of how the LH regulates feeding, reward and metabolism has emerged.

Early lesion studies have focused on the effects of this brain region on feeding and drinking (Anand and Brobeck, 1951; Montemurro and Stevenson, 1957). Electrolytic and chemical lesions have both shown the ability to suppress feeding and drinking (Grossman et al., 1978; Grossman and Grossman, 1982; Stricker et al., 1978). Electrical activation in this area has the ability to cause voracious feeding, as well as reinforce this behavior through self-administered stimulation (Delgado and Anand, 1953; Olds and Milner, 1954). With the advancement of Cre-driver mouse lines and cell type-specific optogenetic targeting, we are able to dissect the functional role of LH populations in controlling feeding and metabolism. Acute stimulation of VGat- expressing neurons in the LH elicited a remarkably similar response to feeding and reinforcement as electrical activation (Jennings et al., 2015). Interestingly, when VGlut2-expressing neurons in the LH were activated, they produced the inverse effect. Food deprived mice displayed suppressed feeding along with aversion to the food zone when photostimulation was applied (Jennings et al., 2013). These opposing behavioral effects were supported by genetic ablation studies. Selective depletion of VGat-expressing neurons caused

reduced feeding, body weight gain and willingness to consume palatable foods (Jennings et al., 2015), while ablation of VGlut2-expressing neurons increased feeding and body weight gain (Stamatakis et al., 2016). As a whole, this divergent signaling pathway directly or indirectly modulates behavioral output.

Neurons that express and release Orx are found solely in the LH. From the precursor gene *hypocretin,* two peptides are derived: orexin A/hypocretin 1 (OrxA) and orexin B/hypocretin2 (OrxB). The mechanism of action is mediated through two GPCRs: orexin receptor type 1 (Orx1R) and orexin receptor type 2 (Orx2R). Both ligands have the ability to bind to either receptor. However, Orx1R has greater affinity for OrxA over OrxB, whereas Orx2R has similar affinity for both. The distinct distribution of the two orexin receptors suggests that they utilize distinct neuronal pathways to modulate different physiological states (Marcus et al., 2001). Orexin neurons are well studied for their role in the regulation of sleep and wakefulness which is evident in experiments in which optogenetic stimulation caused increased wakefulness while genetic ablation elicited narcolepsy (Balcita-Pedicino and Sesack, 2007; Boutrel et al., 2005). Of note, these effects have sparked interests in in the field of metabolic and feeding homeostasis. It has been observed that patients suffering from narcolepsy are at a higher risk of developing obesity, even though these individuals tend to consume less food compared to controls (Schuld et al., 2000). This is consistent with the observation made in orexin deficient mice which develop late-onset obesity (Hara et al., 2005; Willie et al., 2001). Interestingly, ICV injection of OrxA into rats increased food intake (Sears et al., 2013). In addition, orexin-overexpressing transgenic mice have been found to be resistant to a HFD, with evidence suggesting that this effect is mediated predominantly by Orx2R to enhance leptin sensitivity (Funato et al., 2009). Furthermore, OrxA injection into the VMH has been shown to act through Orx1R to increase insulin sensitivity in skeletal

muscle to lower circulating glucose (Shiuchi et al., 2009). As a result, the net effect of increased orexinogenic activity is the maintenance of body weight and blood glucose through the control of leptin and insulin sensitivity.

MCH in the LH is produced from the cleavage of a full length preprohormone sequence (Vaughan et al., 1989). Its functional role has been associated with a wide range of behaviors including energy and glucose homeostasis (Kong et al., 2010). Two receptors for MCH have been identified MCHR1, which is found in all vertebrates, and MCHR2, which is not expressed in rodents, but only higher mammals (Hill et al., 2001). As a result, much of what we know has been based on the MCHR1 pathway due to the lack of in vivo rodent models. Evaluation of MCH KO mice showed a clear reduction of body weight which they contributed to both hypophagia and increased metabolic rate (Shimada et al., 1998). The benefit to MCH neuronal depletion was even more evident in leptin-deficient mice (*ob/ob*) which had improved obesity and glycemic control (Alon and Friedman, 2006). Consistent with these findings, *ob/ob* MCHR1 KO mice also displayed reduced adiposity and increased energy expenditure along with improved glucose tolerance (Bjursell et al., 2006). Inversely, mice with overexpression of MCH gained significantly more body weight and showed clear impairments in glucose and insulin tolerance when challenged with a HFD (Ludwig et al., 2001). More recently, it has been identified that these groups of neurons which are glucose excited respond mechanistically like pancreatic beta-cells. With elevation in glucose levels, ATP production is initiated. When adequate levels of ATP are produced intracellularly, KATP channels close and the cell depolarizes. As a result, when glucose sensitivity is decreased or increased through genetic mutation or specific ablation, it correlates to impairments or enhancements in whole body glucose clearance (Kong et al., 2010). Following these novel discoveries, many attempts were made to develop an MCH1R

antagonist that potentially could be used as a therapy to treat obesity and diabetes. Unfortunately, none have produced any significant therapeutic benefit in clinical trials (Johansson, 2011).

1.1.6 Hindbrain

Various nuclei in the hindbrain have been well studied for their role as integration centers between descending pathways from the hypothalamus and the periphery to in turn modulate sympathetic and parasympathetic outflow. With proximity to the fourth ventricle, the brainstem, like the ARC, can integrate circulating signals from the periphery to modulate efferent activity (Grill and Hayes, 2009). For example, the nucleus of the solitary tract (NTS) is a key hub for detecting and integrating circulating nutrient and hormonal signals from the gut such as GLP-1, ghrelin, and cholencystokinin (CCK) as well as from adipose tissue such as leptin (Chaudhri et al., 2006). The NTS not only receives vagal afferents from the gastrointestinal (GI) tract, but also has reciprocal connectivity with various hypothalamic neurons such as orexin neurons in the LH, POMC neurons in the ARC, as well as multiple neurons in the PVH. The NTS has a high density of MC4R. Direct delivery of MC3/4R agonists or antagonists negatively or positively influence meal size and food intake (Fan et al., 2004; Flak et al., 2014; Sutton et al., 2005). In addition, a small population of POMC neurons is located in the ARC. Although their function is not completely elucidated, some reports show their involvement in acute feeding as well as nociception and cardio respiratory control (Cerritelli et al., 2016). Outputs from the NTS contribute to a variety of neuroendocrine, GI, feeding, and energy expenditure responses. This connectivity with the caudal NTS and vagal efferent neurons in the dorsal motor nucleus of the vagus nerve (DMV) is able to control parasymapthetic GI responses ranging from gastric emptying to insulin secretion. In addition, sympathetic efferents involved in energy expenditure relay

information from the NTS to the POA, DMH and ARC (Grill and Hayes, 2012). Recent work has been done to identify cell-type specificity in the NTS including the CCK and dopamine Beta- hydroxylase (DBH) expressing neurons that relay information to another major brainstem nuclei, the parabrachial nuclei (PBN). The calcitonin gene related protein (CGRP) neurons in the PBN have been shown to be involved in aspects of maladaptive eating behaviors including visceral malaise from nausea, satiation from a meal, and anorexia (Roman et al., 2016). The details of this mechanism have been described previously in this comprehensive review on hindbrain energy homeostasis(Grill and Hayes, 2012).

1.1.7 Midbrain

With connectivity to various hypothalamic regions, the mesolimbic reward system has been shown to directly modulate aspects of hedonic feeding and energy homeostasis. Multiple studies have focused on the cell-type specific connection between the LH and the dopaminergic neurons in the ventral tegmentum area (VTA). This includes orexin neurons for behavioral sensitization to cocaine, drug seeking and reward (Borgland et al., 2006; Harris et al., 2005). Neurotensin neurons mediate hedonic feeding and obesity (Kempadoo et al., 2013; Opland et al., 2013). MCH neurons in this region are involved in sucrose reward behavior (Domingos et al., 2013). In addition, a molecularly distinct population VGAT+ LH neurons has been shown to innervate GABAergic VTA neurons to cause a disinhibition of DA release onto the nucleus accumbens (NAc) to enhance positive reinforcement and reward (Barbano et al., 2016; Jennings et al., 2015; Nieh et al., 2013; Nieh et al., 2016).

In addition to connectivity, various circulating hormones act on receptors in the midbrain to integrate hedonic and homeostatic feeding. DA VTA neurons have been

reported to express LEPR and are inhibited upon leptin application. RNAi knock-down of these LEPR resulted in increased food intake, locomotion, and sensitivity to palatable food (Hommel et al., 2006). Further work revealed that leptin's ability to diminish food palatability involves a presynaptic decrease in the probability of glutamate release onto VTA DA neurons (Domingos et al., 2011). Other work has identified ghrelin receptors in the VTA. Application of ghrelin results in a release of DA into the striatum, amygdala, orbitofrontal cortex, and insula (Malik et al., 2008; Naleid et al., 2005) . More work is needed to elucidate the molecular mechanism of how dysfunction in these pathways affects homeostatic and hedonic feeding in various metabolic disorders.

1.2 The complicated case of leptin's antidiabetic effects

The identification of leptin, its receptor, and its ability to reverse obesity in genetic deficiency were instrumental findings for the field of metabolism (Campfield et al., 1995; Maffei et al., 1995; Zhang et al., 1994). This key hormone released from WAT signals to the CNS resulting in decreased food intake, increased energy expenditure, and restored normoglycemia. Mice lacking functional leptin or leptin receptors exhibit early onset obesity, diabetes, and other neuroendocrine problems. Intravenous or ICV leptin administration to leptin deficit mice (ob/ob) completely reverses the diabetic and obesity phenotypes (Kamohara et al., 1997; Pelleymounter et al., 1995a). Even more attention was drawn to leptin's therapeutic potential as ICV leptin was able to reverse the hyperglycemia in multiple models of insulin-deficient mice (Fujikawa et al., 2013; Fujikawa et al., 2010; Yu et al., 2008). Many studies with cell-type and region specificity have identified CNS regions where leptin exerts its anti-diabetic effects. Nevertheless, leptin therapy is unlikely to improve conditions for diabetes in humans due to the characteristic leptin resistance found in these patients (Myers and Olson, 2012). Considering that insulin is not necessarily required, teasing apart the insulin-independent

and dependent molecular mechanisms may be an avenue for both insulin-deficient (T1DM) and insulin-resistant (T2DM) diabetes therapies.

LEPRs are expressed throughout the CNS with the highest density in the hypothalamus and brainstem. Within the hypothalamus, leptin responsive neurons have been identified in the ARC, DMH, LHA, and VMH (Dhillon et al., 2006; van de Wall et al., 2008). Postulated to be the first order neurons mediating leptin's response are leptin-excited POMC and leptin-inhibited AgRP neurons in the ARC. In addition, studies have shown that re-expression of leptin receptors in these ARC neurons can mediate leptin's glucose lowering effects (Berglund et al., 2012; Goncalves et al., 2014). Interestingly, disruption of GABAergic hypothalamic neurons results in hyperphagia and obesity (Vong et al., 2011). Recent identification of a population of DMH VGAT+ DYN+ LEPR + neurons projecting to the ARC has been shown to mediate food sensory cues (Garfield et al., 2016). Although these circuit's ability to regulate leptin's effects remains untested. Downstream targets of these first order neurons are still unclear, although candidates include MC4R+ or CRH+ neurons in the PVH, neurons that have been shown in separate studies to modulate sympathetic outflow and suppress hepatic glucose production (Klieverik et al., 2009; Perry et al., 2014). Downstream projections modulate sympathetic and parasympathetic outflow to improve glycemic control (Fujikawa and Coppari, 2015). Recent studies have also looked into the ability for non-neuronal cells in the brain to contribute to leptin's effects. Astrocytes have been shown to sense and adjust their activity to changes in energy, pH levels, and glucose. Leptin has been shown to have effects on glutamate and glucose transporter expression levels in hypothalamic astrocytes (Fuente-Martin et al., 2012) and deletion of LEPR in GFAP-Cre mice weaken leptin's anorexigenic effect (Kim et al., 2014). In addition, LEPRs on tanycytes, which line the third ventricle, have also been shown to be sensitive to HFD (Balland et al.,

2014). Although the work on glial cells and their role in mediating leptin's effects is new, it is something to consider in the complexity of leptin signaling.

In addition to investigating the cell-type specificity underlying leptin's antidiabetic effects, elucidating the downstream molecular signaling of leptin action could identify new therapeutic targets. Leptin acts via the long form of the leptin receptor (LepRb) (although other forms exist) to activate the JAK/STAT pathway to induce transcription of genes regulating energy homeostasis and neuroendocrine functions (Ducy 2000; Vaisse 1996; Munzberg 2005). Specifically, it has been identified that STAT3 signaling through LepRb+ neurons mediates the majority leptin's antidiabetic effect (Bates 2003; Piper 2008). Leptin's other signaling pathways include the phosphatidylinositol 3' kinas(PI3K)-AKT pathway, which converges with downstream signaling of insulin (Niswender 2000; Hill 2008). AKT inhibits transcription of factor FoxO1 which regulates the expression of POMC, AgRP and NPY (Kim 2006). Other targets of the PI3K-AKT pathway include mTOR and S6K which have been shown to be involved in attenuating leptin's anorexigenic effects (Cota 2006; Gong 2007). Leptin has been shown to inhibit adenosine monophosphate-activated protein kinase (AMPK) activity to reduce food intake and bodyweight (Claret 2007). Additionally, investigating the molecular mechanisms of negative regulators of the leptin receptor could be another avenue for therapeutic potential. This includes SOCS3 and other phosphatases such as protein tyrosine phophatase1B (PTP1B), T-cell PTP (TCPTP), and RPTP which have been reported to be elevated in obesity models (Bjorbaek 1998; Wauman 2017). These signaling pathways have been discussed in more details elsewhere (Coppari 2011; Wauman 2017).

Early findings showing leptin's ability to rescue the diabetic phenotype in mouse models of insulin-deficient T1D led to the initial belief that leptin could be powerful in

treating diabetes. Moreover, acute administration of leptin can reverse the obesity phenotype in leptin deficient animals and humans. However, leptin deficiency only accounts for a small number of obesity cases. The majority of cases of human obesity include high circulating leptin levels and leptin resistance. As for human therapies, clinical trials have only highlighted that leptin attenuates insulin-deficient diabetes and is an effective treatment for lipodystrophy and restores menstruation in hypothalamic amenorrhea (Coppari 2011). More work is necessary to find a potential therapy that could increase leptin responsiveness or modulate downstream targets of leptin signaling, rather than just administering more leptin.

1.3 The potential of fibroblast growth factors in treating diabetes

Fibroblast growth factors (FGFs) are proteins that are secreted mainly through the endoplasmic reticulum-Golgi secretory pathway(Beenken and Mohammadi, 2009). Their functions have been well documented through FGF mutation studies that have led to impairments in development and even to the pathogenesis of cancer (Kan et al., 2002; Turner and Grose, 2010). FGFs act by binding to the FGF receptor (FGFR), which initiates a downstream signaling cascade. Recently, a few FGFs have drawn much attention for their ability to regulate blood glucose levels and reverse diabetes (Perry et al., 2015; Scarlett et al., 2016).

FGF19 is secreted from ileal enterocytes in the intestines following activation of the farnesoid-X receptor by bile acids (Song et al., 2009). Classically, FGF19 has been shown to control bile salt synthesis in the liver through a negative feedback loop(Chiang, 2009). Interestingly, direct infusion of FGF19 has been shown to reduce body weight and improve glucose tolerance in T2D mouse models (Fu et al., 2004). In addition, deletion of FGF15, the mouse orthologue of FGF19, leads to impairment in glucose

tolerance (Kir et al., 2011), while transgenic expression of FGF19 in mice has been shown to improve insulin sensitivity and reduce basal glucose levels (Tomlinson et al., 2002). These mice were also resistant to obesity and diabetes induced by a HFD. Initially, these effects were believed to be mediated mainly through FGF receptor 4 (FGFR4) in the liver (Yu et al., 2000). Surprisingly, deletion of FGFR4 in mice had negligible effects on FGF19 treatment (Wu et al., 2011a). This suggests an alternative FGFR subtype independent of the liver. Growing evidence has implicated FGFR1 as the primary alternative pathway to affect glucose homeostasis. Administration of a mutated FGFR19 has been shown to reduce whole body glucose in vivo through the activation of FGFR1, independent of FGFR4 (Wu et al., 2010a). Specific agonists for FGFR1 have the ability to ameliorate the hyperglycemia in leptin receptor deficient mice (Wu et al., 2011b). Although expression of FGFR1 has been well documented in WAT and skeletal muscle, which may contribute in part to glucose maintenance, this receptor is highly expressed in the hypothalamus (Yang et al., 2012). Central administration of FGF19 has been shown to significantly reduce the hyperglycemia in both T1 and type T2D models(Morton et al., 2013; Perry et al., 2015; Ryan et al., 2013) by modulating the neuronal activity of specific sub-groups of neurons important for metabolic and glycemic control(Marcelin et al., 2014). However, the central contributions of FGF19 in controlling insulin secretion and insulin sensitivity to reduce blood glucose are still up for debate. Early work has implicated FGF19 in the modulation of insulin secretion and sensitivity in the periphery (Marcelin et al., 2014), while other groups have suggested that the glucose lowering effect is caused by an insulin-independent glucose clearing mechanism (Morton et al., 2013; Perry et al., 2015; Ryan et al., 2013). What is clear is that central and peripheral administration of FGF19 cause a rapid glucose lowering effect. The therapeutic potential of FGF19 has been dampened by the adverse effects caused by chronic administration. It has been well established that overexpression of FGF19

promotes the development of hepatocellular carcinoma (Nicholes et al., 2002). Currently, variants of FGF19 are in development to overcome these caveats (Degirolamo et al., 2016), however due to the incomplete understanding of the underlying molecular mechanisms and pathways, the efficacy and safety of an FGF19 therapy is still awaiting further investigation.

Within the last few years, interest in FGF1 for its therapeutic potential to treat diabetes has risen. Originally, due to the importance of FGF1 in wound healing, neurogenesis and angiogenesis, the first clinical trials using FGF1 were geared towards artery and capillary repair and in restoring motor function in paralyzed patients (Beenken and Mohammadi, 2009). It was not until evidence came out showing that FGF1 KO mice treated with a HFD developed significantly higher BG compared to control mice that investigation into FGF1's role in glycemic control began (Suh et al., 2014). Since that point, the benefits of FGF1 over FGF19 have become evident. Unlike FGF19, FGF1 is not limited to a sub-set of FGFRs due to the need for a co-receptor to aid in binding and activation (Ornitz and Itoh, 2015). The duration of glucose lowering following central administration of FGF1 also surpasses that of FGF19 (Morton et al., 2013; Suh et al., 2014). A single administration of recombinant FGF1 (rFGF1) into the CNS was sufficient to cause a sustained glucose-lowering effect without the risk of hypoglycemia in multiple T2D mice models (Scarlett et al., 2016). Finally and maybe most importantly, is our ability to separate FGF1's mitogenic function from its glucose lowering ability. By creating targeted mutations or deletion in FGF1, binding to FGFR3/4, a key contributor to mitogenicity, can be avoided while keeping glycemic regulation through FGFR1 activation intact (Suh et al., 2014). However, a constant concern is the role of FGF1 in the pathogenesis of certain cancers. Gene expression studies have shown elevated levels of FGF1 in ovarian and breast cancer, but a direct causal mechanism has yet to

be established (Birrer et al., 2007; Finak et al., 2008). The inability to illicit a robust glucose lowering effect in DIO mice following central administration of FGF1 has raised question about its therapeutic potential, as well. In order to answer these questions, data from human or non-human primate trials are required. Currently, no such study has been completed.

1.4 The gut microbiota and the brain

The gut microbiota is essential for the maintenance of a healthy host, including the digestion of food, protection against pathogens, and the synthesis of certain vitamins (Clarke et al., 2014). It is mainly composed of bacteria, archaea, and viruses. The classical belief is that the developing fetus is sterile in utero, rapidly obtaining the microbial population following birth and progressing until stability is reached at 2- 3 years of age (Maynard et al., 2012; Yatsunenko et al., 2012). In healthy individuals, the microbiota acquired during these early years remain remarkably stable throughout adulthood (Faith et al., 2013). In instances when the gut microbiota composition is altered, there has been strong correlations linking dysregulation to the pathogenesis of a myriad of diseases; maybe none more important than diabetes (Mikkelsen et al., 2015; Suez et al., 2014). As a result, there has been a resurgence in the study of the gut microbiome and its role in metabolic, physiological, psychology, and immunological regulation (Desbonnet et al., 2014; Faith et al., 2013).

The shift in microbiota composition in diabetic models has been well characterized. In leptin deficient *ob/ob* mice compared to *ob/+* lean litter mates, a significant change in the ratio of Firmicutes to Bacteroidetes in the cecum was observed (Ley et al., 2005). Diet has also been shown to rapidly alter the microbial community (David et al., 2014). In mice feed a western diet consisting of high-fat/high-sugar foods, a

similar shift in microbiota composition was detected (Turnbaugh et al., 2008). However, it is still unclear whether the altered microbiota drives the development of diabetes or if it is a secondary effect due to the diet and physiological changes. Interestingly, mice lacking microorganisms or germ-free (GF) mice, which received microbiota transplants from obese mice, promoted fat mass accumulation (Turnbaugh et al., 2006). Direct infusion of intestinal microbiota from lean to obese subjects has been shown to increase insulin sensitivity in humans (Vrieze et al., 2012). Finally, the use of antibiotics, which disrupts intestinal homeostasis, has been associated with increased risk of developing T2D (Mikkelsen et al., 2015). Based on this evidence, it can be speculated that in some cases the alterations in microbiota may be the driving factor in the pathogenesis of diabetes.

An increasing number of studies have shown that homeostasis is maintained in part by the gut-brain axis (Collins et al., 2012; Rhee et al., 2009). This is a complex physiological system that connects the GI system to the brain. Utilizing primary visceral afferent nerve fibers, the gut can mediate the sympathetic and parasympathetic outflow of the autonomic nervous system(Furness, 2012). These signals are then compiled by the hindbrain nucleus and in turn relayed to the forebrain region and the hypothalamus, where the information can be interpreted (Rinaman, 2007). In addition, the gut is also able to inform the brain of the current nutrient state by releasing hormones into the circulation. Within the GI tract, enteroendocrine cells secrete orexigenic ghrelin, anorexigenic cholecystokinin (CCK), and insulin mediating glucagon-like peptide-1 (GLP-1) (Breen et al., 2013; Cummings and Overduin, 2007). Of these peptides, analogues of GLP-1 has been widely used for the treatment of T2D, in particular for patients who do not respond to metformin, one of the most prescribed medication for blood glucose control (Prasad-Reddy and Isaacs, 2015). Of note, central administration

of GLP-1 has been shown to improve glucose tolerance, while inhibition of the GLP-1 receptor in the CNS impairs glucose tolerance(Sandoval et al., 2008). This indicates the importance of central GLP-1 signaling in the maintenance of glucose homeostasis. However, these findings are in debate, as glucose lowering was still observed after administration of a GLP-1 analogue in mice lacking the GLP-1 receptor in the CNS (Sisley et al., 2014).

Compared to pharmacological intervention, surgical methods have been shown to be the most effective treatment for diabetes and obesity (Mingrone et al., 2012; Schauer et al., 2014). The most common bariatric surgery which produces the greatest sustained improvement in metabolic and weight reduction is the Roux-en-Y gastric bypass (RYGB) (Sjostrom et al., 2007; Werling et al., 2013). This procedure involves creating a small gastric pouch from the fundus of the stomach. The stomach and proximal small intestine are bypassed by attaching the newly formed pouch with the small intestine below the main body of the stomach, in turn restricting the amount of food that can be ingested. Despite the obvious benefit of food restriction, this mechanism does not fully explain the benefits of this procedure on weight management and diabetes remission, leading to many hypotheses. It has been shown that following surgery there is increased release of GLP-1 from the gut, changes in bile acid metabolism, elevated levels of gastric emptying, and alterations in food preference, all of which may contribute to the observed benefits of this surgical intervention(le Roux and Bloom, 2005; Miras and le Roux, 2013). Growing evidence has also shown changes in gut microbiota composition and diversity following bariatric surgery, suggesting that it may contribute to the beneficial effects as well (Furet et al., 2010; Graessler et al., 2013; Kong et al., 2013; Tremaroli et al., 2015). As stated previously, there are abundant pathways by which the gut can communicate with the CNS. To determine the role of central control in the

sustained success of bariatric surgeries, key homeostatic regulators have been investigated, one of the most important being the melanocortin signaling pathway. This pathway is crucial for maintaining normal food intake, blood glucose levels, and energy expenditure (Cone, 2005). Mouse models lacking the melanocortin-4 receptor (MC4R) develop early-onset obesity and diabetes. Following RYGB surgery, these mice lost significantly less body weight and saw fewer improvements to glucose tolerance, suggesting that central melanocortin signaling is necessary for the effects of bariatric surgery(Hatoum et al., 2012; Zechner et al., 2013). Further work needs to be performed to fully understand the molecular pathways and neural circuits involved in this homeostatic recalibration. If successful, this may lead to novel treatments for obesity and diabetes with the same therapeutic outcomes without the need for surgery.

1.5 Understanding the physiological role of ARC POMC neurons in energy and glucose balance

As previously stated, one of the most well-defined and studied mechanisms of controlling energy balance is the central melanocortin system. It has the ability to assess current and future energy levels and tune physiological and behavioral responses to compensate accordingly (Krashes et al., 2016). The sensory input comes from two divergent populations of neurons located in the ARC (Cone, 2005; Garfield et al., 2009): orexigenic AgRP containing neurons (Aponte et al., 2011; Atasoy et al., 2012; Krashes et al., 2011) and anorexigenic POMC containing neurons (ARC^{POMC}) (Atasoy et al., 2012; Dodd et al., 2015; Zhan et al., 2013). Their ability to sense circulating hormones from the periphery (Garfield et al., 2009; Gautron et al., 2015) and receive significant synaptic inputs from the hypothalamus and forebrain nucleus (Wang et al., 2015) suggest that they integrate both peripheral and brain-based inputs. The functional outflow is controlled by MC4R expressing neurons. In the CNS, α-MSH derived from

POMC activates MC4R, while AgRP is a high-affinity MC4R antagonist. Only mutations in *POMC* and *MC4R* genes have been shown to cause increased prevalence of early-onset obesity in humans, characterized by hyperphagia and a reduction in energy expenditure (Krude et al., 1998; Vaisse et al., 1998; Yeo et al., 1998). Genetic ablation of the *AgRP* gene does not result in any of the expected phenotypes including hypophagia or leanness (Qian et al., 2002). As a result, our work focuses on ARC^{POMC} neurons and their role in energy and glucose homeostasis.

Deciphering the molecular mechanisms and neural circuits underlying the physiological role of POMC neurons has been a longstanding goal, a major obstacle being the heterogeneity of ARC^{POMC} neurons. POMC neurons in the hypothalamus do not uniformly express the same surface receptors. *POMC-hrGFP* mice expressing humanized Renilla green fluorescent protein driven by transcription of the *POMC* gene were one of the first models to determine the direct effects of leptin on ARC^{POMC} neurons. In combination with electrophysiological recordings, initial reports demonstrated a 90% depolarization rate in POMC cells washed with a 100nM concentration of leptin (Cowley et al., 2001). Further studies produced varying results with some reporting as low as 38% leptin responsiveness (Choudhury et al., 2005). Similarly, investigation into insulin effects on ARC^{POMC} neurons produced varying results, from as few as 50% to as many as 82% hyperpolarization due to direct insulin action (Choudhury et al., 2005; Claret et al., 2007). Some of the variability can be explained with sample size and slight variations in experimental procedures, but in more extreme cases a novel explanation is required. It was not until there was a systematic characterization of leptin-activated and insulin-inhibited POMC cell distribution within the ARC that a clear explanation was proposed. Based on topographical regions, cell response to either leptin or insulin can vary dramatically. Leptin responsive POMC

neurons were concentrated in the medial ARC while insulin inhibited POMC cells were mainly focused in the rostro medial area of the ARC. On average, they determined that 35% of POMC neurons responded to leptin while 25% were affected by insulin (Williams et al., 2010). This variability may extend to the ability of these neurons to respond to changes in glucose levels as well. In earlier work using the same transgenic mouse model, the reduction of extracellular glucose from 10mM to 5mM was sufficient to reduce the baseline firing rate to 83% of POMC cells (Ibrahim et al., 2003). More recent work with a larger sample size and physiologically relevant glucose levels showed that the proportion of glucose excited POMC neurons was only 50% of the population (Parton et al., 2007b). Another interesting dichotomy is the expression of fast acting neurotransmitters GABA and glutamate. In situ hybridization techniques used to study mRNA expression of VGLUT2 and glutamic acid decarboxylase 67 (GAD67), markers for glutamatergic and GABAergic synthesis respectively, identified two relatively even distributed populations. In mice, 43% of POMC neurons expressed VGLUT2 while 54% expressed GAD67 mRNA. In rats, the distribution was slightly inversed with 58% of POMC cells containing VGLUT2 and 37% containing GAD67 mRNA (Wittmann et al., 2013). To date no reports of vesicular GABA transporter (VGAT) KO in POMC neurons using the Cre/loxP system have been made. This may be due to the caveats that will be discussed further in the introduction on the use of POMC-Cre mice. On the other hand, selective deletion of VGLUT2 in POMC neurons did not alter body weight when mice were placed on a normal chow diet. However, when placed on HFD VGLUT2 KO mice developed slight body weight gain compared to controls (Dennison et al., 2016). These distinct populations of POMC neurons, with varying surface receptors, gene expression and topography, suggest segregation in their physiological roles and signaling outputs. In addition, due to the lack of evidence for the role of GABA and the mild phenotypical change from selective deletion of vGLUT2 in POMC neurons, it is suggested that

specific neuropeptides rather than fast acting neurotransmitters may be the driver for energy and glucose homeostasis.

Previous models used to study POMC neurons have limitations. POMC-null mice were created to mimic the phenotype of severe obesity and hyperglycemia observed in humans with congenital deficiency of POMC (Farooqi et al., 2006; Yaswen et al., 1999).Early studies showed that POMC-null mice were overweight and developed hypoglycemia at six to eight weeks of age. However, POMC-derived ACTH is required for normal adrenal gland development. Early reports in POMC-null mice described the complete lack of adrenal medulla, resulting in non-detectable levels of circulating corticosterone and aldosterone (Yaswen et al., 1999). In contrast, others have reported visible but underdeveloped adrenal glands with clear cortical and medulla structures. Consistent with previous findings, corticosterone levels in these mice were undetectable and aldosterone levels were markedly reduced (Coll et al., 2004). Unsurprisingly, subcutaneous injection of CRH caused a significant elevation in circulating corticosterone levels in WT mice when compared to heterozygous POMC-null mice (Coll et al., 2004). This shows a direct impairment of the HPA axis in POMC-null mice, which as previously stated is essential for the maintenance of glucose levels in times of stress (Jamieson et al., 2006) (Figure 1.4). With global depletion of POMC, these mice succumb to obesity induced hyperglycemia at three months of age (Hochgeschwender et al., 2003). Prolonged obesity caused elevated levels of glucose and insulin resistance up to the completion of the monitoring period when the mice were eight months old (Smart et al., 2006). Inconsistent with previous findings, recent studies using mice with POMC deletion solely in the ARC have demonstrated improved glucose tolerance (GT) even with the development of severe obesity and insulin resistance. This counterintuitive finding stems from impaired central POMC signaling which reduces the sympathetic

outflow. This in turn lowers the secretion of epinephrine from the adrenal gland and the increase in glycosuria through elevated expression of renal GLUT2 (Chhabra et al., 2016). As a result, the direct role of *POMC* in the ARC as it pertains to glucose homeostasis is still controversial.

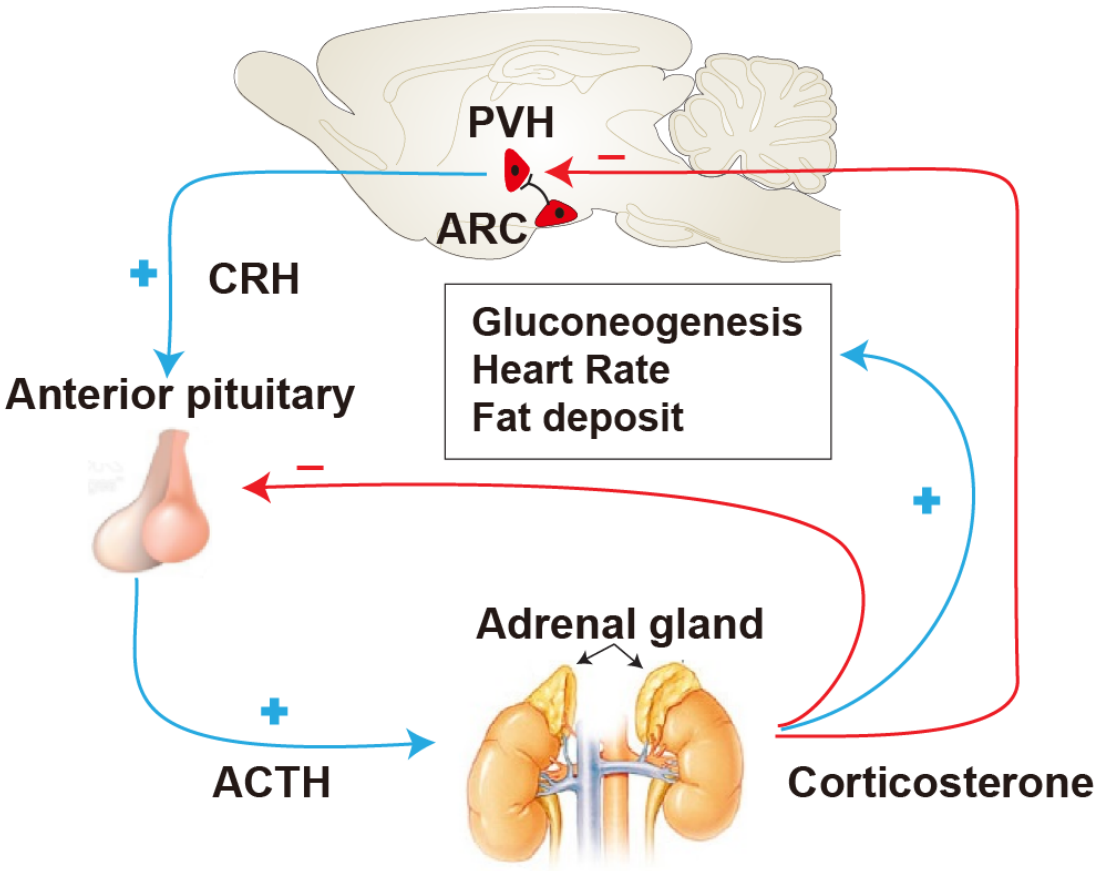

Figure 1.4: The hypothalamic pituitary axis. Corticotrophin-releasing hormone (CRH) neurons are predominately found in the medial parvocellular region of the PVH. Activation of these neurons from upstream effectors causes the release of CRH into the median eminence. CRH stimulates adrenocorticotropic hormone (ACTH) production and secretion from the pituitary gland. Once released, ACTH binds to receptors on the adrenal gland which increases synthesis and release of corticosterone. The circulating corticosterone then acts on peripheral organs and tissues to increase gluconeogenesis, heart rate and fat deposition. In addition, corticosterone acts as a negative feedback signal in the hypothalamus and pituitary gland to suppress CRH and ACTH levels respectively. Image modified from (Santulli, 2015).

A pivotal advancement in the field has been the development of the *POMC*-Cre transgenic mouse line (Balthasar et al., 2004b). The use of the Cre/loxP system to test

the functional importance of surface receptors and peptides found within POMC neurons has provided insight into the upstream effectors and how they modulate changes in the periphery. However, it too has caveats which have cast a shadow on previous discoveries. First, this mouse line utilizes the POMC promotor to drive Cre expression in the central nervous system. Unfortunately, POMC expression during development is dynamic, with transient expression in many sites including the forebrain, hindbrain, spinal cord, hypothalamus and retina. This fleeting expression of POMC in the developing brain has been reported to be sufficient to cause Cre-mediated recombination of floxed alleles. When crossed with a ROSA reporter strain 62 sites of recombination were observed in adult mouse brains (Padilla et al., 2012). Importantly, earlier work has also shown that AgRP neurons, which exert apposing actions to POMC neurons in regards to food intake and energy balance, share a common progenitor. As a result, a quarter of mature AgRP neurons expressed POMC transiently at one point or another during development (Padilla et al., 2010). With the ability to invoke significantly increased feeding with photostimulation of as few as 300 AgRP neurons (Aponte et al., 2011), genetic alteration to even a small subpopulation is sufficient to elicit a physiological response. As a result, approaches utilizing the POMC promotor to control expression of the cre transgene and affect loxP modified alleles are not as temporally or tissue specific as previously thought, bringing doubt to some conclusion drawn about the role of ARC^{POMC} neurons in the regulation of energy and glucose balance (Berglund et al., 2012; Konner et al., 2007). As stated previously, outside of the ARC POMC is expressed in the NTS and the pituitary gland (Balthasar et al., 2004a). Briefly, chemogenetic studies have shown that acute stimulation of POMC neurons in the NTS has the ability to suppress feeding immediately following CNO injection (Zhan et al., 2013). POMC-derived ACTH secreted from the pituitary gland has long been documented as a key regulator of energy balance and glucose homeostasis, in main

part due to its ability to regulate glucocorticoid expression and secretion from the adrenal cortex (Toda et al., 2017). Even though in POMC-null mice it has long been postulated that the ARC^{POMC} neurons are the key mediators for the observed obesity and diabetic phenotypes (Yaswen et al., 1999), the role of other POMC neuron containing regions cannot be ruled out. Finally, manipulation or deletion of elements early in development may result in developmental compensation (as in the case of AgRP ablation)(Morrison and Munzberg, 2012). Therefore, some of these findings may need to be revisited. In order to move the field forward, new tools need to be developed to overcome many of the caveats associated with current techniques. Ideally, a novel method should be developed that increases neuronal and spatial specificity while using techniques that have been well established in the field.

In the present study, using chemogenetics to rapidly depolarize POMC neurons, we have observed an increase in thermogenesis, locomotion and an acute reduction in whole body glucose levels. Furthermore, we elucidated a negative feedback loop which prevents the development of hypoglycemia from excessive POMC neuronal activation. Utilizing clustered regularly interspaced short palindromin repeats (CRISPR) technology in vivo; we sought to identify the key mediators of this homeostatic regulation. Our first candidate, *POMC,* was deleted and re-expressed only in ARC *POMC*-Cre neurons and it was determined that its primary role is modulating feeding and energy expenditure, while hyperglycemia is secondarily caused by physiological changes due to obesity. Taking advantage of the novel Cas9 immune re-expressing viral constructs, we further dissected the role of key biologically active fragments derived from POMC and found that α–MSH is necessary to maintain appropriate thermogenesis and β-endorphin significantly impacts locomotion. Using a similar approach, we established that *CART* in ARC^{POMC} neurons is necessary for maintaining glucose homeostasis. In addition, after

viral over-expression of CART we identified its role in the pathogenesis of both HFD induced T2D and STZ treated T1D mouse models. Finally, using an unbiased approach and the combination of optogentics and chemogenetics, we have determined the downstream target of ARC^{POMC} for glucose regulation. The above findings provide a novel framework for how hypothalamic neurons integrate metabolic signals and maintain whole body homeostasis through clear physiological roles of individual neuropeptides.

Chapter 2: Methods and Materials

2.1 Animal Care

All animal care and experimental procedures were approved and performed in accordance by the Tufts University/Tufts Medical Center Institutional Animal Care and Use Committee (IACUC).In addition, all animal care and experimental procedures were in accordance with NIH guidelines. Mice were housed at 22°C-24°C in groups (2-5 siblings) with *ad libitum* access to a regular chow diet and water. The light cycle began at 7 am and ended at 7 pm daily resulting in 12-h light/dark cycles. Mice were fasted for 16-18 hrs if required for an experiment. Mice were euthanized by CO_2 narcosis. Adult male mice from each line were used for all experiments. Following stereotaxic injection, cannula implantation or fiber optic implantation, mice were individually housed with *ad libitum* access to regular chow diet and water. Littermates of the same sex were randomly assigned to experimental or control groups.

2.2. METHOD DETAILS

2.2.1 Genetic Mouse Models

All mice used in this study have been previously described:Npy-hrGFP (B6.FVB-Tg(Npy-hrGFP)1Lowl/J)) (van den Pol et al., 2009), POMC-hrGFP(FVB-Tg(Pomc1-hrGFP)1Lowl/J) (Parton et al., 2007a), AgRP-IRES-Cre ($AgRP^{Cre}$) (Tong et al., 2008), Rosa26-LSL-Cas9 knockin (B6;129-*Gt(ROSA)26Sor*$^{tm1(CAG-cas9*,-EGFP)Fezh}$/J) (Platt et al., 2014a), *POMC*-Cre (Tg(Pomc1-cre)16Lowl/J) (Balthasar et al., 2004a), .

2.2.2 STZ Injections

Streptozotocin (STZ) (Sigma-Aldrich Cat#S0130) was injected intraperitoneally (i.p.) at varying doses from 75 to 150 mg/kg body weight. Based on injections into *C57BL/6* mice 125 mg/kg was chosen as the optimal dosage to induce gradual onset of hyperglycemia, characteristic of Type 1 diabetes. As a result all experiments involving STZ utilized this dosage. Following injection of STZ the health condition of the mice were monitored closely twice per day for two days and once per day on the third day. Blood glucose

measurements to determine the extent of the STZ-induced diabetes began three days following injection. Other studies performed on these mice included body weight, food intake, micturition analysis, mRNA expression analysis, serum insulin, and serum leptin levels.

2.3 Metabolic Studies

Food intake, body weight, blood glucose, body composition, oxygen consumption and locomotion were measured as follows. Food intake was measured by measuring the initial weight and final weight of food in grams during each indicated session. Daily food intake assays consisted of weighing food pellets at 8 a.m. each day for 4 continuous days, an average of 3-day food intake was calculated. Light cycle food intake was measured from 7 a.m. to 7 p.m. and dark cycle food intake was the inverse unless stated. Body weight and food intake were measured weekly during the duration of the experiment including the week before surgery. For excitatory hM_3Dq-related studies, mice were singly housed and food pellets were weighed before and after CNO i.p. injection (0.3mg/kg) during light or dark cycle. Blood glucose concentrations were measured using a glucose meter and strips (OneTouch). Body fat mass was measured using echoMRI analysis, and oxygen consumption was measured using metabolic chambers of a Comprehensive Lab Animal Monitoring system (CLAMS, Columbus Instruments, Columbus, OH) from the Adipose Tissue Biology and Nutrient Metabolism Core at the Boston Nutrition and Obesity Research Center (BNORC). Mice were acclimatized in the chambers for 48 h prior to data collection. Spontaneous activity was measured using home cage (photobeam break) from the Tufts Behavior Core. Mice were acclimatized in the chambers for 48 h prior to data collection. Mice with missed or partial injection of the virus were excluded from analysis after post hoc examination of mCherry or GFP expression. In this way, all measurements were randomized and blind to the experimenter.

2.3.1 iBAT Temperature

Thermal imaging was performed using a thermal imaging camera attachment (FLIR One). Animals were anesthetized and fur was shaved to expose the region covering the interscapular brown adipose tissue (iBAT) and flank area. After a 1 week recovery and acclimation period, mice were thermally imaged and subcutaneous iBAT and flank temperatures were measured.

2.3.2 Glucose Tolerance Test (GTT)

Mice were fasted for 16 hours overnight. Blood glucose was measured using OneTouch Ultra 2 glucose meter and strips (OneTouch). After fasting, mice received i.p. injection of 20% glucose and blood glucose levels were measured at 0, 15, 30, 60, and 120 min time points. Chemogenetic stimulation of POMC neurons was achieved by injecting CNO (0.3mg/kg) 15 minutes before glucose administration.

2.3.3 Insulin Tolerance Test (ITT)

Mice were fasted for 4 hours and basal blood glucose levels were measured. Mice received i.p. injection of insulin (0.75U/kg BW) and blood glucose levels were measured at 0, 15, 30, 60, and 120 min time points. Chemogenetic stimulation of POMC neurons was achieved by injecting CNO (0.3mg/kg) 15 minutes before insulin administration.

2.3.4 Pyruvate Tolerance Test (PTT)

Mice were fasted for 16 hours overnight. Blood glucose was measured using OneTouch Ultra 2 glucose meter and strips (OneTouch). After fasting, mice received i.p. injection of pyruvate (2g/kg BW) and blood glucose levels were measured at 0, 15, 30, 60, and 120 min time points. Chemogenetic stimulation of POMC neurons was achieved by injecting CNO (0.3mg/kg) 15 minutes before pyruvate administration.

2.4 Quantitative PCR Assay

Mice were sacrificed by decapitation and relevant tissues (hypothalamus region, IBAT, liver and skeletal muscle) were extracted and stored in RNA*later* solution (ThermoFisher

Scientific AM7020). RNA was extracted using TRIzol Reagent (ThermoFisher Scientific #15596-018) and reverse transcribed using AffinityScript QPCR cDNA Synthesis Kit (Agilent Technologies # 600559). Assay probes used were *Agrp* (Mm00475829_g1), *Npy* (Mm00445771_m1), *Pomc* (Mm01323842_m1), *Cartpt* (Mm04210469_m1), *Ucp1* (Mm01244861_m1), *Pck1* (Mm01247058_m1), *G6pc* (Mm00839363), and *Mstn* (Mm01254559_m1). Relative expression of mRNA was normalized for total RNA content by 18S ribosomal RNA quantitative PCR (Applied Biosystems). qPCR was performed on a StepOnePlus Real-Time PCR System (Applied Biosystems).

2.5 Electrophysiology

2.5.1 Slice Preparation

The protocols of slice preparation and whole cell recording have been previously described (Kong et al., 2012). Briefly, 5-7 week-old mice were anesthetized by inhalation of isoflurane. 300 μm thick coronal sections were cut with a Leica VT1000S vibratome and then incubated in carbogen saturated (95% O_2 / 5% CO2) ACSF (in mM: 125 NaCl, 2.5 KCl, 1 $MgCl_2$, 2 $CaCl_2$, 1.25 NaH_2PO_4, 25 $NaHCO_3$, 10 glucose) at 34 °C for 30-40 min before recording. Sucrose was used to adjust the osmolarity of the test solution depending on the concentration of glucose used (0.5 mM or 10 mM). All recordings were obtained within 4 h of slicing at room temperature. Whole-cell recordings were obtained from arcuate POMC neurons visualized under infrared differential interference contrast (IR-DIC) using patch pipettes with pipette resistance of 2.5–4.5 MΩ. *POMC-GFP* mice were used to identify the GFP labeled POMC neurons using epifluorescence illumination. For sIPSC recordings, the internal solution contained (in mM) 135 $CsMeSO_3$, 10 HEPES, 1 EGTA, 3.3 QX-314 (Cl^- salt), 4 Mg-ATP, 0.3 Na-GTP, 8 Na_2-phosphocreatine (pH 7.3 adjusted with CsOH; 295 mOsm·kg^{-1}). For 2-DG group, 2-DG containing ACSF (in mM: 125 NaCl, 2.5 KCl, 1 $MgCl_2$, 2 $CaCl_2$, 1.25 NaH_2PO_4, 25

$NaHCO_3$, 10 glucose, 10 2-DG) was used for recording. Recordings were made using an Axoclamp 700B amplifier (Axon Instruments) at room temperature. Data were filtered at 3 kHz and sampled at 10 kHz. Series resistance, measured with a 5 mV hyperpolarizing pulse in voltage clamp, was on average under 20 MΩ and less than 25 MΩ, uncompensated. All voltage-clamp recordings were made from cells held at −60 mV.

2.6 Immunohistochemistry

Immunohistochemistry was performed as previously described (Kong et al., 2016). Mice were deeply anesthetized with isoflurane and perfused transcardially with 0.9% saline followed by 10% formalin (Sigma Aldrich). Brains were extracted and fixed in 10% formalin overnight at 4°C and transferred to 30% sucrose solution. 40 µm sections were cut on a microtome and collected in a PBS solution, with every fourth section of the whole-brain used for staining. Following PBS washes (3x10 min) brain slices were blocked in PBT-Azide with 3% normal donkey serum for 2 hrs. Primary antibodies used were: anti-DsRed (Clontech #632496, 1:2000), anti-mCherry (EnCor Biotechnology CPCA-mCherry, 1:2000), anti-eGFP (Aves Labs GFP-1010, 1:2000), anti-hrGFP (Agilent Technologies #240142, 1:2000), anti-CART (Phoenix Pharmaceuticals # H-003-62, 1:5000), anti-POMC (Phoenix Pharmaceuticals # H-029-30, 1:2000), anti-αMSH (EMD Millipore #AB5087, 1:2000), anti-β-endorphin(Peninsula Laboratories #T4044, 1:1000), and anti-c-fos (Santa Cruz Biotechnology SC-52-g, 1:150).Sections were washed with PBS (0.1% triton) and incubated for 45 min at room temperature in dye-conjugated secondary antibody (1:200). Sections were washed with PBS (0.1% triton) and incubated for 45 min at room temperature in dye-conjugated secondary antibody (1:200).

Images were taken using Leica TCS SPE Confocal Microscopy (Leica Microsystems) using 10X, 40X oil immersion, or 63X oil immersion, and analyzed using ImageJ software. c-Fos and pS6 positive cells were indicated by immunostaining whole-brain

slices and imaging using Olympus VS120 Virtual Slide Microscope (Olympus). Background was subtracted and a threshold value was set for each brain region, and images were binarized to obtain quantification of c-Fos and cells in each brain region.

2.7 ICV Studies

Intracerebroventricular (icv) cannula implantation was performed as previously described (Fujikawa et al., 2010). Briefly, mice were anesthetized with ketamine (75 mg/kg) and xylazine (5 mg/kg) diluted in saline (0.9% NaCl in water) and fixed on a stereotaxic apparatus (KOPF model 922) with ear-bars. After exposing the skull via a small incision, a small hole was drilled for a cannula implantation into the cerebral lateral ventricle (AP: -0.50 mm, ML: ±1.3 mm, DV: -2.3 mm), PVH (AP: -0.80 mm, ML: ±.020 mm, DV: -4.6 mm) or ARC (AP: -1.4 mm, ML: ±0.20 mm, DV: -5.8 mm). After 1 week recovery and acclimation, subsequent experiments were performed.

2.8 Insulin and Leptin ELISA

Tail vein blood was collected for ELISA assays as previously described (Fujikawa et al., 2010). Briefly, tail vein blood (20-50 µl) was collected in mice that were food restricted 2 hrs prior to blood collection procedure. Blood was collected using heparinized capillary tubes (Fisher Scientific, Cat#22-260-950).Blood was centrifuged at 3,000 x g for 20 min to collect serum blood and stored at -80°C. For insulin levels, Ultra-Sensitive Mouse Insulin ELISA Kit (Crystal Chem# 90080) was used. For leptin levels, Mouse Leptin ELISA Kit (Crystal Chem#90030) was used.

2.9Stereotaxic Injections/Optogentic Fiber implantation

2.9.1Surgery

Stereotaxic injections were performed as previously described (Kong et al., 2016). Mice were anesthetized with ketamine (75 mg/kg) and xylazine (5 mg/kg) diluted in saline

(0.9% NaCl in water) and fixed on a stereotaxic apparatus (KOPF model 922) with ear-bars. After exposing the skull via a small incision, a small hole was drilled for injection based on coordinates to bregma. A pulled-glass pipette with 20-40 μm tip diameter was inserted into the brain and AAV viruses (50-150 nl per injection site) were injected by a lab-built air-puff system. A micromanipulator (Grass Technologies, Model S48 Stimulator) was used to control injection speed at 25 nl/min and the pipette was left in position for another 5 min before being withdrawn to allow enough absorption and spreading of AAVs. For postoperative care, mice were injected intraperitoneally with meloxicam (0.5 mg/kg) for two continuous days. All stereotaxic injection sites were verified under electrophysiological microscopy (for electrophysiology-related studies) or by immunohistochemistry (for anatomy and *in vivo* studies). All 'missed' or 'partial-hit' animals were excluded from data analyses. Animals were allowed to recover from surgery for 1 week and their body weight and health conditions were closely monitored during recovery. Coordinates and injection volume used in the studies are: the ARC (AP: -1.40 mm, DV: -5.80 mm, LR: ±0.30 mm, 150 nl/side).

2.9.2 AAV Viral Injections

AAV8-hSyn-DIO-hM3Dq-mCherry and AAV5-EF1a-DIO-eNPHR3.0-EYFP were purchased from UNC Chapel Hill Vector Core. The following viruses were constructed for this paper and packaged at the Boston Children's Hospital Viral Core: AAV2/DJ-U6-gRNA(POMC)-DIO-mCherry, AAV2/8-EF1a-DIO-ciPOMC, AAV2/8-EF1a-DIO-ciPOMC ΔαMSH, AAV2/8-EF1a-DIO-ciPOMC Δβ-endorphin, AAV2/DJ-U6-gRNA(CART)-DIO-mCherry, and AAV2/8-EF1a-DIO-ciCARTpt. Virus preparation were injected unilaterally or bilaterally into the arcuate nucleus (AP: -1.40 mm, ML: ±0.25 mm, DV: -5.80 mm) of 6-8 week old mice. All virus preparation were injected at a volume of 150nL.

2.9.3 Optogenetic Fiber implantation

Separate craniotomies were made for optogenetic implantation. Mice were anesthetized with ketamine (75 mg/kg) and xylazine (5 mg/kg) diluted in saline (0.9% NaCl in water) and fixed on a stereotaxic apparatus (KOPF model 922) with ear-bars. After exposing the skull via a small incision, a small hole was drilled for optogenetic fiber implantation above the PVH (AP: -0.80 mm, ML: ±.00 mm, DV: -4.5 mm).Cannulas were secured to the skull using adhesive dental cement prepared with 5% gentamycin. The incision at either ends were closed using non-absorbable synthetic sutures. Mice were allowed to recover for a minimum of 1-2weeks before the initiation of experiments.

2.9.4 Excitatory DREADD

AAV_8-hSyn-DIO-hM3Dq-mCherry virus (Krashes et al., 2011) was bilaterally injected into the arcuate nucleus in 6 week old *POMC-Cre* and *POMC-Cre/*LSL-Cas9-eGFP mice. The mice were singly housed and allowed to recover from surgery for 1 week and their body weight and health was closely monitored during this recovery time. Following an additional week for viral incorporation and expression mice received either i.p. injections of CNO or saline control. A single saline or CNO i.p. injection (0.3mg/kg) was administered at the start of following studies: food intake, thermogenesis, and locomotion and glucose metabolism. All stereotaxic injection sites were verified by immunohistochemistry. Animals with 'missed' or 'partial-hit' were excluded from data analyses. Coordinates and injection volume used in the studies are: the ARC (AP: -1.40 mm, DV: -5.80 mm, LR: ±0.30 mm, 150 nl/side).

2.9.5 Synaptic Silencing Studies

Briefly, AAV_8-hSyn-DIO-hM3Dq-mCherry virus and AAV_5-EF1a-DIO-eNPHR3.0-EYFP were co-injected bilaterally into the arcuate nucleus of 6 week old *POMC-Cre* mice. Following 1 week of recovery time and an additional week for proper viral expression, mice were implanted with optogenetic fiber for the target region using the following

coordinates: PVH (AP: -0.80 mm, ML: ±.00 mm, DV: -4.5 mm). Following 1 week of recovery period from surgery, mice were given a single i.p injection of CNO (0.3mg/kg) or saline with or without optogenetic inhibition consisting of orange light (620nm). For *in vivo* experiments, the light source (Plexon, LED, 620nm, #40652-105) was connected to the implanted fiber with a fiber optic cable (Plexon, 200/230um fiber, #94059-100). LED Commutator (Plexon, #91397-003) was used as well to allow animals to move without twisting the fiber. The light was controlled by a manually programmable Waveform Generator (Rigol, #DG1022U). Light intensity was measured and calibrated by a Photodiode Power Sensor (Thorlabs). Mice were connected with fiber 30 mins before experiment to reduce the effects from stress. Orange light (max 10mW) was delivered continuously for 60 mins for the experiment. Blood glucose measuring tests were performed right before and right after the photo-inhibition. All stereotaxic injection sites were verified by immunohistochemistry. Animals with 'missed' or 'partial-hit' were excluded from data analyses. Coordinates and injection volume used in the studies are: the ARC (AP: -1.40 mm, DV: -5.80 mm, LR: ±0.30 mm, 150 nl/side).

2.9.6 Virus Production

Cre-dependent adeno-associated virus (AAV) viral vectors were constructed based on pAAV-pEF1α-FLEX-mCherry-WPRE-pA plasmid[38]. For the AAVs to deliver single-guide RNAs (sgRNAs) into the hypothalamus, sgRNAs were designed using online CRISPR tools (http://crispr.mit.edu/[39] and http://chopchop.cbu.uib.no/)[40]. The pU6-sgRNA-scaffold cassettes to express single sgRNAs, including those in AAV vectors AAV-U6-gRNA(POMC)-hSyn-DIO-mCherry and AAV-U6-gRNA(CARTpt)-hSyn-DIO-mCherry, were constructed using a lab-designed "Snap-Ligation" kit (Xu and Kong, unpublished), followed by cloning into the MluI site on *pAAV-pEF1α-FLEX-mCherry-WPRE-pA* plasmid. GeneArt CRISPR Nuclease Vector Kit (ThermoFisher Scientific) was used to

ligate U6-gRNA-tracrRNA region into AAV-hSyn-DIO-mCherry backbone.AAV-U6-gRNA(POMC)-hSyn-DIO-mCherry (serotype 2/DJ) viral construct, POMC gRNA (GATTCTGCTACAGTCGCTCA) was generated using crispr.mit.edu (ranked #3) in which exon 2 was targeted. AAV-U6-gRNA(CARTpt)-hSyn-DIO-mCherry (serotype 2/DJ) viral construct, *CARTpt* gRNA (GAGTAGATGTCCAGGGCTCG) was generated using crispr.mit.edu (ranked #3) in which exon 1 was targeted. For the AAVs to express CRISPR-immune (ci) cDNAs in cre-expressing neurons, including *AAV-pEF1α-FLEX-ciPOMC* and *AAV-FLEX-ciCART,* cDNAs were generated from the total RNAs extracted from the hypothalamus of *C57BL/6* mice by reverse transcription. The DNA fragments containing coding DNA sequences (CDS) of *POMC* and *CART* were amplified with the following pairs of PCR primers: ciPOMC Forward: 5'AATTGCTAGCGCC ACCATGCCGCGGTTTTGTTATTCGAGAAGCGGGGCCCTGTTGCTGGCCCTCCTGC TTCAGACCTC3'. ciPOMC Reverse: 5'AATTGGCGCGCCTCACTGGCCCTT CTTGTGCGC3'ciCART Forward: 5'TTATGCTAGCAGAACCATGGAGAGCTCCCGCC TGCGGCTGCTACCCCTCCTGGGCGCCGCCCTGCTGCTACTGCTACCTTTGCTGGG TGCCCGTGCCCAGGAGGACGCCGAGCTGCAGCCAAGGGCATTAGATATATATAGC GCCGTGGATGATGCGTCCCACG3'.ciCART Reverse: 5'GCATGGCGCGCCCCTTCA CAAGCACTTCAAGAGG3'. For the *AAV-pEF1α-FLEX- ciPOMC*$^{\Delta\alpha\text{-}MSH}$ and *AAV-FLEX-ciPOMC*$^{\Delta\beta\text{-}endorphin}$ virus to express both CRISPR-immune (ci) cDNAs and in cre-expressing neurons, cDNA were generated using plasmids which constructed previously to express *ciPOMC*. The DNA fragments of *ciPOMC*$^{\Delta\alpha\text{-}MSH}$ and *ciPOMC*$^{\Delta\beta\text{-}endorphin}$ were amplified with the following PCR primers:Δα-MSH Forward: 5'AAGTTCCATGGGTGTGGGCAAGAAACGGCGCCCGGTG3'. Δα-MSH Reverse: 5'AATTGGCGCGCCTCACTGGCCCTTCTTGTGCGC3'. Δβ-endorphin forward: 5'AATTGCTAGCGCCACCATGCCGCGGTTTTGTTATTCGAGAAGCGGGGCCCTGTT GCTGGCCCTCCTGCTTCAGACCTC3'. Δβ-endorphin Reverse: 5'AATTGGCGCG

CCTCAGCCACCGTAACGCTTGTCCTTGGGCGGGTTGC3'. Following Sanger DNA sequencing to verify the mutations, the obtained DNA fragments were ligated into the AscI and NheI restriction enzyme sites of *pAAV-pEF1α-FLEX-mCherry-WPRE-pA* plasmid. The above listed AAV vectors were packaged at the Boston Children's Hospital Viral Core. Viral aliquots were stored at -80 ºC before stereotaxic injection.

2.10 N2A gRNA validation method

Neuro2A (N2A) cells were cultured in Dulbecco's modified Eagle's Medium (DMEM) accompanied by glutamine, 10% fetal bovine serum, and 1% penicillin/streptomycin antibiotics and maintained at 37 degrees Celsius in 5% CO2. For indel detection assay, N2A cells were plated at 1:10 density in 6 well plates. The "Snap-ligation" PCR product was digested with MlU1-HF to isolate the u6-sgRNA-scaffold vector, and ligated into Cas9-egfp plasmid (addgene #44719).N2A cells were transfected with empty or a sgRNA-Cas9-eGFP plasmid was transfected using Lipofectamine 3000. Cells were harvested 48 hours later. Genomic DNA was digested by proteinase K and extracted by ethanol precipitation. Following purification, PCR amplification of a 400-600 bp genomic region containing the sgRNA target was conducted in both reference and test samples. 400 ng of the PCR product was hybridized to form heteroduplexes. Next, the hybridized products were treated with SURVEYOR nuclease and enhancer S (IDT transgenomic) for 60 minutes at 37 degrees, in accordance with the manufacturer's protocol. The final product was separated on an ethidium bromide 2% TAE Agarose gel. The DNA fragments of *POMC* and *CART* were amplified with the following PCR primers: POMC Forward: 5'TGGGCCAAGTGATATGGCAA3' POMC reverse: 5'ACATACCAG CAGGTTGCTCT3' (Product length= 552bp and Cut bands =360/192bp).CART Forward: 5'TTTCTGCGCTCTAGCCCATC3' CART reverse: 5'GCAAGGACCCTGTGGTAGTC3' (Product length= 547bp and Cut bands =344/203bp). The DNA fragments of POMC and

CART off-target were amplified with the following PCR primer: RGS12 Forward: 5' TCCTGCACATGGTGATTGCT' RGS12 reverse: 5' TGTCAGTGACCAGTTGCACA 3' (Product length= 591bp). TRPS1 Forward: 5' CCCCATCTGAAGGCACTTGT' TRPS1 reverse: 5' TCAAACCCTGGAGCCAACAG 3' (Product length= 527bp). CAND2 Forward: 5' AGACTTGGGTCAGCCTTGGA' CAND2 reverse: 5' GCCTTTTCAGCTTGGGACCTA 3'(Product length= 595bp). ETF1 Forward: 5' CCACAGTGGCCTTTAGAGACT' ETF1 reverse: 5' AAGGTTTATAGTTGTGAGCTA CCAT 3' (Product length= 456bp).

2.11 Statistical Analyses

Offline data analysis for electrophysiology was performed using custom scripts in Igor Pro 6 (Wavemetrics) and MATLAB (MathWorks). Statistical analyses were performed using GraphPad PRISM 6 software (GraphPad). Imaging data analyses were performed with ImageJ (NIH). All values were expressed as the mean ± SEM.

Table 2.1: Star Method

Reagent or Resource	Source	Identifier
Antibodies		
Rabbit Polyclonal anti-DsRed	Clontech	Cat#632496
Chicken Polyclonal anti-mCherry	EnCor Biotechnology	CPCA-mCherry
Chicken Polyclonal anti-eGFP	Aves Labs	GFP-1010
Rabbit Polyclonal anti-hrGFP	Agilent Technologies	Cat#240142
Rabbit Polyclonal anti-CART	Phoenix Pharmaceuticals	H-003-62
Rabbit Polyclonal anti-POMC	Phoenix Pharmaceuticals	H-029-30
Sheep Polyclonal anti-αMSH	EMD Millipore	AB5087
Rabbit Polyclonal anti-β-endorphin	Peninsula Laboratories	T-4044
Goat Polyclonal anti-cFos	Santa Cruz Biotechnology	sc-52-g
Chemicals, Peptides, and Recombinant Proteins		
CART (55-102)	Phoenix Pharmaceuticals	Cat#003-62
(-)-Bicuculline Methiodide	Enzo Life Sciences	Cat#89157-518
Clozapine-N-oxide	ApexBio	A3317
Streptozocin	Sigma-Aldrich	S01230;CAS:18883-66-4
2-Deoxy-D-glucose	Sigma-Aldrich	D6134;CAS:154-17-6
Humulin	Lilly	HI-210
Neuropeptide Y	GenScript	RP10492
Critical Commercial Assays		
Mouse Leptin ELISA Kit	Crystal Chem	Cat#90030
Ultra Senstitive Mouse Insulin ELISA Kit	Crystal Chem	Cat#90080
Experimental Models:Organisms/strains		
Mouse:NPY-hrGFP:B6.FVB-Tg(Npy-hrGFP)1Lowl/J	The Jackson Laboratory	6417
Mouse:POMC-hrGFP:FVB-Tg(Pomc1-hrGFP)1Lowl/J	The Jackson Laboratory	6421
Mouse:Pomc-Cre:Tg(Pomc1-cre)16Lowl/J	The Jackson Laboratory	5965
Mouse:Agrp-Ires-Cre:Agrptm1(cre)Lowl/J	The Jackson Laboratory	12899
Mouse:Rosa26-LSL-Cas9:B6;129-Gt(ROSA)26Sortm1(CAG-cas9*,-EGFP	The Jackson Laboratory	24857
Mouse:Ai9:B6.Cg-Gt(ROSA)26Sortm9(CAG-tdTomato)Hze/J	The Jackson Laboratory	7909
Recombinant DNA		
AAV8-hSyn-DIO-hM3Di-mCherry	UNC Chapel Hill Vector Core	NA
AAV5-EF1a-DIO-eNPHR3.0-EYFP	UNC Chapel Hill Vector Core	NA
AAV2/DJ-U6-gRNA(POMC)-DIO-mCherry	This paper(packaged by Ch	NA
AAV2/8-EF1a-DIO-ciPOMC	This paper(packaged by Ch	NA
AAV2/8-EF1a-DIO-ciPOMC ΔαMSH	This paper(packaged by Ch	NA
AAV2/8-EF1a-DIO-ciPOMC Δβ-endorphin	This paper(packaged by Ch	NA
AAV2/DJ-U6-gRNA(CART)-DIO-mCherry	This paper(packaged by Ch	NA
AAV2/8-EF1a-DIO-ciCARTpt	This paper(packaged by Ch	NA
AAV2/8-FLEX-CARTpt	This paper(packaged by Ch	NA
Sequence-Bases Reagents		
Agrp TaqMan probe	ThermoFisher Scientific	Mm00475829_g1
NPY TaqMan probe	ThermoFisher Scientific	Mm00445771_m1
Pomc TaqMan probe	ThermoFisher Scientific	Mm01323842_m1
Cartpt TaqMan probe	ThermoFisher Scientific	Mm04210469_m1
Ucp1 TaqMan probe	ThermoFisher Scientific	Mm01244861_m1
Pck1 TaqMan probe	ThermoFisher Scientific	Mm01247058_m1
G6pc TaqMan probe	ThermoFisher Scientific	Mm00839363
Mstn TaqMan probe	ThermoFisher Scientific	Mm01254559_m1
Software and Algorithm		
GraphPad Prism7.0	GraphPad	NA

Chapter 3: Results

3.1 Chemogenetic Stimulation of POMC Neurons Acutely Reduced Whole Body Glucose.

To examine the dynamic expression of POMC during development, we crossed *POMC*-Cre to a ROSA-eGFP reporter strain and observed expression in the ARC and other regions including dentate gyrus, periventricular nucleus, posterior hypothalamic nucleus and pituitary, consistent with prior findings (Figure 3.1A)(Padilla et al., 2012). Since *POMC* is transiently expressed in AgRP neurons in the ARC(Padilla et al., 2010), we assessed its ability to cause Cre-driven recombination. A triple cross between *POMC*-Cre, ROSA-tdTomato and NPY-GFP was performed to quantify the proportion of tdTomato labeled NPY containing neurons in the ARC (Figure 3.1B). It was determined that ~24% of tdTomato-positive neurons express neuropeptide Y (NPY), a neuropeptide that co-localizes exclusively with AgRP neurons within the ARC (Figure 3.1C). Due to the stabilization of *POMC* in adulthood, it has been suggested that the use of Cre-dependent viral constructs could dramatically reduce off-target recombination (Morrison and Munzberg, 2012; Padilla et al., 2012). Therefore, we unilaterally injected a Cre-dependent mCherry (mCh) labeled viral construct into *POMC*-Cre /NPY-hrGFP crossed mice allowing for the endogenous labeling of AgRP neurons with an enhanced green fluorescent reporter and Cre induced mCh expression in mature POMC neurons. We found no recombination events occurring in AgRP neurons and expression was restricted solely within the ARC (Figure 3.1D and 3.1E). Using an anti-POMC antibody to look for co-localization with virally infected neurons (Figure 3.1F), we determined the efficiency of this approach in targeting POMC neurons was ~98% (Figure 3.1G). This provides evidence that the viral approach in adult *POMC*-Cre mice yields neuronal and spatial specificity when inducing recombination events.

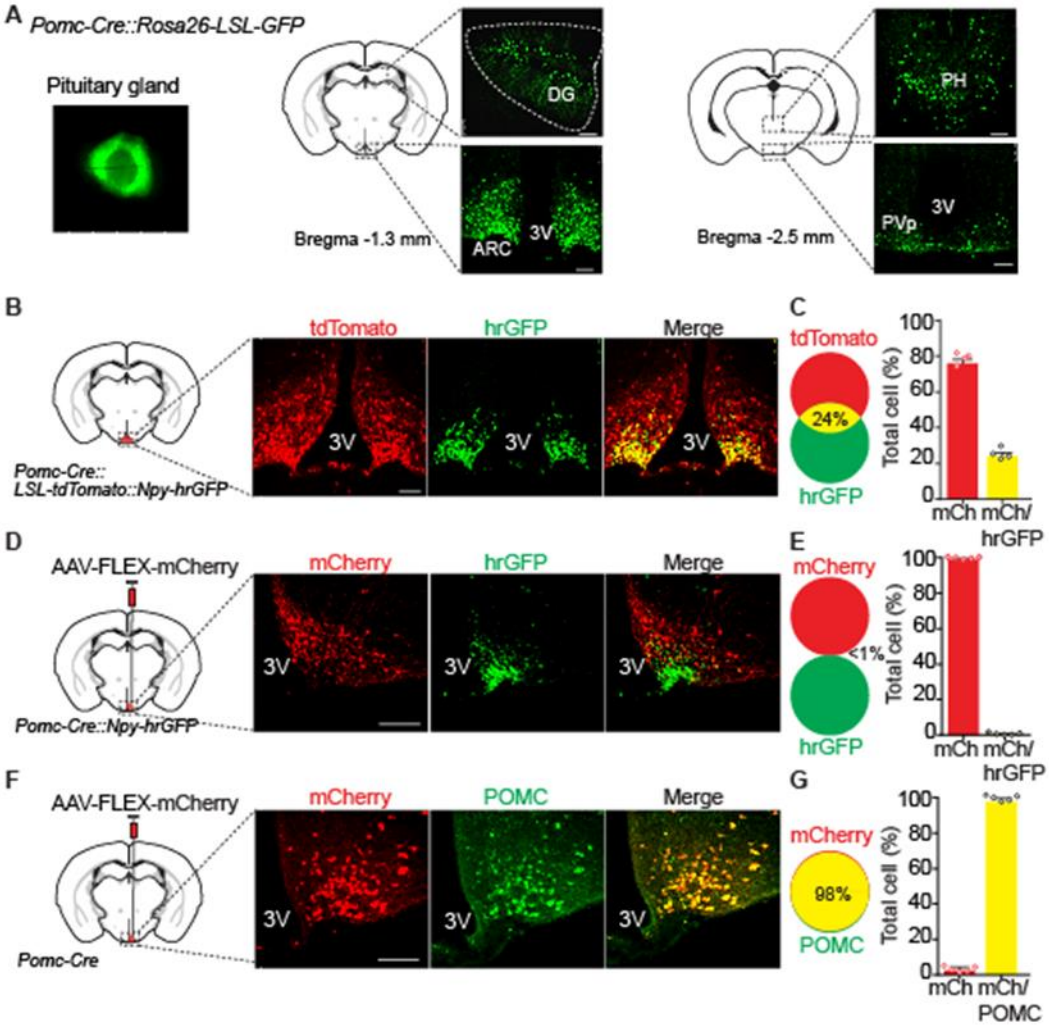

Figure 3.1: Validation of viral approach in adult *POMC*-Cre mice. (A) Schematic and confocal imaging of GFP in *POMC*-Cre mice crossed with Rosa26-LSL-eGFP reporter mice. (B and C) Schematic indicating site of confocal imaging, representative image and (C) quantification of tdtomato and hrGFP co-localization in *POMC*-Cre mice crossed with Npy-hrGFP and LSL-tdTomato reporter line (n=4). (D and E) Schematic indicating site of unilateral injection, representative image and (E) quantification of mCherry and hrGFP co-localization in *POMC*-Cre mice crossed with Npy-hrGFP mice (n=5). (F and G) Schematic indicating site of unilateral injection, representative image and (G) quantification of mCherry and POMC co-localization in *POMC*-Cre mice (n=5). Data are presented as mean ± SEM. *p< 0.05; **p< 0.01, and***p< 0.001 as determined by paired t-test. Scale bars size=100µm

Next, we sought to characterize the functionality of POMC neurons following acute stimulation. To accomplish this we utilized virally packaged excitatory Designer Receptors Exclusively Activated by Designer Drugs (DREADDs), designated hM3Dq (Alexander et al., 2009; Armbruster et al., 2007; Ferguson et al., 2011). Adult male

POMC-Cre mice received bilateral stereotactic injections of AAV8-hSyn-DIO-hM3D-mCherry (hM3D) virus into the ARC (Figure 3.2A). Co-immunostaining of c-Fos, a marker for neuronal activity, with mCh (Figure 3.2B) showed that clozapine N-oxide (CNO) significantly activates hM3Dq-expressing POMC neurons (Figure 3.2C). Consistent with prior findings, CNO administration did not alter acute light or dark cycle food intake (FI) compared to saline control (Figure 3.2D-3.2F) (Zhan et al., 2013). However, thermal imaging of treated mice (Figure 3.2G) indicated a significant increase in thermogenesis in both the interscapular and flank region following CNO injection (Figure 3.2H).In addition, video tracking (Figure 3.2I) showed a significant increase in locomotion following CNO administration (Figure 3.2J). Blood sampling from the tail tip was used to monitor fluctuations in peripheral blood glucose (BG) levels (Figure 3.2K). Notably, an acute reduction in BG was observed 1 hour post CNO injection followed by a sharp normalization to control levels (Figure 3.2L). Serum collected at the 1 hour time point did not indicate any changes in circulating insulin levels suggesting that the reduction in BG is independent of hormone secretion (Figure 3.2M). Thus, acute activation of ARC^{POMC} neurons modulates energy, locomotion and glucose homeostasis with no effect on FI.

To further investigate the effects of acute POMC neuronal activation on BG regulation, we performed a glucose tolerance test (GTT). When the mice were challenged with an injection of glucose, the mice treated with CNO initially showed a rapid decline in plasma glucose compared to saline injected control, indicating a short lived GT enhancement (Figure 3.2N). Using the insulin tolerance test (ITT) CNO treated *POMC*-Cre mice showed a significant reduction in BG at 1 hour compared to saline injection, indicating increased insulin sensitivity (IS) (Figure 3.2O). Given that the liver can use pryruvate to produce glucose through gluconeogenesis, using the pyruvate

tolerance test (PTT) we found that hepatic glucose production (HGP) was lower in CNO injected animals compared to saline control at the 1 hour time point (Figure 3.3A). Previous hyperinsulinemic-euglycmeic clamp experiments have shown that POMC neurons can alter liver function (Berglund et al., 2012). Therefore, we tested mRNA levels of both rate limiting enzymes responsible for gluconeogenesis in the liver, glucose 6-phosphatase (*G6pase*) and phosphoenolpyruvate carboxykinase (*PCK1*), and found both to be significantly reduced at the peak glucose reduction time point (Figure 3.3B and 3.3C). In addition, the expression of myostatin (*Mstn*), which has been shown to contribute to peripheral insulin resistance (Steculorum et al., 2016), was significantly reduced in brown adipose tissue (Figure 3.3D). This indicates that reduced gluconeogenesis in the liver and IS in BAT plays a key role in maintaining glucose homeostasis post POMC neuronal excitation.

3.2 Pathological Roles of ARC^{POMC} Neurons in T1D and T2D.

Since we found that POMC neurons contribute to BG regulation we went further and examined the peripheral changes in our diabetic mice models. We repeated our experiments on *POMC*-Cre mice that were fed a 60% HFD to induce T2D (Figure 3.3E) or injected with STZ to cause T1D (Figure 3.3I). Consistent with prior reports, we observed increases in body weight (BW) (Figure 3.3F) and BG (Figure 3.3G) in mice fed a HFD (Figure 3.3I H). In addition, STZ injected mice displayed key characteristics of T1D including increased basal BG (Figure 3.3 J), diminished circulating insulin levels (Figure 3.3 K), and micturition (Figure 3.3 L). Robust neuronal activity of POMC neurons in HFD treated mice produced a similar acute temporal change, but a dramatically larger magnitude of reduction in basal BG was observed (Figure 3.2P). In addition, CNO administration in our T2D model ameliorated GT (Figure 3.2Q) and IS (Figure 3.2R).

Finally, following administration of CNO in our T1D mice, we once again observed significant improvement in resting BG 1hr post CNO administration (Figure 3.2S). Therefore, acute excitation of hypothalamic POMC neurons temporarily improves whole body BG in our diabetic models to regular chow fed *POMC*-Cre mice levels.

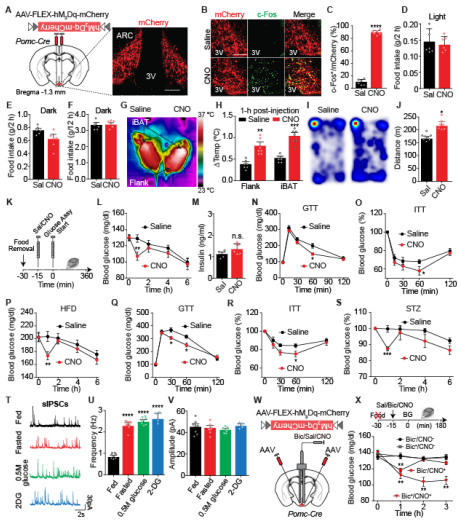

Figure 3.2: Chemogenetic stimulation of POMC neurons acutely reduced whole body glucose. (A) Schematic and expression of hM3D in POMC neurons. (B and C) c-Fos immunoreactivity and quantification in hM3Dq-expressing POMC neurons following saline or CNO administration (0.3mg/kg BW) mice (n=6). (D) 2hr food intake of hM3D *POMC*-Cre mice following saline or CNO injection during the light cycle (n=6). (E) 2hr food intake of hM3D *POMC*-Cre mice following saline or CNO injection during the dark cycle (n=6). (F) 12hr food intake of hM3D *POMC*-Cre mice following saline or CNO injection during the dark cycle (n=6).(G and H) Infrared thermography and quantification of interscapular (n=7) and flank region (n=7) 1 hr following injection of saline or CNO(I and J) 2hr heat map and quantification of distance traveled following saline or CNO injection during the light cycle (n=7-8).(K) Schematic of blood glucose monitoring protocol. (L, P and S) Blood glucose monitoring performed in (L) *POMC*-Cre^{hM3D} mice (n=8), (P) HFD treated *POMC*-Cre^{hM3D} mice (n=6), and (S) STZ treated *POMC*-Cre^{hM3D} mice following saline or CNO injection (n=6). (M) 1hr serum insulin levels following saline or CNO injection in *POMC*-Cre^{hM3D} mice (n=5-6). (N and Q) Glucose tolerance test (GTT) performed in (N) *POMC*-Cre^{hM3D} mice (n=6) and (Q) HFD treated *POMC*-Cre^{hM3D} mice following saline or CNO injection (n=8). (O and R) Insulin tolerance test (ITT) in (O) *POMC*-Cre^{hM3D} mice (n=7), (R) HFD treated *POMC*-Cre^{hM3D} mice following saline or CNO injection (n=8). (T, U and V) Representative traces of sIPSCs, and quantification of (U) frequency and (V) amplitude (n= 4-8 per group). (w) Schematic of cannula injection into *POMC-Cre^{hM3D}*. (S) Schematic of protocol and blood glucose monitoring of cannulated *POMC*-Cre^{hM3D} mice (n=6 per group).Data are presented as mean ± SEM. *p< 0.05; **p< 0.01, and***p< 0.001 as determined by unpaired t-test or paired t-test. Scale bars size=100µm.

3.3 ARC^{POMC} Neurons and Their Negative Feedback.

To confirm these findings, we used POMC-eGFP mice and performed whole cell patch clamp recordings on ARC^{POMC} neurons at varying states of glucose availability (Figure 3.3 M). Notably, reducing glucose levels *in vivo* by overnight fasting or *in vitro* by reducing external glucose levels to 0.5mM significantly increased sIPSC frequency in POMC neurons but neither amplitude nor sEPSC when compared to the control (Figure 3.2T-1V and 3.3N-3.3P). Inhibition of glucose metabolism by using a non-metabolizable glucose analog (2-deoxy-D-glucose) also increased sIPSC onto POMC neurons while amplitude and sEPSC remained unaltered (Figure 3.2T-1V and 3.3N-3.3P). Hence, these results suggest that glucose availability plays a key role in the inhibitory tones onto ARC^{POMC} neurons.

To determine if GABAergic mechanisms are responsible for the compensation of the observed glucose lowering effects of POMC neurons, we specifically administered a GABA receptor antagonist, bicuculline (BIC), through a bilateral cannula into the ARC to block any inhibitory input (Figure 3.2W). Cannulated *POMC*-Cre mice were pre-infected with excitatory DREADD virus for acute stimulation of POMC neurons (Figure 3.3Q). Validation of cannula position and ability to deliver agents selectively into the ARC was assessed through lesions and administration of trypan blue (Figure 3.3R). Serial dilutions of BIC were tested for its effects on both FI (Figure 3.3S) and basal BG (Figure 3.3T), and since no changes were observed we chose 0.05 µg of BIC as our working dose. Injection of 0.05 µg BIC or CNO behaved as previously observed; however, BIC in combination with CNO caused a prolonged BG reduction (Figure 3.2X). This persistent reduction in BG suggests that a GABAergic negative feedback loop is responsible for preventing hypoglycemia due to POMC neuronal excitation.

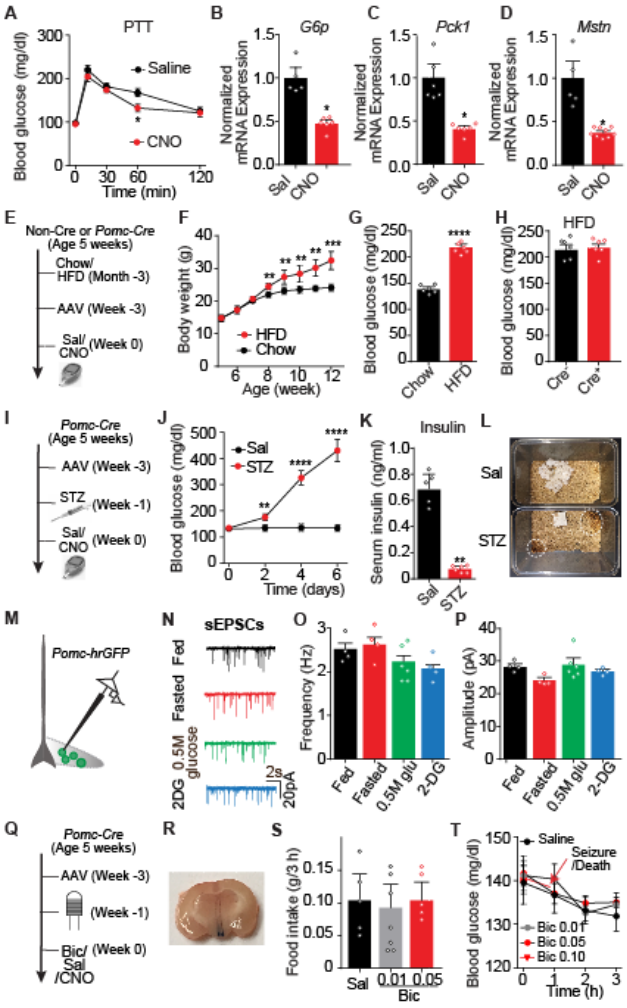

Figure 3.3: Acute effects of modulating POMC neuronal activity. (A) Pyruvate tolerance test (PTT) in hM3D *POMC*-Cre mice following saline or CNO injection (n=6). (B, C and D) Quantification of (B) *G6pase* (n=5-6) and (C) *Pck1* (n=6) mRNA expression in the liver and (D) *Mstn* (n=5-9) mRNA expression in the iBAT of *POMC*-Cre^{hM3D} mice 1hr following saline or CNO injection (n=8). (E) Schematic of experimental protocol. (F) Weekly body weight change following chow or HFD feeding (n=6). (G) Basal blood glucose following 12 weeks of chow or HFD feeding(n=6).(H) Basal blood glucose following 12 week HFD in hM3dq injected Cre^{-} or Cre^{+} litter mates (n=6). (I) Schematic of experimental protocol. (J) Daily blood glucose levels following saline or STZ injection(n=6). (K) Insulin levels 6 days following saline or STZ injection (n=5-6). (L) Representative image of micturition following saline or STZ injection. (M) Schematic of whole cell patch clamping. (N, O and P) Representative traces of (N) sEPSCs, and quantification of (O) frequency and (P) amplitude (n= 4-6 per group). (Q) Schematic of surgery timeline and blood glucose monitoring.(R) Representative image of cannula guided injection of trypan blue into the ARC.(S) Average total 3 hr food intake following saline or BIC injection at the start of the light cycle(n= 5-7).(T) Blood glucose levels following injection of saline or BIC(n= 6). Data are presented as mean ± SEM. *p< 0.05; **p< 0.01, and***p< 0.001 as determined by unpaired t-test or paired t-test. Scale bars size=100µm.

3.4 POMC Deletion Causes Impaired Energy Homeostasis.

To assess the physiological role of POMC and its encoded peptides, we utilized the novel CRISPR-CAS9 knock-in mice (Platt et al., 2014b) and specifically deleted POMC from the ARC of adults ($ARC^{\Delta POMC}$). This allows the Cre-driven endogenous expression of Cas9, which overcomes many of the issues associated with its delivery. Previously, it has been shown that viral specific guide RNA (sgRNA) is sufficient to cause targeted DNA double-strand breaks (DSBs), which results in indels and loss-of-function mutations (Hsu et al., 2014). In order to obtain neuronal specificity, we crossed *POMC*-Cre mice with the cre-dependent Rosa26 Cas9 knock in mice (LSL-Cas9). Validation of Cas9 expression was performed using IHC for the eGFP tag inserted into the Rosa 26 locus. With a viral gRNA targeting the 5' coding region of Exon 2 of POMC gene, a DSB in the coding region causes an insertion or deletion of one or more nucleotides, rendering all of POMC substrates inactive through alterations in the reading frame (Figure 3.5A). Hence, we packaged our gRNA into an adeno-associated virus (AAV) along with a Cre-recombinase-dependent mCh fluorescent tag to monitor expression (Figure 3.4A). When the AAV-sgRNA specific to the *POMC* locus ($sgRNA^{POMC}$) was stereotaxically injected bilaterally into the ARC of *POMC*-$Cre^{LSL\text{-}Cas9}$ mice, robust expression of mCh was observed solely in the ARC (Figure 3.4C). No expression was observed following injection into non-Cre litter mates (data not shown). Viral toxicity was assessed by quantification of eGFP positive neurons with or without viral infection; no change in neuronal cell count was observed (Figure 3.5B-3.5D). Only one off-target site was predicted in exon of *Rgs12 gene* by multiple online designer software's (Figure3.5E). To confirm that there was no effect on this gene, a construct consisting of both Cas9 and U6-$sgRNA^{POMC}$ was transfected into N2a mouse cell line to detect indels introduced by CRISPR/Cas9 genome editing (Figure 3.5F and 3.5G).

Indels were observed only on the on-target site of *POMC* locus, indicating efficient genome editing by sgRNA^{POMC} (Figure 3.5H).The concerns regarding the recombination event in AgRP neurons was addressed through injection of sgRNA^{POMC} into *AgRP-IRES-*Cre$^{LSL\text{-}Cas9}$ mice (Figure 3.5I). As reported there was no observable change in BW (Figure 3.5J), FI (Figure 3.5K) or basal blood glucose (Figure 3.5L) during the monitoring period, providing direct evidence that expression of sgRNA^{POMC} in ARC AgRP neurons, does not have any physiological effect on the system. To determine the efficiency of ARC$^{\Delta POMC}$, we stereotaxically injected sgRNA^{POMC} unilaterally into the ARC of *POMC-Cre*$^{LSL\text{-}Cas9}$ mice as an endogenous control. ARC$^{\Delta POMC}$ efficiency was observed by immunohistochemistry (IHC) against the POMC protein.POMC protein expression in CRISPRed mice was completely ablated compared to the endogenous control (Figure 3.4A and 3.4B). In addition, when POMC hypothalamic mRNA levels were quantified using qPCR, a significant reduction was observed compared to Cre negative litter mate controls with no effect on AgRP and NPY levels (Figure 3.4D). Thus, POMC is reliably and specifically depleted in the ARC of *POMC-Cre*$^{LSL\text{-}Cas9}$ mice.

Characterization of bilaterally injected ARC$^{\Delta POMC}$ mice showed induced obesity (Figure 3.4E and 3.5M) and increased body length (Figure 3.4F and 3.5N). Weekly measurements tracking BW gain showed a significant increase compared to non-Cre control only 1 week following injection of sgRNA^{POMC} (Figure 3.4G). This BW gain was found to be solely due to increased fat mass accumulation (Figure 3.4H and 3.5O). Initial characterization of ARC$^{\Delta POMC}$ mice revealed that they developed significant hyperphagia following injection of the sgRNA^{POMC} (Figure 3.4I), suggesting that alteration in consumption contributes to the BW gain.

Thermogenesis is a major factor in non-activity induced energy expenditure, using infrared thermography, we found that body temperature was severely reduced in

$ARC^{\Delta POMC}$ mice compared to non-Cre controls (Figure 3.4J). The average ambient temperature of the interscapular region of $ARC^{\Delta POMC}$ mice was markedly reduced at week 3 (Figure 3.5P and 3.5Q). This downward trend was observed in both the interscapular and the flank region by week 8 (Figure 3.4K) and continued until the end of the monitoring period. Expression of *Ucp1* mRNA, a BAT-specific uncoupling protein essential for non-shivering thermogenesis, was significantly lower in $ARC^{\Delta POMC}$ mice (Figure 3.4L). Further metabolic testing indicated oxygen metabolism of $ARC^{\Delta POMC}$ mice was consistently lower than non-Cre litter mate controls and the difference was still apparent when data was expressed based on the lean mass of each animal at both 3 (Figure 3.5R and 3.5S) and 8 weeks following viral injection (Figure 3.4M and 3.4N). Interestingly, analyses of locomotor activity showed dramatic reduction in spontaneous activity during the dark phase at 3 weeks post injection, before significant weight gain was observed (Figure 3.5T and 3.5U). This reduction in activity persisted until the end of monitoring at 8 weeks post injection of $sgRNA^{POMC}$ (Figure 3.4O AND 3.4P). These results indicate that ARC^{POMC} neurons regulate energy expenditure through a synergistic effect, which incorporates BAT thermogenic function, oxygen metabolism and spontaneous activity.

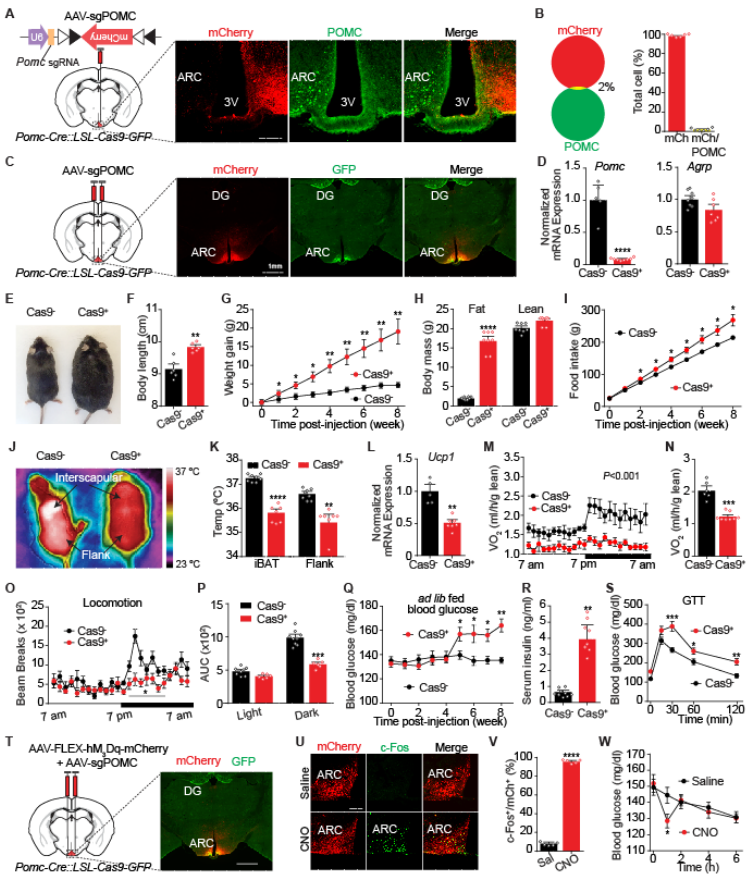

Figure 3.4: CRISPR/Cas9 Knockout of POMC in ARC causes hyperphagia and obesity but not hyperglycemia. (A and B) Schematic of unilateral injection, images and (B) quantification of co-localization. Scale bars size=100µm. (n=6). (C) Schematic of bilateral injection and images of co-localization of sgRNA^{POMC} and LSL-Cas9-eGFP. Scale bars size=1mm. (D) Quantification of *POMC* and *Agrp* mRNA expression in the ARC of sgRNA^{POMC} injected mice (n=5-8). (E) Image 8 weeks following sgRNA^{POMC} injection. (F). Average body length at 8 weeks (n=6). (G) Body weight change at 8 weeks (n=5-6). (H) Body Composition (n=8). (I) Total food intake curve (n=5-6). (J) Infrared thermography at 8 weeks. (K) Quantification of interscapular and flank temperature at 8 weeks (n=7-8). (L) Expression of *ucp1* mRNA in iBAT of sgRNA^{POMC} injected mice(n=5-7).(M and N) Distribution of oxygen uptake (VO2) over a 24-hr period and (N) average daily VO2 (n=6-8). (Q and P) Locomotor activity over 24-hrs and (P) total activity during the light and dark phase (n=6-9). (Q) Weekly blood glucose levels in sgRNA^{POMC} injected Non-Cre and *POMC*-Cre /LSL-Cas9 mice(n=5-6).(R) Insulin levels at the end of the study (n=8-9). (S) GTT performed at 8 weeks following viral injection. (n=8). (T) Schematic and expression of hM3D with sgRNA^{POMC} and colocalization of sgRNA^{POMC} and LSL-Cas9-eGFP. Scale bars size=1mm. (U and V) Immunoreactivity and quantification of c-Fos following saline or CNO administration (0.3mg/kg BW) mice (n=5). (W) Blood glucose monitoring following saline or CNO injection (n=6). Data are presented as mean ± SEM. *p< 0.05; **p< 0.01, and***p< 0.001 as determined by unpaired t-test or paired t-test.

Surprisingly, there was no observed change in basal BG levels 4 weeks post injection. However following this latent period, basal BG levels rose dramatically starting at 5 weeks post injection (Figure 3.4Q). Quantification of serum insulin at the end of the monitoring periods revealed significantly higher levels in $ARC^{\Delta POMC}$ mice (Figure 3.4R), indicating the development of insulin resistance. Even when challenged with a bolus injection of glucose, no observable difference was detected between the control and the $ARC^{\Delta POMC}$ mice at 3 weeks post viral injection (Figure 3.5V). Following 3 additional weeks of monitoring, the mice were once again subjected to a GTT, and remarkably the $ARC^{\Delta POMC}$ mice exhibited severe GT impairment (Figure 3.4S). Taken together these results indicate that hyperglycemia is a secondary effect caused by the compounding stresses of obesity.

To determine if the observed acute reduction in whole body glucose remains unaltered after rapid perturbation of POMC neurons, hM3D virus was bilaterally injected into $ARC^{\Delta POMC}$ mice (Figure 3.4T). Consistent with our previous findings, intraperitoneal injection of CNO induces rapid neuronal activation visualized through c-Fos staining (Figure 3.4U). Quantification of c-Fos positive cells revealed almost identical activation efficiency as observed in our initial characterization of the functionality of POMC neurons (Figure 3.4V). Importantly, following CNO injection, an acute reduction in basal BG was observed in 3 week $sgRNA^{POMC}$ injected mice (Figure 3.4W). This suggests that POMC or its precursor polypeptides are not primarily responsible for maintaining whole body glucose but is necessary for maintaining energy homeostasis.

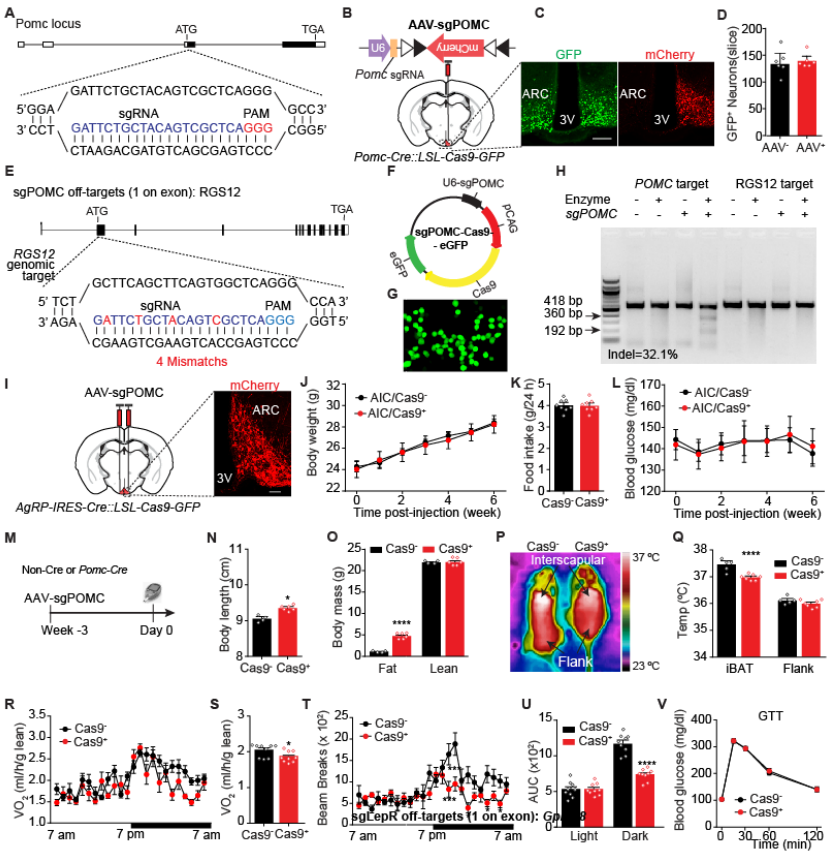

Figure 3.5: Early effects of POMC deletion in the ARC. (A) Schematic of sgRNA design and targeting of *POMC* locus. (B and C) Schematic of AAV vector for sgRNA^{POMC} expression and site of unilateral injection, (C) representative image of mCherry and eGFP co-localization in *POMC*-Cre mice crossed with LSL-Cas9-eGFP mice. (D) Quantification of average eGFP expressing neurons in non-virally and virally injected sides of the ARC (n=6). (E) Schematic of sgPOMC off-target locus.(F) Plasmid construct for in-vitro indel testing. (G) N2a cells transfected with U6-sgPOMC plasmid. (H) Gel image indicating indels in *POMC* locus but not in off-target sites. (I) Schematic indicating site of unilateral injection and representative image of mCherry expression in the ARC. (J) Weekly body weight change following viral injection (n=8). (K) Average total food intake 6 weeks following viral injection (n=8). (L) Weekly blood glucose measurements following surgery (n=8). (M) Schematic of experimental protocol.(N) Average body length 3 weeks following AAV-sgRNA^{POMC} injection (n= 4-6). (O) Body composition 3 weeks following AAV-sgRNA^{POMC} injection (n= 4-6). (P) Infrared thermography 3 weeks following AAV-sgRNA^{POMC} injection. (Q) Quantification of subcutaneous temperatures in the interscapular and flank region at 3 weeks following viral injection(n= 5-7). (R and S) Distribution of oxygen uptake (VO2) over a 24-hr period and (S) average daily VO2 between Non-Cre and *POMC*-Cre /LSL-Cas9 mice 3 weeks post-viral injection (n=9). (T and U) Locomotor activity over 24-hrs and (U) total activity during the light and dark phase following viral injection between Non-Cre and *POMC*-Cre /LSL-Cas9 mice (n=9). (V) GTT performed at 3 weeks following viral injection in Non-Cre and *POMC*-Cre /LSL-Cas9 mice n=8. Data are presented as mean ± SEM. *p< 0.05; **p< 0.01, and***p< 0.001 as determined by unpaired t-test). Scale bars size=100µm.

3.5 Expression of ciPOMC Prevents Metabolic Dysregulation

To validate that the observed metabolic dysregulation was indeed a product of $ARC^{\Delta POMC}$ and not due to off target effects, we generated a Cre-enabled AAV virus modified from a widely used AAV-Flex-ChR2 template (Atasoy et al., 2008), expressing a Cas9 immune POMC cDNA sequence (ciPOMC) (Figure 3.7A). This sequence allows for the unhindered re-expression of POMC by altering the Cas9 binding site in the cDNA sequence without affecting the amino acid sequence. We packaged our ciPOMC cDNA sequence into a Cre-recombinase-dependent AAV without a fluorescent tag to prevent any interference with post-translational modifications. The virus was then bilaterally injected into the ARC of *POMC-Cre*$^{LSL\text{-}Cas9}$ and non-Cre littermate controls. Since viral depletion of POMC occurs acutely, we designed our experiment to allow sufficient time for ciPOMC transcription and translation (Figure 3.7B). Additionally, *POMC-Cre*$^{LSL\text{-}Cas9}$ mice received either an injection of $sgRNA^{POMC}$ or ciPOMC as positive or negative controls, respectively. Unilateral injection of ciPOMC and $sgRNA^{POMC}$ indicated no reduction in protein expression following staining (Figure 3.6A and 3.6B). As shown in figure 3.6C, targeting of $sgRNA^{POMC}$ in the ARC was validated through mCh expression bilaterally in the ARC. POMC transcription showed significant elevation in *POMC-Cre*$^{LSL\text{-}Cas9}$ mice either injected with ciPOMC alone or in addition with $sgRNA^{POMC}$ (Figure 3.6D), while Agrp levels remained unchanged in all groups (Figure 3.6E). Analyses of body length (Figure 3.6F), BW (Figure 3.6G), body composition (Figure 3.7C and 3.7D), and FI (Figure 3.6H) indicated that expression of ciPOMC completely attenuated the effects of $ARC^{\Delta POMC}$. The expression of ciPOMC also prevented the dysregulation of body temperatures in the interscapular (Figure 3.6I) and flank regions (Figure 3.6J) of the $sgRNA^{POMC}$ treated mice (Figure 3.7E). In addition, metabolic and locomotor testing was performed on all groups (Figure 3.7F and 3.6K). Quantification of average oxygen

consumption and spontaneous activity indicated no significant difference in CRISPRed mice expressing ciPOMC (Figure 3.7G, 3.6L and 3.6M). Following weekly BG monitoring, hyperglycemia was no longer observed when ciPOMC was expressed (Figure 3.6N). Finally, GTT performed at the end of the monitoring period did not indicate any differences in POMC restored mice compared to cas9 deficient control (Figure 3.7H). Together, the results from the ARC$^{\Delta POMC}$ and the expression of ciPOMC prove that ARC^{POMC} is responsible for metabolic regulation while secondarily modulating BG.

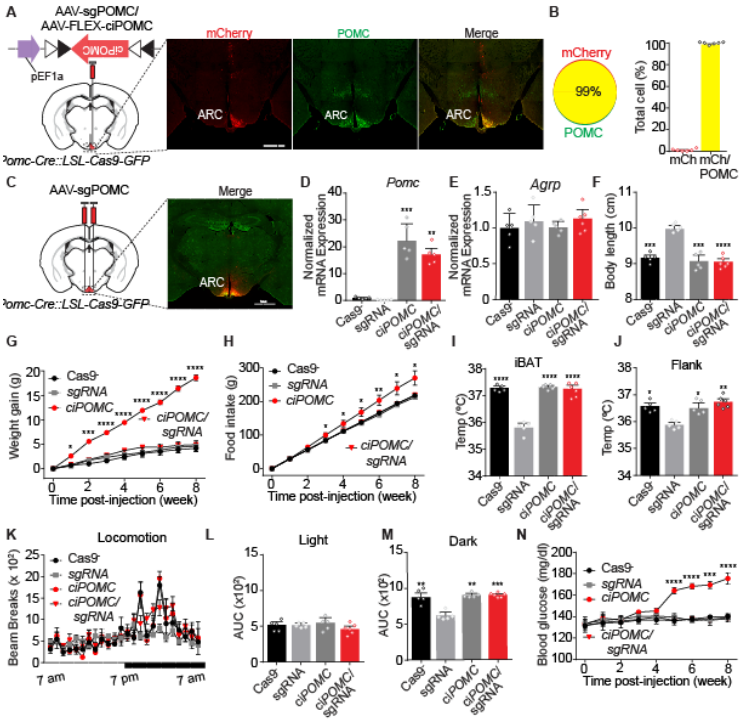

Figure 3.6: Expression of ciPOMC Prevents Metabolic Dysregulation. (A and B)Schematic of unilateral injection, images and (B) quantification of co-localization (n=6). C) Schematic of bilateral injection and image of co-localization. (D and E) Quantification of (D) *POMC* and (E) *Agrp* mRNA expression in the ARC of sgRNA^{POMC} and/or ciPOMC injected mice (n=4-6). (F) Quantification of average body length 8 weeks following viral injection (n=5-6). (G) The change in body weight following sgRNA^{POMC} and/or ciPOMC injection (n=5-6). (H) Total food intake curve after sgRNA^{POMC} and/or ciPOMC injection (n=5-6). (I and J) Quantification of subcutaneous temperatures in the (I) interscapular and (J) flank region at 8 weeks following viral injection (n=5-6). (K, L and M) Locomotor activity over (K) 24-hrs and total activity during the (L) light and (M) dark phase following viral injection (n=5-6). (N) Weekly blood glucose levels (n=5-6). Data are presented as mean ± SEM. *p< 0.05; **p< 0.01, and***p< 0.001 as determined by unpaired t-test or one-way ANOVA (Tukey's multiple comparison test). Scale bars size=1mm.

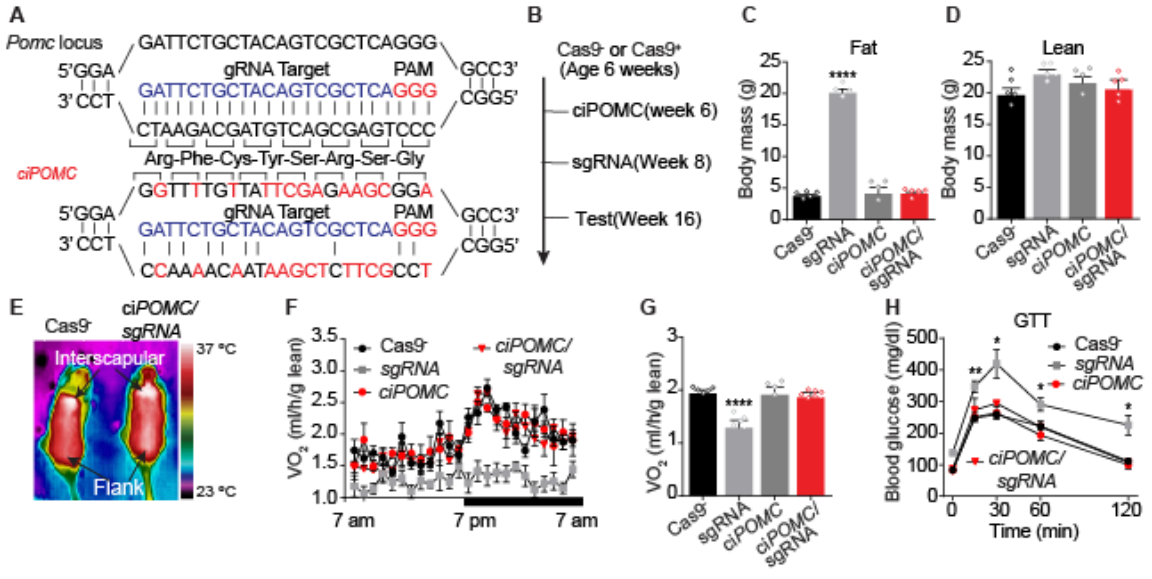

Figure 3.7 Preventing POMC deletion attenuates metabolic impairment. (A) Schematic of Cas9 immune POMC (ciPOMC) design and strategy. (B) Timeline of viral injections.(C and D) Average (C) fat and (D) lean mass accumulation 8 weeks following viral injection n=4-5. (E) Infrared thermography 8 weeks following viral injection. (F and G) Distribution of oxygen uptake (VO2) over a 24-hr period and (G) average daily VO2 8 weeks post-viral injection (n=4-6). (H) GTT performed at 8 weeks following viral injection n=4-6. Data are presented as mean ± SEM. *p< 0.05; **p< 0.01, and***p< 0.001 as determined by unpaired t-test).

Taking advantage of the ability to not only ablate POMC from ARC^{POMC} neurons but also attenuate all the energy dysregulations using ciPOMC expression, we took on the challenge of dissecting the role of certain biologically active fragments derived from POMC. Both α-MSH (Huszar et al., 1997; Meister, 2007) and β-endorphin (Koob, 1992; Veening and Barendregt, 2015) have been implicated in the regulation of whole body homeostasis. However, direct evidence is lacking. Thus, we designed and constructed a Cas9 immune POMC cDNA sequence which was devoid of the sequence coding either for α-MSH (ciPOMC$^{\Delta\alpha\text{-MSH}}$) (Figure 3.8A) or β-endorphin (ciPOMC$^{\Delta\beta\text{-endorphin}}$) (Figure 3.8B). Constructs were packaged in AAVs as described previously. To validate proper expression and posttranslational modification, we performed unilateral injection of

sgRNA^{POMC} with either ciPOMC$^{\Delta\alpha\text{-MSH}}$ (Figure 3.8C) or ciPOMC$^{\Delta\beta\text{-endorphin}}$ (Figure 3.8H) and stained for the corresponding neurotransmitters. Co-localization between the mCH tagged sgRNA^{POMC} and either α-MSH or β-endorphin revealed that when co-injected with ciPOMC$^{\Delta\alpha\text{-MSH}}$, α-MSH was significantly ablated from the virally injected side (Figure 3.8D and 3.8E) while β-endorphin remained consistent (Figure 3.8F and 3.8G). Similarly when ciPOMC$^{\Delta\beta\text{-endorphin}}$ was injected with sgRNA^{POMC}, β-endorphin was almost completely absent from the injection site (Figure 3.8I and 3.8J), while no observable difference in α-MSH expression could be ascertained (Figure 3.8K and 3.8L). Weekly BW measurements showed significant elevation for mice co-injected with ciPOMC$^{\Delta\alpha\text{-MSH}}$ or ciPOMC$^{\Delta\beta\text{-endorphin}}$ when compared with non-Cre control. However, the weight gain was not to the extent of sgRNA^{POMC} injection alone (Figure 3.8M). This was corroborated by the increase in fat mass accumulation at the end of the study (Figure 3.8N). Interestingly, only ARC$^{\Delta\alpha\text{-MSH}}$ mice showed an increasing trend of FI, but this was not significantly different from that of ARC$^{\Delta\text{POMC}}$ mice (Figure 3.8O). Infrared thermography of ARC$^{\Delta\alpha\text{-MSH}}$ (Figure 3.8P) and ARC$^{\Delta\beta\text{-endorphin}}$ (Figure 3.8Q) mice showed a stark contrast in thermoregulation. The average temperature of the interscapular region of ARC$^{\Delta\alpha\text{-MSH}}$ mice was reduced, indicating that heat production was suppressed (Figure 3.8R). This contrast was also observed in locomotor activity (Figure 3.8S); the only reduction in dark cycle activity was observed in ARC$^{\Delta\beta\text{-endorphin}}$ and ARC$^{\Delta\text{POMC}}$ mice (Figure 3.8T). Ablation of α-MSH or β-endorphin from the ARC had no effect on BG within the first four weeks, consistent with ARC$^{\Delta\text{POMC}}$ mice (Figure 3.8U). Thus, two biologically active fragments derived from POMC has distinct roles in regulating energy expenditure: α-MSH in thermoregulation and β-endorphin in locomotor activity.

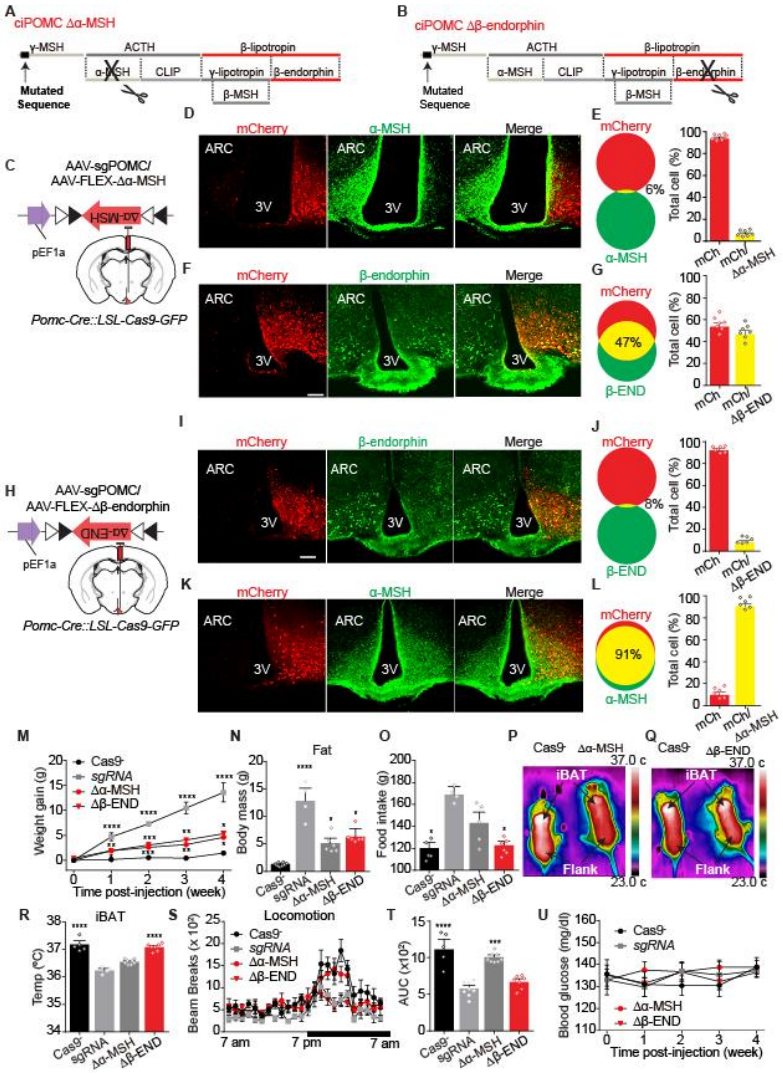

Figure 3.8: Deletion of α-MSH or β-endorphin in ARC^{POMC} neurons. (A and B) Comparative schematic of ciPOMC$^{\Delta\alpha\text{-MSH}}$ and ciPOMC$^{\Delta\beta\text{-endorphin}}$ design. (C) Schematic of unilateral injection. (D and E) Representative images and (E) quantification of sgRNA^{POMC} co-localization with α-MSH (n=7). (F and G) Representative images and (G) quantification of sgRNA^{POMC} co-localization with β-endorphin (n=7). (H) Schematic of unilateral injection. (I and J) Representative images and (J) quantification of sgRNA^{POMC} co-localization with α-MSH (n=6). (K and L) Representative images and (L) quantification of sgRNA^{POMC} co-localization with β-endorphin (n=6). (M) Body weight change (n=4-8 mice per group). (N) Fat mass at 4 weeks (n=4-8 per group). (O) Total food intake curve following viral injection (n=4-6 mice per group).(P and Q) Infrared thermography 4 weeks following viral injection. (R) Interscapular temperature 4 weeks following viral injection(n=4-8 per group.(S and T) Locomotor activity over 24-hrs and (T) total activity during the dark phase following viral injection (n=5-8 mice per group). (U) Weekly blood glucose levels (n=4-8 mice per group). Data are presented as mean ± SEM. *p< 0.05; **p< 0.01, and***p< 0.001 as determined by unpaired t-test or one-way ANOVA (Tukey's multiple comparison test). Scale bars size=100μm.

3.6 Central Administration of CART Acutely Reduces Blood Glucose and Improves Glucose Tolerance.

We were surprised to find that neither POMC nor its active fragments played a direct role in BG regulation. We reassessed the known neurotransmitters released by ARC^{POMC} neurons to determine a potential candidate. The only common neuropeptide to the majority of POMC neurons in the ARC is CART (Elias et al., 1998; Elias et al., 2001; Vrang et al., 1999). However, the function of CART in ARC^{POMC} is still unclear. We centrally administered CART to test the direct physiological role of CART on glucose homeostasis. We surgically implanted a cannula into the lateral ventricle of 8 week old C57BL/6J mice (Figure 3.9A). To validate proper cannulation, NPY, a strong orexigenic neuropeptide, was injected to stimulate FI during the light cycle to determine positive responders (Figure 3.10A and 3.10C). Following injection, lesions were assessed to determine accurate targeting of the cannula (Figure 3.10B). Once experimentally viable mice were selected, intracerebroventricular (ICV) injection of 0.2 µg CART (55-102) were performed. As shown, CART administration caused no change in FI compared to saline injection at the start of the light cycle (Figure 3.9B). However, a short term reduction in basal BG was observed (Figure 3.9C). Remarkably, the trend and magnitude almost identically matched DREADD stimulated neuronal activation of POMC neurons. After further testing, this similarity persisted as GT (Figure 3.9D) and insulin resistance (Figure 3.9E) improved following CART administration. Collectively, this suggests that CART may be the glucose lowering neurotransmitter released from ARC^{POMC} neurons.

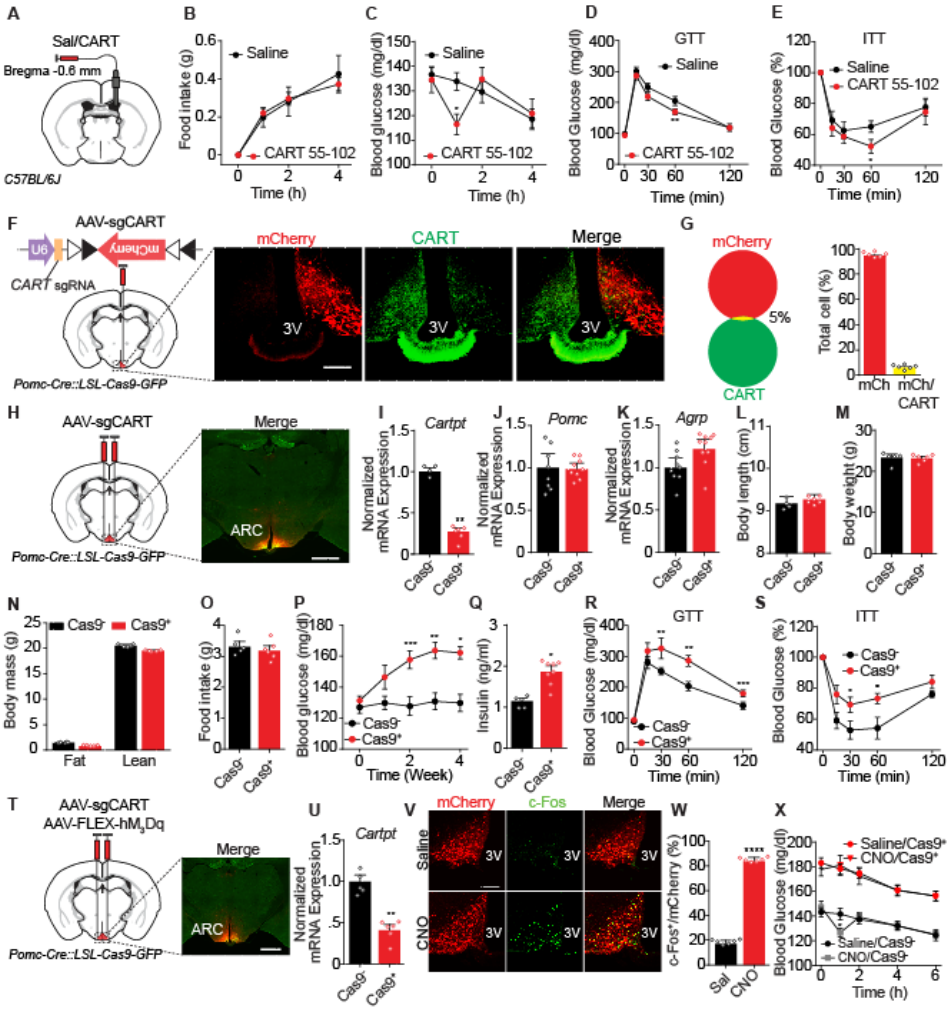

Figure 3.9: The role of CART in glucose and energy homeostasis. (A) Schematic of injection into C57BL/6J mice.(B) 4hr food intake following saline or CART administration (n=7).(C) Blood glucose monitoring following saline or CART injection(n=9). (D and E) GTT and ITT following saline or CART injection (n=9). (F and G) Schematic of unilateral injection, images and (G) quantification of sgRNA^{CARTpt} and CART(n=6). Scale bars size=100µm.(H) Schematic of injection and co-localization of sgRNA^{CARTpt} and LSL-Cas9-eGFP. Scale bars size=1mm. (I, J and K) Expression of (I) *CARTpt,* (J) *POMC, and* (K) *Agrp* mRNA in sgRNA^{CARTpt} injected mice (n=4-10). (L) Average body length at 8 weeks (n=4-6). (M) Average body weight of sgRNA^{CARTpt} injected mice (n=5-6). (N) Body Composition (n=5). (O) Average daily food intake 4 weeks following injection (n=5-6). (P) Weekly blood glucose levels (n=6). (Q) Insulin levels at 4 weeks (n=5-8). (R and S) GTT and ITT 4 weeks following injection of sgRNA^{CARTpt} (n=5or6) (T) Schematic of injection with hM3D+sgRNA^{CARTpt} and image of sgRNA^{CARTpt} and LSL-Cas9-eGFP co-localization. Scale bars size=100µm. (U) Expression of *CARTpt* mRNA in hM3D and sgRNA^{CARTpt} injected mice (n=5-6). (V and W) Immunoreactivity and quantification of c-Fos following saline or CNO administration (0.3mg/kg BW) mice (n=6). Scale bars size=100µm. (X) Blood glucose monitoring following saline or CNO injection (n=8). Data are presented as mean ± SEM. *p< 0.05; **p< 0.01, and***p< 0.001 as determined by unpaired t-test or paired t-test.

3.7 CART Deletion Impairs Glucose Homeostasis But Not Energy Balance.

Neuronal specificity is necessary to delineate the role of CART in the ARC similar to the ARC$^{\Delta POMC}$ approach, we designed a sgRNA targeting the 3' coding region of Exon 1 of *CART* (Figure 3.10D). Using the previously described online software three off target sites were predicted in exons (Figure 3.10E-3.10G). Similarly, a construct containing Cas9 and U6-sgRNA^{CARTpt} was assembled and transfected in N2A mouse cell line. Of note, no off-target indels were detected within *Trps1, Cand2* and *Etf1* locus (Figure 3.10H). Next, we packaged our sgRNA into an adeno-associated virus (AAV) along with a Cre-recombinase-dependent mCh fluorescent tag (Figure 3.9F). When the AAV-sgRNA(CART)-DIO-mCherry (sgRNA^{CARTpt}) was stereotaxically injected bilaterally into the ARC of *POMC*-Cre /LSL-Cas9 mice, robust expression of mCh was observed only in the ARC (Figure 3.9H). To confirm the effects of the ARC$^{\Delta CARTpt}$ virus, we sterotaxically injected sgRNA^{CARTpt} unilaterally into the ARC of *POMC-Cre*$^{LSL-Cas9}$ mice in order to obtain an endogenous control. ARC$^{\Delta CARTpt}$ efficiency was assessed by IHC staining for CART protein. As shown in figure 3.9F and 3.9G, CART protein expression was dramatically reduced compared to the endogenous control. CART positive fibers were also reduced in the paraventricular nucleus (PVH), a known POMC neuronal projection site (Figure 3.10I and 3.10J). Non-specific CART deletion was not observed in the LH of MCH neurons, attesting to the specificity of the Cas9 expression and gRNA targeting (Figure 3.10K). *CARTpt* mRNA levels were significant reduced in sgRNA^{CARTpt} treated vs non-Cre litter mate controls (Figure 3.9I), *Agrp/POMC* levels remained unchanged (Figure 3.9J and 3.9K). No observable changes in body length (Figure 3.9L), BW (Figure 3.9M), body composition (Figure 3.9N), or FI were detected following viral injection (Figure 3.9O). Detailed characterization of energy homeostasis showed no change in thermal regulation (Figure 3.10L-3.10N), oxygen consumption (Figure 3.10O

and 3.10P) or locomotion (Figure 3.10Q and 3.10R). This indicated that CART in ARC^{POMC} neurons is not required to maintain energy balance. However, weekly BG monitoring revealed an increase in basal BG levels starting almost immediately after $sgRNA^{CARTpt}$ injection and become significantly greater than non-Cre litter mates 2 weeks post-injection (Figure 3.9P). Elevated levels of circulating insulin were also observed in serum samples from these mice (Figure 3.9Q). Further physiological testing revealed impaired GT (Figure 3.9R), IS (Figure 3.9S), and gluconeogenesis (Figure 3.10S). Of interest, mRNA levels of both *G6pase* and *PCK1* were significantly elevated in the livers of $ARC^{\Delta CARTpt}$ mice (Figure 3.10T and 3.10U). *Mstn* mRNA levels in BAT were consistently higher in $ARC^{\Delta CARTpt}$ mice as well (Figure 3.10V). Therefore, CART in ARC^{POMC} neurons is required to maintain BG levels by modulating IS and HGP.

To assess if the acute glucose lowering effect of POMC neuronal stimulation was still intact following $ARC^{\Delta CARTpt}$, we injected $sgRNA^{CARTpt}$ into $POMC\text{-}Cre^{LSL\text{-}Cas9}$ mice pre-infected with hm3D virus; localized and robust expression of mCh was observed specifically in the ARC (Figure 3.9T). CART mRNA expression was significantly reduced in $ARC^{\Delta CARTpt}$ mice (Figure 3.9U). Following CNO injection, consistent neuronal activation was observed in POMC neurons (Figure 3.9V). Quantification of c-Fos positive cells did not reveal any irregularities in activation efficiency (Figure 3.9W). Consistent with our prior findings, total daily FI (Figure 3.10W) or dark cycle (Figure 3.10X and 3.10Y) were not altered following CNO or saline injection. However, the acute hypoglycemic effects caused by POMC activation were completely ablated in $ARC^{\Delta CARTpt}$ mice (Figure 3.9X). This further supports that CART is the main glucose lowering neuropeptide found within POMC neurons.

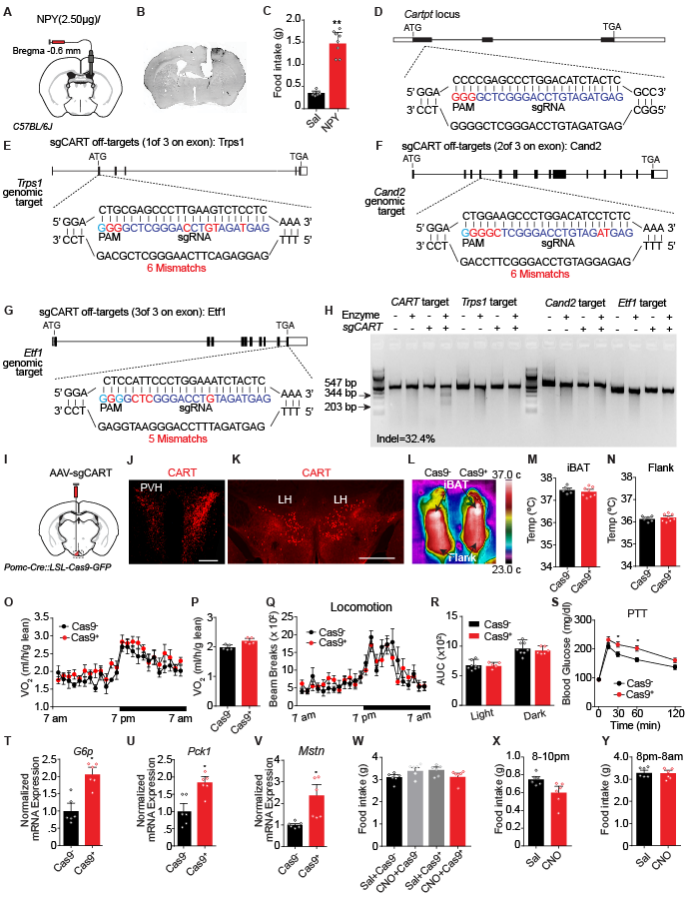

Figure 3.10: Validation of sgCART (A)Schematic of cannula injection. (B) Representative coronal section of mice brain showing typical lesion produced by cannula.(C) Total 2 hr food intake following saline or NPY injection (n=7-8). (D) Schematic of sgRNA design and targeting of *CARTpt* locus. (E, F and G) Schematic of sgCART off-target locus. (H) Gel image indicating indels in *Cartpt* locus but not in off-target sites. (I, J and K) Schematic indicating site of (I) unilateral injection, representative image of (J) CART positive fibers in the PVH and (K) CART expressing neurons in the LH. Scale bars size=100µm for PVH and 1mm for LH. (L) Infrared thermography 4 weeks following sgRNA^{CARTpt} injection.(M and N) Quantification of the (M) interscapular and (N) flank temperature at 4 weeks following viral injection(n=6-8). (O and P) Distribution of oxygen uptake (VO2) over a 24-hr period and (P) average daily VO2 between Non-Cre and *POMC*-Cre /LSL-Cas9 mice 4 weeks post-viral injection(n=5). (Q and R) Locomotor activity over 24-hrs and (R) total activity during the light and dark phase following 4 weeks viral injection between Non-Cre and *POMC*-Cre /LSL-Cas9 mice (n=6-8). (S) Pyruvate tolerance test (PTT) 4 weeks following viral injection (n=6-8).(T, U and V) Quantification of (T) *G6pase* (n=6) and (U) *Pck1* (n=6) mRNA expression in the liver and (V) *Mstn* (n=6) mRNA expression in the iBAT 4 weeks following viral injection(n=6-8). (W) Average total food intake following saline or CNO injection (n=6). (X) 2hr food intake following saline or CNO injection during the dark cycle (n=6). (Y) 12hr food intake following saline or CNO injection during the dark cycle (n=6). Data are presented as mean ± SEM. *p< 0.05; **p< 0.01, and***p< 0.001 as determined by unpaired t-test or one-way ANOVA (Tukey's multiple comparison test).

3.8 Expression of ciCART Prevents Hyperglycemia

We validated the observed hyperglycemia by generating a Cre-recombinase-dependent AAV packaged with a Cas9 immune *Cartpt* cDNA sequence (ciCARTpt) (Figure 3.11A) and staggered our viral injections. The virus was then bilaterally injected into the ARC of *POMC-Cre*$^{LSL\text{-}Cas9}$ and non-Cre littermate controls. In addition, a separate set of *POMC-Cre*$^{LSL\text{-}Cas9}$ mice received only a bilateral injection of sgRNA^{CARTpt} as a positive control. As shown in figure 3.11B, mCh was expressed in both sides of the ARC. Unilateral injection of ciCARTpt and sgRNA^{CARTpt} showed no reduction in protein expression following staining (Figure 3.11C and 3.11D) while qPCR analyses of CART mRNA in the hypothalamus showed a 6-fold increase following viral overexpression of ciCARTpt (Figure 3.11E). Analyses of BW (Figure 3.11F) and FI (Figure 3.11G) did not yield any significant differences among the 3 groups; however, preventing the depletion of CART from ARC^{POMC} neurons completely attenuated hyperglycemia (Figure 3.11H). Of note, the overexpression of ciCART also normalized circulating insulin levels in the serum (Figure 3.11I) and mRNA levels of *G6pase* and *PCK1* in the liver (Figure 3.11J and 3.11K). Thus, ARC$^{\Delta CARTpt}$ is solely responsible for the observed elevation in basal BG levels and has no observed effect on energy homeostasis.

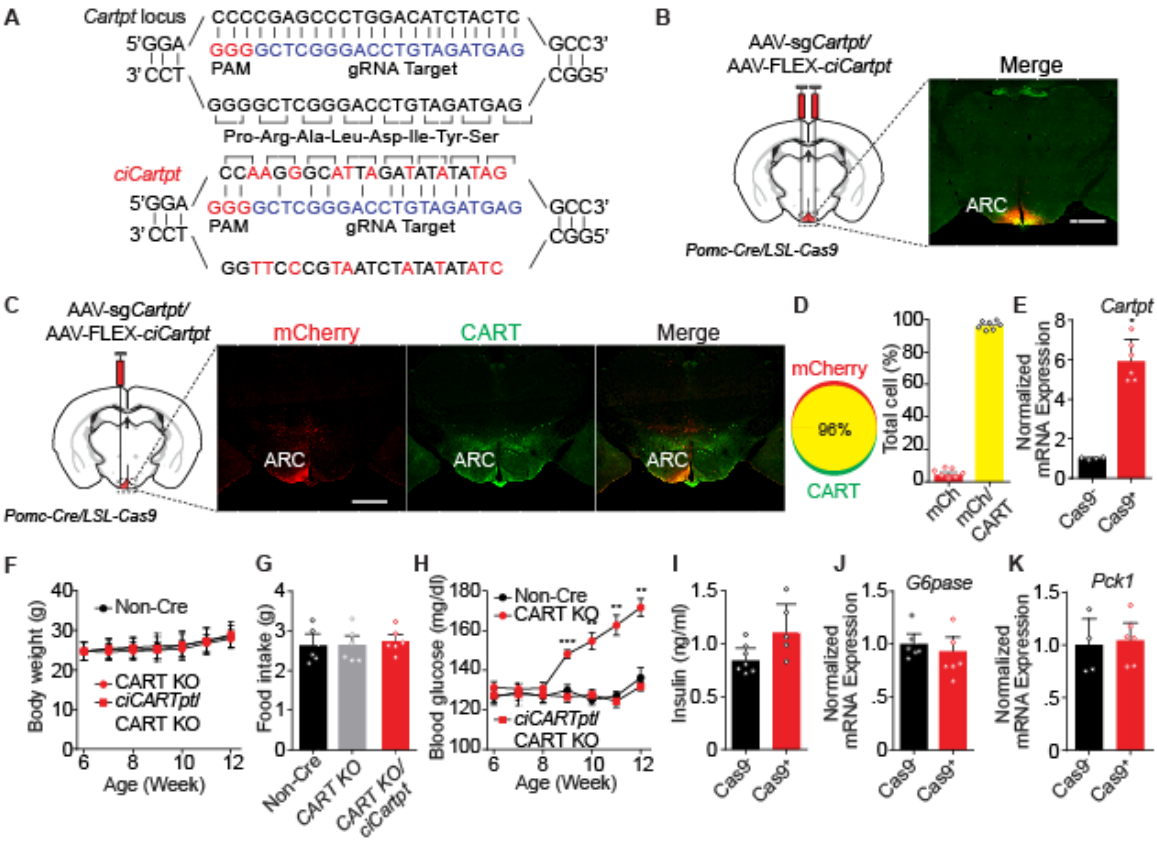

Figure 3.11: Expression of ciCART Prevents Hyperglycemia (A) Schematic of Cas9 immune CARTpt (ciCARTpt) design. (B) Schematic of injection and image of sgRNA^{CARTpt} and LSL-Cas9-eGFP co-localization. (C and D) Schematic of injection, image and (D) quantification of sgRNA^{CARTpt} and CART co-localization(n=4-7).(E) Expression of *CARTpt* mRNA expression in ciCARTpt injected mice (n=7).(F) Body weight change following sgRNA^{CARTpt} and/or ciCARTpt injection (n=6). (G) Average daily food intake 6 weeks following viral injection (n=5-6). (H) Weekly blood glucose levels (n=6). (I) Insulin levels at 6 weeks (n=5-7)(J and K) Expression of (J) *G6pase* and (K) *Pck1* mRNA in the liver of sgRNA^{CARTpt} and ciCARTpt injected mice(n=4-6). Data are presented as mean ± SEM. *p< 0.05; **p< 0.01, and***p< 0.001 as determined by unpaired t-test. Scale bars size=1mm.

3.9 Reduction of Hypothalamic CART in Diabetic Models

To determine the contribution of CART in POMC neurons to the pathogenesis of diabetes we first examined whether CART expression is reduced in T1D (STZ treated) and T2D (60%HFD feed) models in the ARC. We employed IHC and qPCR techniques to quantify and observe both CART protein and mRNA expression levels in the

hypothalamus of our diabetic mice. In both our T2D (Figure 3.13A and 3.13B) (Kristensen et al., 1998; Tian et al., 2004) and T1D model (Figure 3.13M and 3.13N) (Xu et al., 2016) protein and mRNA expression of CART was markedly reduced compared to either chow feed or saline injected controls, consistent with prior findings. Thus, CART levels in the ARC are suppressed in both diabetic models, consistent with previous findings by others.

3.10 CART Overexpression in POMC Neurons Has No Effect on Energy or Glucose Homeostasis.

To test if preventing CART reduction in our diabetic models would have any therapeutic benefit, we constructed a Cre-enabled AAV virus vector to specifically deliver native *Cartpt* cDNA into POMC neurons. Validation of CART viral expression was performed by unilateral injection into the thalamus of Vglut2-IRES-Cre mice; robust Cre-dependent expression of CART was detected by strong immune-reactive signal (Figure 3.12A). The specificity of viral expression was further tested in the ARC at the single-cell level. It is known that AgRP neurons co-express Neuropeptide Y (NPY) and do not express CART. We stereotaxically injected the CART virus into the ARC of Agrp-IRES-cre/Npy-hrGFP mice. As shown in figure 3.12B, CART was solely expressed in GFP labeled neurons, demonstrating that the virus can be used as an efficient tool to overexpress CART in Cre^{+} neurons. The virus was then stereotaxically injected into the ARC of *POMC*-Cre mice (Figure 3.12C). *CARTpt* mRNA expression levels within the ARC confirmed significant over-expression of *CARTpt* in mice treated with AAV-Flex-*CARTpt* (Figure 3.12D). Consistent with over-expression of *ciCARTpt* there was no effect on BW (Figure 3.12E), FI (Figure 3.12F), or basal BG (Figure 3.12G). Even when challenged with a bolus of glucose, no observable difference was detected between *CARTpt* overexpressing and non-Cre litter mates (Figure 3.12H). Finally, IHC staining for

CART in virally injected models of T2D (Figure 3.13A) and T1D (Figure 3.13M) showed preservation against diabetes induced depletion. Therefore, our Cre-enabled AAV virus vector expressing *CARTpt* is capable of assuring CART expression in the ARC of diabetic mice.

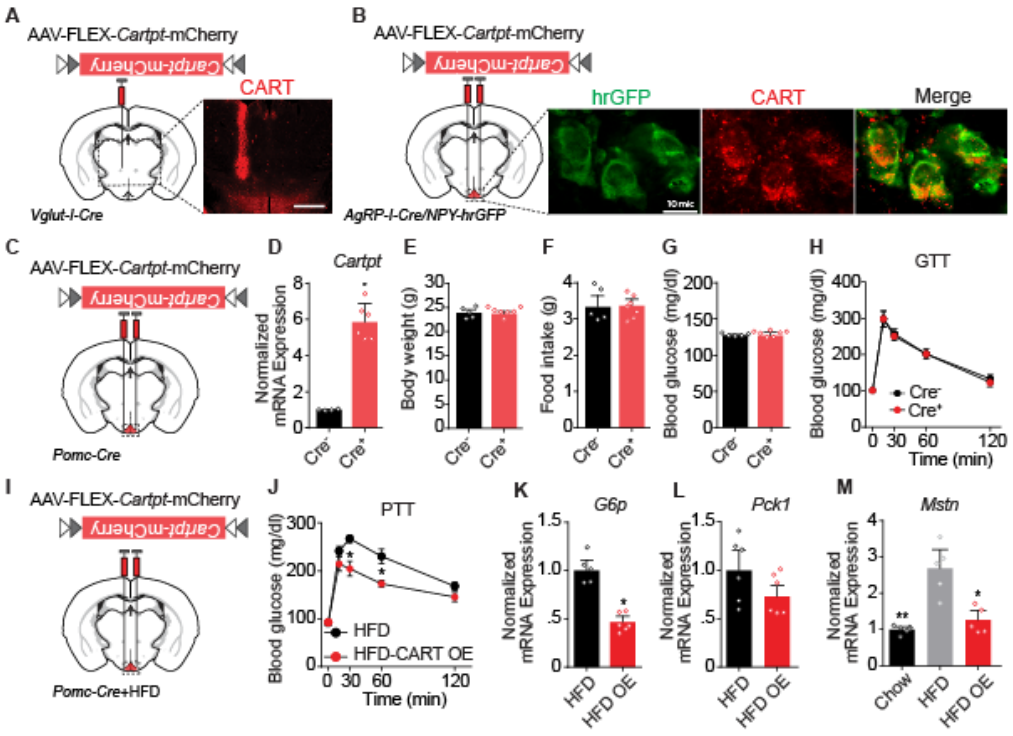

Figure 3.12: Effects of CARTpt overexpression in ARC POMC neurons. (A) Schematic indicating site of unilateral injection and representative image of CART expression in the thalamus of Vglut2-Ires-Cre mice. Scale bars size=1mm (B) Schematic indicating site of bilateral injection and representative image of hrGFP and CART co-localization in Agrp-Ires-Cre mice crossed with NPY-hrGFP mice. Scale bars size=10µm (C) Schematic indicating site of bilateral injection of AAV-FLEX-CARTpt into *POMC*-Cre mice.(D) qRT-PCR analysis of *cocaine-amphetamine regulated transcript (CARTpt)* mRNA expression in the ARC of injected AAV-FLEX-CARTpt mice(n=4-6). (E) Average body weight 4 weeks following viral injection (n=5-7). (F) Average daily food intake 4 weeks following viral injection (n=5-7). (G) Average basal blood glucose at the end of study (n=5-7). (H) GTT performed at 4 weeks following viral injection in Non-Cre and *POMC*-Cre /LSL-Cas9 mice (n=5-7). (I) Schematic indicating site of bilateral injection of AAV-FLEX-CARTpt into *POMC*-Cre mice feed a HFD diet. (J) Pyruvate tolerance test (PTT) 4 weeks following viral injection (n=5-6). (K, L and M) Expression of (K) *G6pase* and (L) Pck1 mRNA in the liver and (M) *Mstn* mRNA in iBAT of chow feed, HFD, and HFD+CART OE mice(n=5-6).Data are presented as mean ± SEM. *p< 0.05; **p< 0.01, and***p< 0.001 as determined by unpaired t-test.

3.11 CART Depletion in the ARC Contributes to the Pathogenesis of Diabetes

We first examined the role of CART in our T2D model by stereotaxically injecting our Cre-dependent CART over-expression virus into the ARC of *POMC*-Cre mice treated with HFD (Figure 3.13C). qPCR analyses revealed an almost 3-fold increase in CART expression compared to non-Cre HFD treated control (Figure 3.13D). Serum insulin level showed a significant improvement but CART over-expression did not completely rescue levels to a chow fed state (Figure 3.13E). Basal BW (Figure 3.13F) and FI (Figure 3.13G) remained consistent with control group throughout the experiment. Cre^{+} HFD treated mice infected with AAV-FLEX-CART showed significant improvement in basal BG (Figure 3.13H) but not following an overnight fast (Figure 3.13I). Overexpression of CART consistently prevented hyperglycemia in our T2D diabetic model (Figure 3.13J), and improved glucose clearance (Figure 3.13K) as well as IS (Figure 3.13L). Therefore, countering CART reduction in the ARC of T2D mice prevents the development of hyperglycemia.

To examine the role of CART in the pathogenesis of T1D, we performed a similar experiment in which we overexpressed CART in mice treated with STZ (Figure 3.13O). Gene expression analysis showed marked increase in *CARTpt* compared to Cre negative litter mates treated with STZ (Figure 3.13P). In all mice treated with STZ, circulating insulin levels were almost completely ablated (Figure 3.13Q). Consistent with prior findings, circulating leptin was dramatically reduced in treated mice as well (Figure 3.13R). Total BW (Figure 3.13S) and FI (Figure 3.13T) were consistent between STZ injected non-Cre controls and STZ injected CART overexpressing mice at all time points while BG monitoring showed attenuation of hyperglycemia before reaching our maximum monitoring threshold, at 6 and 8 days post STZ injection (Figure 3.13U). Interestingly, CART overexpression did significantly prolong the survival of STZ treated

mice (Figure 3.13V). Although preserving CART levels in the ARC of T1D mice does have a therapeutic effect, it is not the main factor regulating survival when deprived of insulin and leptin.

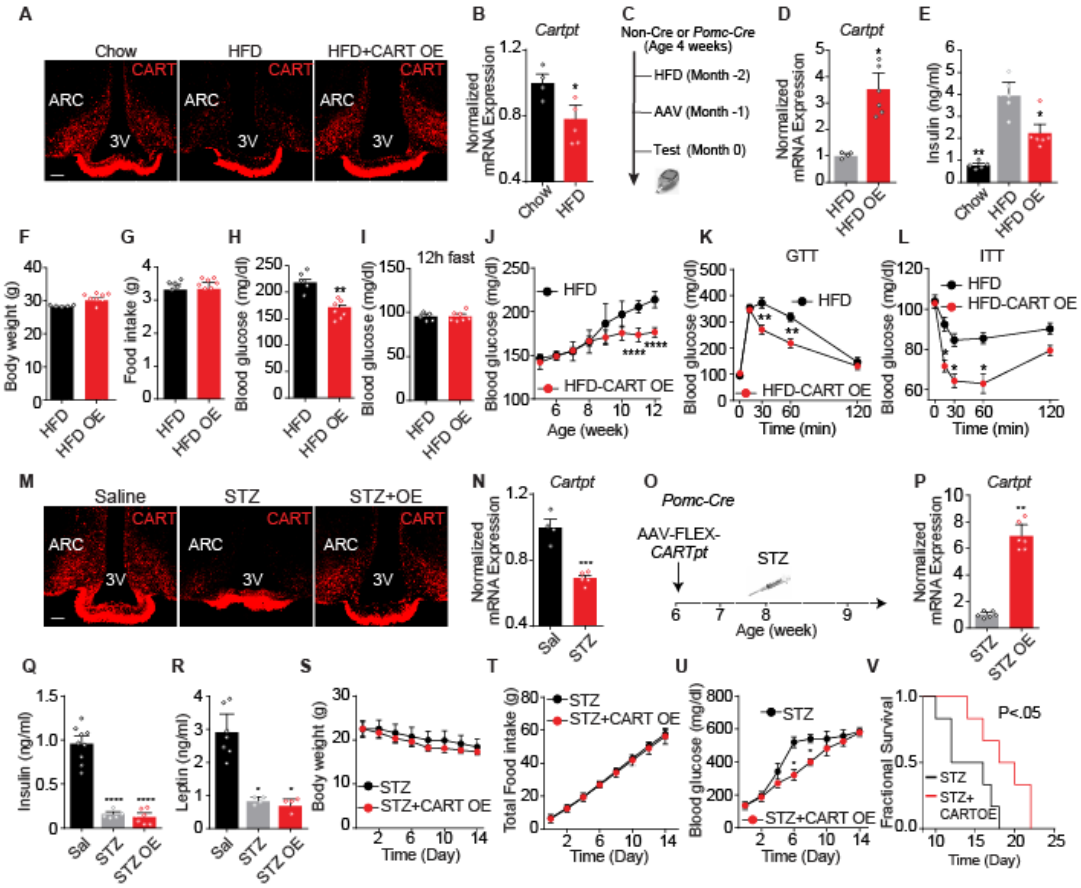

Figure 3.13: *CARTpt* over-expression in HFD and STZ treated mice. (A) CART expression in chow feed, HFD, and HFD+CART OE mice. (B) Expression of *CARTpt* mRNA in chow feed or HFD feed mice (n=4-5). (C) Schematic of monitoring protocol. (D) Expression of *CARTpt* mRNA in HFD feed or HFD+CART OE mice (n=4-6). (E) Insulin levels at 12 weeks of age (n=5-6). (F) Average body weight (n=5-7). (G) Average daily food intake (n=5-7). (H) Basal blood glucose at 12 weeks of age (n=5-7). (I) Blood glucose following 12 hr fast (n=5-7). (J) Weekly blood glucose levels (n=5-7). (K and L) GTT and ITT following 8 weeks of HFD (n=5-6). (M) CART expression in saline, STZ, and STZ+CART OE injected mice. (N) Expression of *CARTpt* mRNA in saline or STZ injected mice (n=4-5). (O) Schematic of monitoring protocol. (P) Expression of *CARTpt* mRNA in STZ or STZ+CART OE injected mice (n=6). (Q and R) Insulin and Leptin levels at the end of the study (n=4-9). (S-U) Average daily body weight, food intake and blood glucose (n=5-6). (V)Survival curves of STZ and STZ+CART OE injected mice (n=6). Data are presented as mean ± SEM. *p< 0.05; **p< 0.01, and***p< 0.001 as determined by unpaired t-test or one-way ANOVA (Tukey's multiple comparison test). Scale bars size=100µm.

3.12 Downstream Glucoregulatory Circuit

To determine the downstream glucoregulatory pathway, we used an unbiased approach utilizing the change in neuronal activity caused by STZ treatment. As observed, expression of c-Fos positive neurons were upregulated in several regions in the brain involved in energy and glucose homeostasis (Figure 3.14A and 3.14B), including the paraventricular hypothalamic nucleus (PVH), dorsomedial hypothalamic area (DMH), and lateral hypothalamic area (LH) (Atasoy et al., 2012; Gao and Horvath, 2008). Since, these regions are known to be innervated by POMC projections (Bouret et al., 2004), and CART acts through an inhibitory G protein-coupled receptor (Lin et al., 2011; Vicentic et al., 2006), we performed a screen to observe regions in which neuronal activity would be attenuated by DREADD stimulation of POMC neurons (Figure 3.14C). Following CNO administration, the region with the most significant reduction in c-Fos activity compared to saline injected control was the PVH (Figure 3.14D and 3.14E). To directly test the glucose regulatory functions of these projections, we co-injected a Cre-dependent AAV vector expressing halorhodopsin (eNpHR3.0) and hM3D into the ARC of *POMC*-Cre mice and implanted an optical fiber above the PVH (Figure 3.14F). As shown in figure 3.14G and 3.14H, ~89% of hM3d expressing POMC neurons also expressed eNpHR3.0. The ability of the orange-light-mediated inhibitions of POMC neurons expressing eNpHR3.0 was assessed using current-clamp recordings (Figure 3.14I). Not surprisingly, co-localization continued to the POMC projected fibers in the PVH as well (Figure 3.14J and 3.14K). Optical inhibition of ARC^{POMC} neuronal projections in the PVH prevented acute reduction of BG at 1hr following CNO administration compared to non-light inhibition (Figure 3.14L and 3.14M). To determine if the suppression is attributed to CART, we implanted a bilateral cannula into C57bl/6J mice and injected either saline or CART 55-102 directly into the PVH following STZ treatment. We observed a dramatic

reduction in neuronal activation solely in the PVH of CART injected mice (Figure 3.14N and 3.14O). In addition, injection of CART 55-102 directly into the PVH acutely reduced resting BG levels but not to the same degree as observed with central administration or acute POMC neuronal excitation (Figure 3.14P). This result indicates that POMC neurons provide inhibitory projection in the form of CART release to the PVH and selectively reduces BG.

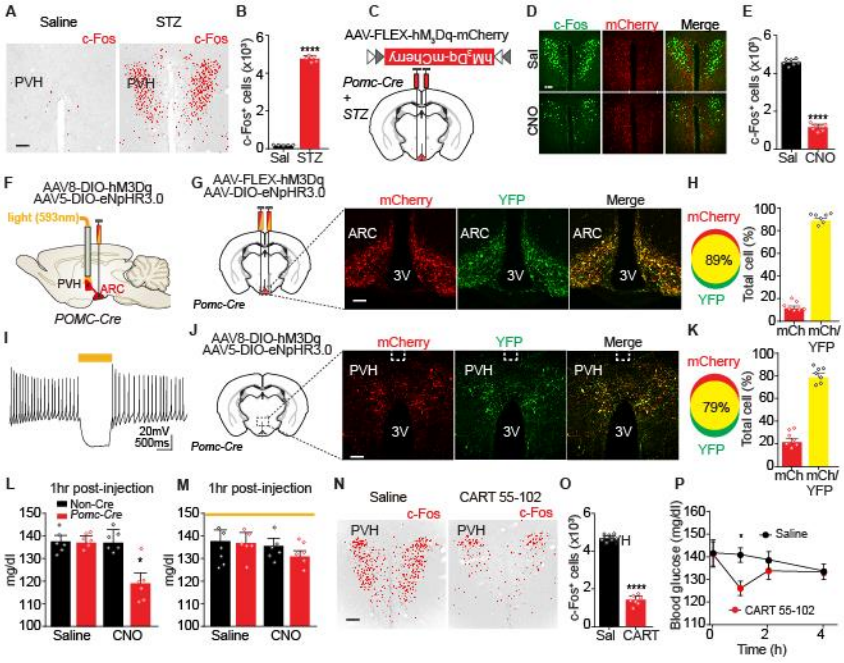

Figure 3.14: POMC to PVH Neurocircuits Modulates Glucose Homeostasis. (A and B) Image and quantification of c-Fos immunoreactivity in saline or STZ injected mice (n=5). (C) Schematic of injection. (D and E) cFos immunoreactivity and quantification of c-Fos in saline or CNO injected mice (n=7). (F) Schematic of injection and optogenetic implantation. (G and H) Schematic of injection, representative image and (H) quantification of AAV8-DIO-hM3d-mCherry and AAV5-DIO-eNpHR3.0-YFP co-localization (n=7). (I) Current-clamp recording of orange-light-mediated inhibition of eNpHR3.0 positive neurons in the ARC. (J and K) Schematic indicating site of confocal imaging, image and (K) quantification of AAV8-DIO-hM3d-mCherry and AAV5-DIO-eNpHR3.0-YFP positive fibers in the PVH (n=7). (L and M) Blood glucose levels 1hr following saline or CNO injection (L) without or (M) with orange-light-mediated inhibition (n=6). (N and O) Image and (O) quantification of c-Fos immunoreactivity in saline or CART 55-102 injected STZ mice (n=7). (P) Blood glucose levels following saline or CART 55-102 injection into the PVH of 8-week-old C57BL/6J mice (n=8). Data are presented as mean ± SEM. *p< 0.05; **p< 0.01, and***p< 0.001 as determined by unpaired t-test or paired t-test. Scale bars size=100µm.

Chapter 4: Discussion

The use of the *POMC*-Cre transgenic mouse line in combination with the Cre/loxP system has previously shown that ARC^{POMC} neurons play a role in energy and glucose homeostasis. However, an understanding of the underlying molecular mechanisms remains unknown. To address this, we took a systematic approach, utilizing novel techniques to remove many caveats and ambiguities. By acutely and rapidly stimulating ARC^{POMC} neurons using a viral chemogenetic approach, we provided direct evidence for their role in lowering whole body glucose (BG). In addition, we elucidated a negative feedback loop which is responsible for preventing hypoglycemia directly caused by POMC neuronal activation. Building on this, we sought to identify the neuropeptide responsible for this BG regulation. By employing advancements in *in-vivo* CRISPR-Cas9 genome editing technology, we established that $ARC^{\Delta POMC}$ causes extreme obesity and dysregulation in energy homeostasis. However, we observed that hyperglycemia is a secondary effect to the physiological dysregulation (Platt et al., 2014a). By dissecting the roles of key neuropeptides derived from POMC, we determined that the separate thermoregulatory and locomotor aspects of energy regulation are distinctly controlled by α-MSH and β-endorphin, respectively. Depletion of CART from ARC^{POMC} neurons displayed another divergent role, showing no signs of energy dysregulation, yet direct effects on BG levels. We then went on to clarify CART's role in the pathogenesis of both T2D and T1D. We observed that in both our HFD-induced T2D mice and STZ treated T1D mice, CART mRNA and protein levels were markedly diminished. Importantly, when CART was virally over-expressed in POMC neurons, it prevented the development of hyperglycemia in our T2D model and significantly improved the survival of mice devoid of insulin. Finally, through an unbiased screening process we have identified the PVH as the key region that POMC neurons utilize to modulate glucose regulation. In summary, we have uncovered the prominent

neuropeptide in ARC^{POMC} neurons that controls glucose homeostasis and unraveled the molecular mechanism for POMC's control of energy expenditure.

4.1 Selective regulation of energy balance and glucose homeostasis

Previously, chemogenetic stimulation of ARC *POMC*-Cre neurons was shown to cause an acute reduction in BG levels while increasing thermogenesis and locomotion, without an acute effect on food intake (FI). Some of these findings are supported by previous work while a portion have either not been repeated or contradictory findings have been reported. Controversy has surrounded the effects of ARC^{POMC} neurons in regulating GT and IS. Recent work utilizing a similar approach of crossing the *POMC*-Cre line with a transgenic mouse strain expressing a Cre-dependent hM3Dq inserted into a ROSA26-locus to initiate endogenous receptor expression did not observe any changes in IS or glucose clearance following CNO activation (Steculorum et al., 2016). The blunted effect of *POMC*-Cre neurons observed in these experiments most likely stem from the strong negative regulation of these neurons. As we have shown and others have described (Lee et al., 2015), the transient expression of POMC is able to induce Cre-driven recombination in various parts of the CNS (Padilla et al., 2012). Importantly, we have observed that recombination occurs in a large population of local GABAergic AgRP neurons in the ARC, which have been shown to project to POMC neurons (Padilla et al., 2010). As a result, CNO activation of these *POMC*-cre Hm3Dq mice likely causes inhibition of ARC^{POMC} neurons. In addition, subsequent attempts to elicit a stronger peripheral effect by hyper exciting these neurons with multiple injections of CNO resulted in the opposite effect. This makes sense considering the negative feedback loop we identified that responds to acute reductions in circulating glucose.

Consistent with previous work looking at the role of ARC^{POMC} neurons in energy regulation, we observed rapid induction of iBAT thermogenesis following chemogentic stimulation. Using similar techniques to induce acute excitation of POMC neurons in the ARC, temperature transponders implanted subcutaneously in the iBAT showed significant increases in heat production following CNO administration. Using this technique, they described a fast acting increase in iBAT temperature which was sustained for four hours (Fenselau et al., 2017). This supports the idea that ARC^{POMC} neurons have the ability to elicit rapid responses, driven by acute excitation. This thought was in doubt following previous work describing ARC^{POMC} neurons' classical role as satiety regulators. Chemogenetic stimulation failed to reduce food intake within a 24 hour period following a single dose of CNO or two injections administered at five hour intervals. Only when these mice were chronically injected with CNO for three days did they finally observe a reduction in BW and FI. In contrast, acute excitation of POMC neurons in the NTS was sufficient to inhibit food intake for up to eight hours (Zhan et al., 2013). Subsequent work did not observe impairment in dark-cycle feeding, following stimulation of ARC^{POMC} neurons, but cumulative FI 24 and 48 hours following a CNO injection were decreased (Fenselau et al., 2017). Surprisingly, we observed an increase in light-cycle locomotion as well. Traditionally within the ARC, AgRP neurons have been shown to increase locomotor activity following chemogenetic stimulation. This was attributed to food-seeking behavior since the mice continually visited the zone which the food was normally located (Krashes et al., 2011) (Dietrich et al., 2015). It is believed that ARC^{POMC} neurons should elicit the opposite response; however this has not been described previously. Selective ablation of ARC^{POMC} neurons by virally expressing diphtheria toxin receptor resulted in reduced locomotion. After taking measurements 20 days following treatment with diphtheria toxin, the phenotype could be attributed to direct ARC^{POMC} neuronal ablation or the development of obesity (Zhan et al., 2013). Of note,

leptin receptor expression solely in ARC^{POMC} neurons was sufficient to increase activity when compared to *db/db* mice. Regrettably, once again the improvement in locomotion can be seen as a result of increased neuronal activation through the leptin pathway or simply through improvement in overall physical health (Huo et al., 2009). In summary, the genetic approaches taken by previous labs to access the role of ARC^{POMC} neurons in glucose homeostasis has been shown to be sub optimal, consequently blunting the effects of neuronal stimulation of POMC neurons. In regards to iBAT thermogenesis and acute FI, our findings are consistent with previous work in the field showing that ARC^{POMC} neurons have the ability to elicit acute responses and that their effects on FI are long-term. Finally, with our observation that these groups of neurons directly control locomotion, it provides clarity to the field and enabled us to further identify the underlying molecular mechanisms.

4.2 Negative feedback loop onto ARC POMC neurons

As previously described, POMC neurons in the ARC are stimulated by elevated levels of glucose through a pancreatic β-cell model. Consistent with our findings, it has been observed that when extracellular levels of glucose are reduced, POMC neurons are inhibited through increased frequency of sIPSCs (Lee et al., 2015). This marked increase in GABAergic tone to POMC neurons was also observed in mice which were fasted for 24 hours (Vong et al., 2011). In part one of the first experiments using transgenic mice expressing eGFP in ARC^{POMC} neurons showed that the addition of leptin decreased the frequency of sIPSCs in 33% of cells, through an auto-inhibitory loop from melanocortin peptides (Cowley et al., 2001). Recently, pharmacological blockage of MC3/4Rs completely attenuated leptins effects on stimulating IPSC frequency (Lee et al., 2015). This suggests a role of presynaptic MC3/4R expressing GABAergic neurons in the regulation of POMC neurons. In agreement with this, subsequent work has shown

that when leptin receptors are ablated from GABAergic neurons there is a large increase in sIPSC frequency onto POMC neurons (Vong et al., 2011). However, leptin has at most only been shown to attenuate a sub population of ARC^{POMC} neurons, leaving the possibility of an independent pathway. A plausible alternative could be the role of glucose inhibited neurons which express GABA. As previously stated, unlike glucose excitation the underlying molecular mechanisms of how glucose inhibits neurons are not as well characterized. Within the ARC 40% of AgRP neurons have been shown to be hyperpolarized and cause inhibition by raising the extracellular glucose from 0.5 to 5mM, through direct post-synaptic action (Fioramonti et al., 2007). In addition, recent work has shown that chemogenetic and optogenetic stimulation of AgRP neurons sends direct GABergic signals to neighboring POMC neurons within the ARC (Atasoy et al., 2012). Interestingly, when VGAT is specifically deleted from AgRP cells, fasting-induced sIPSCs were not attenuated (Rau and Hentges, 2017). Furthermore, mice lacking leptin receptors on AgRP neurons did not show a significant increase in inhibitory inputs onto POMC neurons (Vong et al., 2011). This suggests that GABA release onto POMC neurons during high metabolic need is mediated by non-AgRP GABAergic neurons (Figure 4.1). To access the role of this inhibitory input onto POMC neurons in the context of maintaining glucose homeostasis, we transiently reduced BG through chemogenetic stimulation of ARC^{POMC} neurons while administering BIC specifically into the ARC. Since the first observation that BIC was able to reduce the effects of GABA in the 1970's, it has become a key antagonist for $GABA_A$ receptors (Johnston, 2013). One caveat associated with the use of BIC is that some GABA receptors are insensitive to it; mutation studies in the $GABA_C$ receptor have pointed to specific amino acids residues which prevents binding (Zhang et al., 2008). BIC also has significant actions on other receptors including nicotinic acetylcholine receptors (Demuro et al., 2001). An alternative $GABA_A$ receptor antagonist that could have been use is Gabazine or RU5135. Gabazine has a

very similar action to BIC, but it interacts with different residues on $GABA_A$ receptors (Zhang et al., 2008). However, unlike BIC, Gabazine has been shown to be less potent and a poor blocker of induced currents (Uchida et al., 1996). RU5135 on the other hand is a convulsant steroid derivative which has been shown to be 500 times more potent then BIC(Hunt and Clements-Jewery, 1981), but with its increased potency also comes unspecific interactions (Simmonds and Turner, 1985). BIC provides a balance between having a potent compound while minimizing off target effects. However, on top of the issue discussed, pharmacological manipulations in general are inherently not spatially or cell-type specific. A plausible next step is to utilize the in vivo CRISPR technique described previously to disrupt $GABA_A$ receptors within ARC^{POMC} neurons. $GABA_A$ receptors are heteropentameric channels mainly composed from two α, two β and one γ subunit (Nakamura et al., 2015). Ablation of the channel could be achieved with the targeted disruption of all the variants in one of the main subunits. Based on previously reported packaging limits into AAVs, we are able to incorporate multiple guide RNAs (gRNAs) into the sequence to target multiple genes (Wu et al., 2010b). Ideally, a single Cre inducible AVV packaged with multiple gRNAs targeting a single subunit can be delivered specifically into the ARC of *POMC-Cre/*LSL-Cas9-eGFP mice. The effectiveness of the virus can be determined through whole cell patch recording to determine if any sIPSCs can be detected on POMC cells. Once validated, basal physiological measurements should be obtained to determine if ablation of inhibitory input onto ARC^{POMC} neurons produces any physiological changes or alterations to homeostatic set points. Finally, it would be beneficial to co-inject with the AAV8-hSyn-DIO-hM3Dq-mCherry virus to express the excitatory GPCR in $GABA_A$ receptor KO ARC^{POMC} neurons. This would provide direct evidence that with acute excitation of POMC neurons, there is a negative feedback loop which utilizes inhibitory GABA release onto POMC neurons to prevent hyper excitation and prolonged reduction in BG.

Furthermore, if this pathway is confirmed, then retrograde tracing with specific viral serotypes can be used to dissect the neural circuit and unravel which GABAergic neuronal population maybe the primary upstream effector (Tervo et al., 2016).

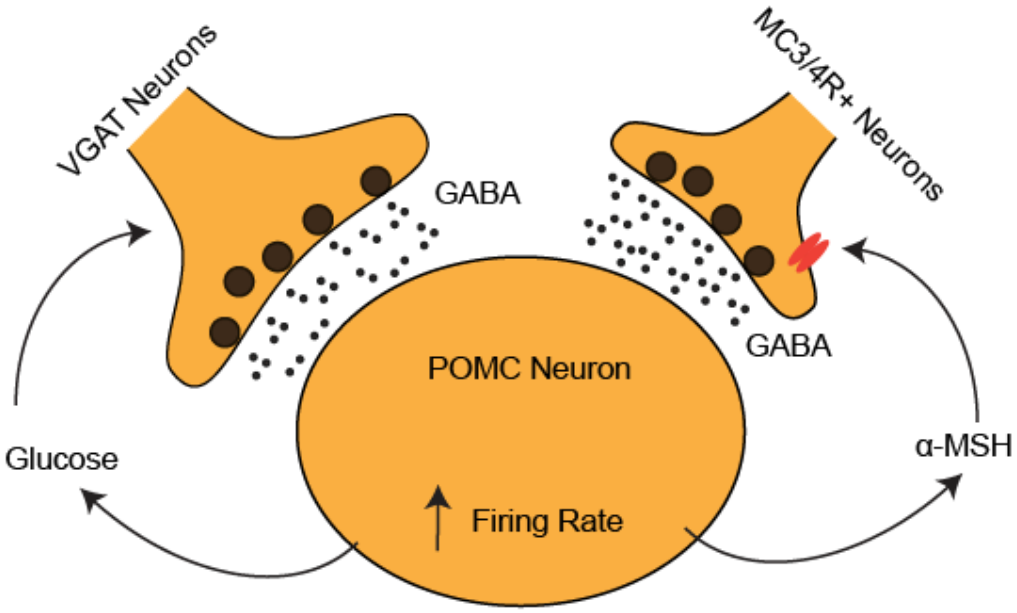

Figure 4.1: Plausible mechanisms for auto-inhibitory loop. Following activation of POMC cell in the ARC, α-MSH is released and subsequently binds to MC3/4R GABAergic neurons, this elicits enhanced GABA release onto ARC^{POMC} neurons. Alternatively, deficits in glucose availability, excites glucose inhibited (GI) neurons as previously discussed and increases inhibitory signaling to ARC^{POMC} neurons.

4.3 POMC deletion and dysregulation of energy expenditure

POMC was our first candidate for mediating *POMC*-Cre neuron-driven glucose homeostasis. It has been established that POMC ablation results in hyperphagia, obesity, reduction in locomotion, energy expenditure and hyperglycemia (Smart et al., 2006; Yaswen et al., 1999; Zhan et al., 2013). However, its effect on glucose homeostasis have not been definitively proven as previously discussed. Similarly, after

viral gRNA injection, we observed the same alteration in FI, BW and energy expenditure. Of note, two observations that will be discussed are the decrease in dark-cycle locomotion before the development of obesity and the staggered onset of hyperglycemia. The observation that ARC POMC deficient mice have reduced locomotion is not novel, however, these tests were performed following the onset of severe BW gain. As a result, it was believed that this phenotype can be attributed to the reduced health of the animal. In all the metabolic and physiological experiments we performed the severity increased over time, except for locomotion which remained surprisingly stable through the monitoring period. This strongly suggests that one or more biologically active fragments derived from POMC are required for normal locomotor activity. Hyperglycemia did not develop until 5 weeks post injection, even when stressed with a bolus injection of glucose shortly before the onset of hyperglycemia, did not reveal any glucose tolerance impairment compared to controls. Nonetheless, when basal BG is elevated, severe impairment to glucose is observed, implying that ablation of ARC POMC contributes to the development of diabetes through the strain caused by obesity. To provide direct evidence, we utilized our previous observation that chemogentic stimulation of ARC^{POMC} neurons causes an acute reduction in basal BG as a readout. As shown previously, $ARC^{\Delta POMC}$ did not ablate the acute reduction in BG following stimulation of ARC^{POMC} neurons. Taken together, these results indicate that ARC^{POMC} is directly controlling energy expenditure with elevation in BG as a secondary effect. Employing similar techniques in the NTS will provide direct evidence to the role of POMC in acute feeding. As described previously, chemogenetic stimulation of POMC neurons in the NTS immediately suppressed feeding, while selective ablation of the cells had no effect on BW, FI or glucose tolerance (Zhan et al., 2013). In order to further these studies, it would be beneficial to repeat these experiments using the viral CRISPR approach. By co-injecting our POMC specific viral

gRNA along with AAV_8-hSyn-DIO-hM3Dq-mCherry into the *POMC-Cre*/LSL-Cas9-eGFP mice, the functional role of POMC in regards to acute feeding can be assessed. If no suppression or a partial reduction in FI is observed, then other drivers must be investigated. But if food suppression is abolished, then it can be concluded that a biologically active fragment derived from POMC is the primary contributor. Using the CRISPR immune re-expression viruses lacking either α-MSH or β-endorphin may reveal further the contribution of each fragment. A primary contributor, if identified, could possibly lead to anterograde tracing and receptor analyses to determine the downstream neural circuits which can be validated with both terminal excitation and inhibition using optogenetics. Finally, it would be interesting to observe the effects of specific ablation of POMC in the NTS^{POMC} neurons to determine if it is consistent with cell ablation. In short, using our novel *in vivo* technique to delete POMC from ARC^{POMC} neurons we have concluded that one or more derivatives of POMC directly modulate locomotion while hyperglycemia is induced by the stresses of obesity. Using this technique the other primary brain region containing POMC neurons can be explored and its role in acute feeding can be assessed.

Concerns about using CRISPR/Cas9 *in vivo* to deplete neuropeptides include off-target effects and neuronal toxicity. Neuronal toxicity was assessed by the quantification of eGFP+ cells in *POMC*-Cre /LSL-Cas9 mice and cell counts remained consistent between our treated regions and an endogenous control. In addition, in vitro work showed efficient genome editing within *POMC* locus without altering potential off-target genes. We validated the targeting by constructing a Cre-enabled AAV virus which expresses a Cas9 immune POMC cDNA sequence. We specifically mutated the nucleotides within the binding region targeted by the gRNA, while keeping the codons consistent. When $sgRNA^{POMC}$ injected mice were pretreated with ciPOMC, endogenous

levels of POMC mRNA expression were significantly elevated. However, with over-expression of ciPOMC it not only prevented ARC$^{\Delta POMC}$, but also the metabolic dysregulation. This not only provided direct evidence that the effects caused by ARC$^{\Delta POMC}$ were not the result of off target effects, but that within the system there is also a pre-existing set point or saturation limit which does not allow over-expression of POMC to affect any physiological function that we have observed. Taken together, the use of viral gRNA to KO POMC in the ARC of adult mice does not cause cell death and is accurate. Initially, it is understandable that *in vitro* testing of the gRNA needs to be performed to ensure proper targeting, but with the use of ciPOMC we provided a great tool to identify that the phenotypes observed with our gene KO is solely due to specific targeting rather than off target effects. However, care needs to be taken to ensure that over expression of that gene does not have its own physiological consequences due to the inability to limit expression of the ciPOMC.

4.4 The Metabolic role of α-MSH and β-endorphin in the ARC

Utilizing the novel Cas9 immune viral construct and the ability to deplete the ARC of endogenous POMC, we were able to dissect this complicated mechanism in detail. It has been well characterized that POMC gives rise to multiple active peptides with diverse physiological roles. However, direct evidence has been lacking to date. A novel mouse model recently created to study α-MSH uses the insertion of a mutation in a POMC protein cleavage site to prevent the production of α-MSH from ACTH. Unsurprisingly, they reported body weight gain, hyperphagia, increased body length and a trend in reduced locomotion. Unfortunately, other prominent fragments derived from POMC including β-endorphin were not detected, leaving the possibility of complete POMC ablation. In addition, this mutation is universally expressed affecting POMC expression in all the regions previously discussed (Mountjoy et al., 2017). A mouse

model lacking β-endorphin was first developed to study its role in pain inhibition. This mouse contains a point mutation in exon three which causes a truncated POMC prohormone to be expressed (Rubinstein et al., 1996). Subsequent characterization of these mice revealed a slight increase in FI which led to an increase in BW, but no other changes in basal metabolic rates were observed. Regrettably, no tests were performed to measure changes in spontaneous activity (Appleyard et al., 2003). But as stated before, global truncation of POMC prohormone is not region-specific. When we specifically ablated α -MSH or β-endorphin, there was a significant increase in BW and fat mass accumulation. Neither, even when combined, seemed to equate to the dramatic BW gain following POMC depletion from the ARC. This suggests either a synergistic effect from these two neuropeptides or the absence of a contribution from a third peptide. While the accumulation of BW by Δα-MSH can be attributed to a trend in increased feeding and reduced thermogenesis, the significant fat mass accumulation by Δβ-endorphin seems to be caused by a single deficit in locomotion. Therefore, Δα-MSH and Δβ-endorphin can account for the reduction in thermogenesis and locomotion, but not total BW gain or the hyperphagia observed in ARC$^{\Delta POMC}$ mice.

Thermogenesis is essential for maintaining normal body temperature and energy balance. Non shivering heat production is mediated by beige and BAT which utilizes UCP1 in the mitochondria to produce heat when the system is subjected to low temperatures. A key sensor and activator of this protective mechanism is the CNS, which drives sympathetic signaling to the BAT (Morrison et al., 2012). It has been hypothesized that leptin might be a key activator of BAT thermogenesis due to its role as a hormonal signal of food consumption. The high metabolic rate caused by heat production requires adequate fuel availability to be sustainable. Early work showed that ICV injection of leptin into ob/ob mice was sufficient to increase thermogenesis (Hwa et

al., 1996). With the ARC expressing high levels of the leptin receptor, focus soon turned to the neuronal populations found within this region (Myers et al., 2008). Administration of leptin into mice increased sympathetic nerve activity to the BAT, which was abolished when leptin receptors were depleted from the ARC (Harlan et al., 2011). As stated previously, leptin signaling activates the JAK/STAT pathway signaling to induce transcription of genes including *POMC* and *AgRP* (Myers et al., 2008). When insulin and leptin signaling is enhanced in ARC POMC neurons through the inactivation of protein tyrosine phosphatases PTP1B and TCPTP, which dephosphorylates JAK2 and STAT3 respectively, it promotes WAT browning and increased energy expenditure (Dodd et al., 2015). ICV administration of MT-II, an agonist of MC4-R provided a dose-dependent excitation of sympathetic nerve activity to the BAT. Antagonizing MC4-R using SHU9119 completely blocked this signaling (Haynes et al., 1999). Consistent with these findings, chronic infusion of SH9119 using an osmotic pump attached to the cannula in the lateral ventricle induced decreased thermogenesis and reduced UCP1 expression (Verty et al., 2010). Thus, in combination with our findings the importance of the melanocortin pathway in BAT thermogenesis has been shown.

In contrast, the bulk of the studies in regards to β-endorphin have mainly focused on its role in pain management. In the central nervous system, β-endorphin binds to μ opioid receptors to exert its action on presynaptic nerve terminals. In the context of pain, the analgesic effect is mediated by the inhibition of GABA release, which allows for the production and release of dopamine. The release of this particular neurotransmitter has been strongly associated with the feeling of pleasure or euphoria (Sprouse-Blum et al., 2010). Early work in rats has shown that ICV injection of β-endorphin stimulated locomotion at low to moderate doses, however at high doses it led to catalepsy (Spanagel et al., 1991). In μ opioid receptor KO mice, no significant change in basal

locomotion was observed (Hall et al., 2004). Finally, characterization of β-endorphin ablated mice yielded mild phenotypes mainly associating increased feeding with a slight elevation in BW (Appleyard et al., 2003). As a result, the role of this neuropeptide in energy expenditure has been greatly overlooked. By combining the benefits of neuronal and spatially specific deletion in adult mice, we have shown that β-endorphin is a major contributor to maintaining basal energy balance.

In the future, the inability to account for the dramatically elevated FI and BW of $ARC^{\Delta POMC}$ mice requires further investigation. As previously stated, when the fragments were independently deleted we observed unique impairments in thermogenesis and locomotion but neither accounted for the hyperphagia and BW gain, even when taken together. We hypothesize that there could be two explanations for this phenomenon. First, both α-MSH and β-endorphin may work together to produce a greater effect. Second, one or more neuropeptides besides α-MSH or β-endorphin derived from POMC may play a partial role. Of interest, previous work that crossed β-endorphin KO mice with MC4R KO mice observed significantly higher FI then with β-endorphin KO or MC4R KO mice alone. Unfortunately, changes in BW were not reported (Appleyard et al., 2003). However, this does implies that our first hypothesis could be correct. To validate this, we would simply construct a CRISPR immune re-expression virus lacking both α-MSH and β-endorphin. Identical to our previously discussed experiments, the endogenous expressing POMC in the ARC would be ablated through the administration of our gRNA. Then with the incorporation of our virally delivered Δα-MSH/β-endorphin, we can determine if the absence of both peptides results in a greater phenotypical response then single deletion alone. If unsuccessful, then further ablation of POMC derived fragments will have to be performed systematically to interpret their individual roles. Briefly, this novel technique could be further utilized to decipher the role of other

complicated systems involving a gene that is post-translationally cleaved to give rise to multiple biologically active fragments. In summary, we have identified the roles of two key POMC derived fragments: α-MSH and β-endorphin. Further work needs to be done to fully understand how POMC regulates energy balance.

4.5 CART in the regulation of whole body glucose

In pursuit of a secondary target for whole body glucose control, we came across the neuropeptide CART. It was first described in the early 1980's due to the upregulation of its mRNA following acute administration of cocaine or amphetamine. It was later named cocaine and amphetamine regulated transcript for this fact (Douglass et al., 1995; Spiess et al., 1981). *CART* produces two alternatively spliced mRNAs of different lengths, called pro-CART 1-89 and proCART 1-102 (Douglass and Daoud, 1996). Of note, the differences in mRNA splicing do not affect the final peptides produced, since the sequence is downstream of the splice regions. However, the proCART peptides are post-translationally modified to produce at least two biologically active peptides, CART 55-102 and CART 62-102 (Dey et al., 2003). These active peptides are highly conserved between rodents and humans, sharing 95% of their amino acid sequence(Dominguez, 2006). This suggests that CART could serve a critical physiological function. Due to the nature of its discovery, the bulk of the research involving CART initially focused on its potential role in addiction and reward (Vicentic and Jones, 2007). Interestingly, CART mRNA was found to be expressed in high levels in the hypothalamus, especially in the ARC (Gautvik et al., 1996). This suggests that CART may play a significant role in homeostatic regulation. Importantly, 95% of POMC neurons in the ARC are found to express CART (Elias et al., 2001; Vrang et al., 1999) and its expression has been linked to the metabolic state, correlating to circulating leptin levels (Elias et al., 1998). CART has been shown to be significantly reduced in the ARC in leptin deficiency induced

diabetic rodent models (Kristensen et al., 1998). In the ARC, peripheral leptin administration was sufficient to elevate levels of CART mRNA (Elias et al., 2001). Even though evidence has shown the potential of CART to regulate glucose homeostasis, much is still unknown due to the lack of tools. Currently, the CART receptor has yet to be identified preventing the development of efficient pharmacological blockers for CART. In the late 1990s, binding studies were performed using radiolabeled CART to find its receptor (Hubert et al., 2008). Disappointingly, none of the studies were able to conclusively provide a suitable target. Plausible reasons for the inability to identify the receptor include low affinity to the radiolabeled peptide, low receptor number and non-specific binding. Alternative approaches included the use of known receptors and ligands to determine if CART 55-102 administration could block or alter these interactions (Vicentic et al., 2006). Following the study of a large number of peptide receptors, no interaction was detected. This implies that the CART receptor has yet to be identified. Nonetheless, there have been promising findings which suggest that CART acts through an inhibitory G-protein-coupling receptor that couples to $G_{i/o}$ proteins. Following a screen of numerous cell lines, AtT20 cells were identified as CART responsive. It was shown that CART 55-102 administration to these cells resulted in an increase in P-ERk-1 and P-ERK-2 (Lakatos et al., 2005). These findings were also confirmed by another group which replicated the experiment (Vicentic et al., 2005). More importantly, the addition of pertussis toxin which blocks G_i or G_o from interacting with its receptors was able to completely ablate CART's actions on these cells, indicating the importance of this pathway in CART signaling (Lakatos et al., 2005). Following this work, others have also shown that CART binds to rat adrenal pheochromocytoma PC12 cells (Maletinska et al., 2007). Consistent with work done in AtT20 cells, treatment with CART increased P-ERK and application of pertussis toxin blocked this effect (Lin et al., 2011). As a result, there is ongoing work to develop good agonists and antagonists for the

CART receptor, but to date none are considered viable as a therapeutic agent (Rogge et al., 2008). Thus, many have relied on direct injection of active CART peptide (Kong et al., 2003; Lambert et al., 1998) or utilizing different strains of CART KO mice (Moffett et al., 2006) to identify CART's physiological roles. The majority of the initial findings have shown that ICV administration of the CART peptide inhibits feeding in rats (Lambert et al., 1998; Lau and Herzog, 2014). Consistent with these findings, chronic central infusion of CART inhibited FI and attenuated BW gain in lean and obese Zucker rats (Larsen et al., 2000). Contradictorily, reports have shown that specific administrations of high doses of CART in discrete hypothalamic nuclei are sufficient to significantly increase feeding (Abbott et al., 2001). Along these lines, chronic twice daily intra-arcuate injections of CART increased daytime FI and BW (Kong et al., 2003). Adding to the controversy are the observations that ICV administration of CART alters motor control and at high doses (5 µgram), even induces seizures (Aja et al., 2001; Keating et al., 2008). This opens the door to the possibility that the anorexic effect could be secondary to the impairment in locomotion. Central injection of CART is neither neuronal specific, nor has it provided clear evidence to CART's role in FI and energy regulation. Currently, there are two strains of CART KO mice available. The first group deleted exon one and two from the CART gene and replaced it with a neomycin resistant gene (Asnicar et al., 2001). The second group replaced all three exons of the gene with a His/Neo cassette (Wierup et al., 2005). In CART KO mice lacking exon one and two, no difference in BW and FI were observed in all three groups (WT, $CART^{+/-}$ and $CART^{-/-}$) during the monitoring period, which lasted 17 weeks. When placed on a HFD, only $CART^{-/-}$ mice showed modest increases in FI and BW gain compared to WT controls. The conclusions drawn from these findings were that CART may constitute a minor protective mechanism against obesity, but it does not seem to be a major anorectic signal like POMC (Asnicar et al., 2001). The CART KO strain with complete deletion of the whole gene also reported no

change in FI when placed on a normal chow diet. However at 40 weeks, there was a slight increase in BW compared to WT controls. Of note, they observed increased basal blood insulin and impaired glucose elimination when challenged with a bolus of glucose. They contributed their findings to reduced islet function which they hypothesized may come from an unknown neural pathway (Wierup et al., 2005). With CART KO mice, the main concerns are developmental compensation and the global nature of the depletion. However, with CRISPR/Cas9 *in vivo* neuropeptide deletion, we were able overcome many of the discussed caveats. Our detailed physiological characterization of $ARC^{\Delta CARTpt}$ mice indicates that CART in ARC^{POMC} neurons does not affect energy homeostasis. Remarkably, $ARC^{\Delta CARTpt}$ resulted in the development of hyperglycemia. Consistent with acute neuronal activation of POMC neurons, we observed the transverse effects as it pertains to IS and gluconeogenesis. Furthermore, neuronal activation of $ARC^{\Delta CARTpt}$ mice completely attenuates the acute effects on whole body BG as previously reported. As a result, CART in POMC neurons directly controls glucose homeostasis through modulation of IS and gluconeogenesis in the liver without affecting energy expenditure. In combination, with our in-vitro work and the development of our novel ciCART viral vector, which prevents $ARC^{\Delta CARTpt}$, we were able to show that the observed hyperglycemia was not due to off target effects, but exclusively due to depletion of CART in the ARC. With the successful deletion of CART in the ARC an interesting next step may be to explore the other neuronal population that expresses CART in the hypothalamus, MCH neurons in the LH. Early *in situ* hybridization studies have shown that CART mRNA co-localizes with 70% of MCH neurons in the LH (Elias et al., 2001). In MCH KO mice, many interesting phenotypes have emerged including reduced BW, increased locomotion and wakefulness (Kokkotou et al., 2005; Shimada et al., 1998; Willie et al., 2008). In addition, reducing MCH neurons' ability to be excited by elevated levels of extracellular glucose results in impaired glucose tolerance. When these cells

are genetically altered to be hypersensitive to glucose, glucose tolerance is improved (Kong et al., 2010). Of great interest, neuronal ablation using diphtheria toxin resulted in many of the same observation leanness and hyperactivity phenotypes, but inconsistent with MCH KO mice glucose tolerance improved. They concluded that MCH neurons control glucose clearance through a signaling pathway independent of MCH (Whiddon and Palmiter, 2013). Given the CRISPR tools developed in our lab and the availability of MCH-Cre transgenic mice (Kong et al., 2010), it would not be difficult to translate the work done here to this sub-population of neurons. In particular, it would be of great importance to determine if CART plays a role in energy expenditure and if it may be the unknown signaling peptide responsible for glucose control in MCH neurons.

4.6 CART depletion in the ARC contribute to the pathogenesis of T2D and T1D

As stated previously, it has been observed that CART is dramatically reduced in the hypothalamus in diabetic mice. In leptin deficient *ob/ob* mice, CART mRNA levels were dramatically reduced compared to heterozygous controls. Interestingly, expression was also reduced in the LH, but not to the same extent. Following chronic injection of leptin, expression of CART mRNA in the ARC was restored, providing evidence that CART mRNA expression is controlled by the energy state of the system (Kristensen et al., 1998). In addition, rats fed a HFD for 14 weeks showed a marked decrease in CART positive cells in the ARC. As stated previously, it has been shown that hyperglycemia is often a comorbidity with obesity over time. Finally, microarray analysis of STZ-induced T1D mice which developed severe hyperglycemia (>500mg/dl) showed a shift to lower CART gene expression compared to controls (Xu et al., 2016). Following validation of our diabetic models, we came to the same conclusion that both CART mRNA and protein expression levels were markedly reduced. With the development of viral tools earlier in our studies, we answered the previously unexplored question: what is the role

of CART in the pathogenesis of diabetes? Using our Cre-dependent viral expression vector, we maintained elevated levels of CART in the ARC, independent of external stresses caused by the progression of T2D or T1D. In HFD induced T2D mice pretreated with AAV-FLEX-CART, hyperglycemia was significantly attenuated. This is attributed to the maintenance of IS in the periphery and gluconeogenesis in the liver. Although moderate elevation of BG was observed in CART over-expression mice on HFD, this suggests that other neuronal populations might play a role in glucose homeostasis, and which become dysregulated as a result of prolonged exposure to HFD. In addition, it is also possible that incomplete viral infection of the ARC may contribute to the observed variation. Since leptin monotherapies have been previously shown to rescue lethality in insulin deficient T1D models by maintaining normal glucose and lipid metabolism (Fujikawa et al., 2010), we hypothesize that the transient improvement in BG and modest survival benefit we observed is mainly due to the reduction in circulating leptin. One of the main characteristics of T1D is the reduction of WAT, the main source of leptin, from the underutilization of glucose following meals. As a result, the synergistic nature of insulin depletion and reduced circulating leptin could potentially mute the effects of CART in the ARC. An intriguing observation similar to the findings made in leptin deficient *ob/ob* mice is that CART expression is reduced in the LH, which co-localizes with MCH containing neurons It has been suggested that glucose control by these neurons is achieved through an independent pathway separate from MCH (Whiddon and Palmiter, 2013). If the experiment proposed in the previous section elicits impairment in glucose homeostasis, then the logical next step would be to use our viral expression vector to determine if the reduction of CART in MCH neurons has any physiological benefit.

4.7 The downstream glucoregulatory circuit

POMC neurons in the ARC innervate many common second order structures which are known to be important sites for whole body homeostasis (Bouret et al., 2004; Gao et al., 2008). Through our unbiased screening process, we identified the PVH as a key region that is highly modulated by ARC^{POMC} neurons to maintain glucose homeostasis. Unsurprisingly, the connection between the ARC and PVH has been well characterized due to the importance of the melanocortin pathway (Garfield et al., 2015). In addition, the PVH is known to be a key convergent point in the control of consumption and energy expenditure. The PVH utilizes two mechanisms to alter neuroendocrine outflow through the hypothalamic-pituitary axis and affect sympathetic or parasympathetic system through the preganglionic neurons (Hill, 2012). These mechanisms allow the PVH to maintain homeostasis through changes in the peripheral tissues including WAT, BAT, the liver, and pancreas (Jansen et al., 1997; Song et al., 2008; Stanley et al., 2010). The control of key organs and tissues by the PVH coincides with the peripheral alteration observed with both acute excitation of ARC^{POMC} neurons and the ablation of CART from the ARC. If provided the time and resources, we would further investigate which sub-population of neurons is being modulated by CART from the ARC to maintain BG homeostasis. A very simplistic approach is to first perform IHC to determine which population of neurons is effected by CART administration. As shown, ICV administration of CART into the PVH is sufficient to reduce c-Fos activity in STZ treated mice. If good antibodies can be attained, double IHC can be performed and quantified to assess which group of neurons may be potential targets. If a Cre line is available, whole cell patch recordings can be performed on these neurons to determine if CART administration to the buffer can cause hyperpolarization and reduced firing rates. Finally, using viral chemogenetics to inhibit these neurons, we should be able to

observe a reduction in basal BG similar to ARC POMC excitation. This clear readout could be used to validate these findings. Unfortunately, due to current limitations, neuronal sub-populations within the PVH targeted by ARC^{POMC} neurons in BG regulation remain unidentified, making investigation very difficult.

4.8 Conclusion and proposed model

In conclusion, this study reveals novel complexity as pertaining to ARC POMC neuronal control of energy and glucose homeostasis. We have not only reaffirmed the importance of ARC POMC neurons in the regulation of BW and energy balance, but that the hyperglycemic effect is driven by a peptide, CART, which is not derived from POMC. Using the CRISPR techniques (native and Cas9-immune) developed in our lab, we were able to dissect the roles of POMC-derived biologically active fragments and show that there are clear divergent roles for both α-MSH and β-endorphin. This brings clarity to a field that has previously relied on non-specific mouse models. Not only do these studies bring to light the underlying molecular mechanism for energy balance, but they also provide insight into the role of CART in glucose regulation and the pathogenesis of diabetes. The specific deletion of CART from ARC POMC neurons resulted in hyperglycemia without any observable changes to energy homeostasis. Combining our recent findings and previous observations in diabetic models, we were able to show that CART depletion in the ARC plays a significant role in the progression of diabetes. Finally, using our unbiased approach, we were able to isolate a region of interest and establish a downstream gluco-regulatory circuit between ARC POMC neurons and the PVH. The divergent roles of neuropeptides uncovered in this study provide an additional layer of complexity to the regulation of energy and glucose homeostasis by POMC neurons and provide a novel target to treat hyperglycemia and obesity (Figure 4.2). In addition, the identification of this neural circuit provides a promising starting point for

further identification of the connection between the CNS and the periphery. Further investigation into the identification of the CART receptor and its expression pattern is a priority in elucidating the efferent pathways that control glucose homeostasis and could potentially lead to new therapeutic treatments for diabetes. Furthermore, we hope that these techniques can be used to revisit previous findings reveal novel circuits and complex mechanisms in other fields of research, as they proved in ours.

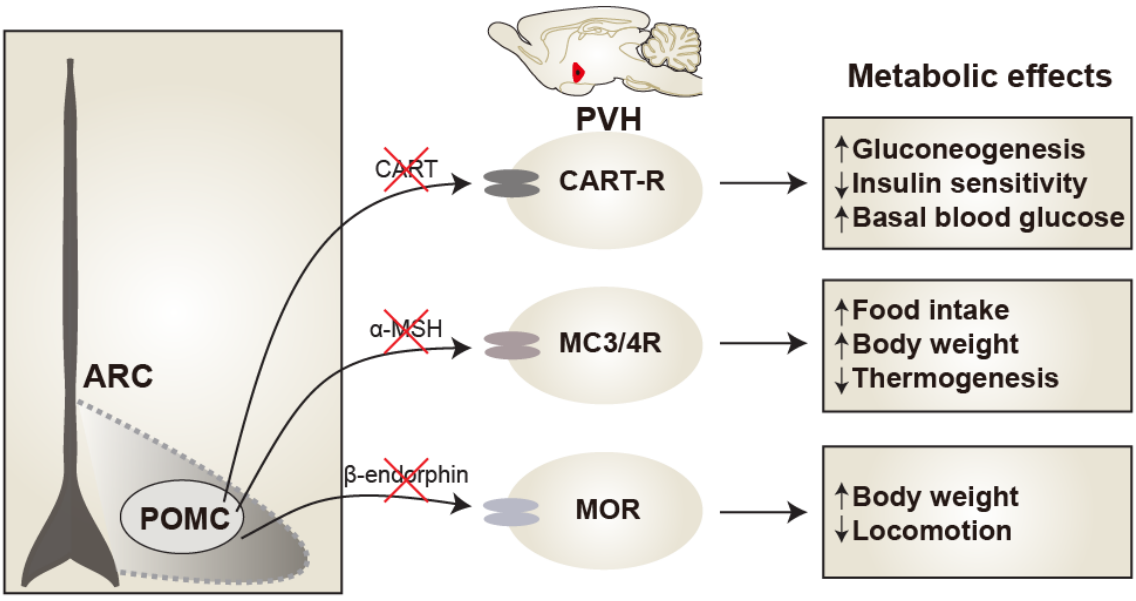

Figure 4.2: A model of ARC^{POMC} neuronal regulation of energy and glucose balance. In our study, we identified clear divergent roles of neuropeptides synthesized and released from ARC^{POMC} neurons. POMC derived α-MSH when released from POMC neurons binds to melanocortin 3/4 receptors (MC3/4R) expressing cells downstream. With specific ablation of α-MSH in the ARC of adult mice using a combination of CRISPR and viral techniques, we noted increases in food intake and a reduction of thermogenesis which resulting in increased body weight. B-endorphin another POMC derived neuropeptide on the other hand, interacts with μ opioid receptors (MOR) and when deleted from ARC^{POMC} neurons resulted in reduced locomotion and increased body weight. Neither α-MSH or β-endorphin ablation contributed to elevated basal blood glucose within the 4 week monitoring period. Alternatively, CART depletion resulted in increased gluconeogenesis in the liver and decreases in insulin sensitivity, culminating in elevated levels of basal blood glucose. Even though the CART receptor has yet to be identified using optogenetics and chemogenetics we identified the PVH as the main downstream glucoregulatory target and the way POMC neurons modulate the periphery.

Chapter 5: Bibliography

Abbott, C.R., Rossi, M., Wren, A.M., Murphy, K.G., Kennedy, A.R., Stanley, S.A., Zollner, A.N., Morgan, D.G., Morgan, I., Ghatei, M.A*., et al.* (2001). Evidence of an orexigenic role for cocaine- and amphetamine-regulated transcript after administration into discrete hypothalamic nuclei. Endocrinology *142*, 3457-3463.
Aguilar-Bryan, L., Clement, J.P.t., Gonzalez, G., Kunjilwar, K., Babenko, A., and Bryan, J. (1998). Toward understanding the assembly and structure of KATP channels. Physiological reviews *78*, 227-245.
Aja, S., Sahandy, S., Ladenheim, E.E., Schwartz, G.J., and Moran, T.H. (2001). Intracerebroventricular CART peptide reduces food intake and alters motor behavior at a hindbrain site. American journal of physiology Regulatory, integrative and comparative physiology *281*, R1862-1867.
Alexander, G.M., Rogan, S.C., Abbas, A.I., Armbruster, B.N., Pei, Y., Allen, J.A., Nonneman, R.J., Hartmann, J., Moy, S.S., Nicolelis, M.A*., et al.* (2009). Remote control of neuronal activity in transgenic mice expressing evolved G protein-coupled receptors. Neuron *63*, 27-39.
Alon, T., and Friedman, J.M. (2006). Late-onset leanness in mice with targeted ablation of melanin concentrating hormone neurons. The Journal of neuroscience : the official journal of the Society for Neuroscience *26*, 389-397.
Anand, B.K., and Brobeck, J.R. (1951). Localization of a "feeding center" in the hypothalamus of the rat. Proceedings of the Society for Experimental Biology and Medicine Society for Experimental Biology and Medicine (New York, NY) *77*, 323-324.
Aponte, Y., Atasoy, D., and Sternson, S.M. (2011). AGRP neurons are sufficient to orchestrate feeding behavior rapidly and without training. Nature neuroscience *14*, 351-355.
Appleyard, S.M., Hayward, M., Young, J.I., Butler, A.A., Cone, R.D., Rubinstein, M., and Low, M.J. (2003). A role for the endogenous opioid beta-endorphin in energy homeostasis. Endocrinology *144*, 1753-1760.
Arletti, R., Benelli, A., and Bertolini, A. (1990). Oxytocin inhibits food and fluid intake in rats. Physiology & behavior *48*, 825-830.
Armbruster, B.N., Li, X., Pausch, M.H., Herlitze, S., and Roth, B.L. (2007). Evolving the lock to fit the key to create a family of G protein-coupled receptors potently activated by an inert ligand. Proceedings of the National Academy of Sciences of the United States of America *104*, 5163-5168.
Asnicar, M.A., Smith, D.P., Yang, D.D., Heiman, M.L., Fox, N., Chen, Y.F., Hsiung, H.M., and Koster, A. (2001). Absence of cocaine- and amphetamine-regulated transcript results in obesity in mice fed a high caloric diet. Endocrinology *142*, 4394-4400.
Atasoy, D., Aponte, Y., Su, H.H., and Sternson, S.M. (2008). A FLEX switch targets Channelrhodopsin-2 to multiple cell types for imaging and long-range circuit mapping. The Journal of neuroscience : the official journal of the Society for Neuroscience *28*, 7025-7030.
Atasoy, D., Betley, J.N., Su, H.H., and Sternson, S.M. (2012). Deconstruction of a neural circuit for hunger. Nature *488*, 172-177.
Balagura, S., and Devenport, L.D. (1970). Feeding patterns of normal and ventromedial hypothalamic lesioned male and female rats. Journal of comparative and physiological psychology *71*, 357-364.

Balcita-Pedicino, J.J., and Sesack, S.R. (2007). Orexin axons in the rat ventral tegmental area synapse infrequently onto dopamine and gamma-aminobutyric acid neurons. The Journal of comparative neurology *503*, 668-684.
Balland, E., Dam, J., Langlet, F., Caron, E., Steculorum, S., Messina, A., Rasika, S., Falluel-Morel, A., Anouar, Y., Dehouck, B.*, et al.* (2014). Hypothalamic tanycytes are an ERK-gated conduit for leptin into the brain. Cell metabolism *19*, 293-301.
Balthasar, N., Coppari, R., McMinn, J., Liu, S.M., Lee, C.E., Tang, V., Kenny, C.D., McGovern, R.A., Chua, S.C., and Elmquist, J.K. (2004a). Leptin receptor signaling in POMC neurons is required for normal body weight homeostasis. Neuron *42*, 983-991.
Balthasar, N., Coppari, R., McMinn, J., Liu, S.M., Lee, C.E., Tang, V., Kenny, C.D., McGovern, R.A., Chua, S.C., Jr., Elmquist, J.K.*, et al.* (2004b). Leptin receptor signaling in POMC neurons is required for normal body weight homeostasis. Neuron *42*, 983-991.
Bamshad, M., Aoki, V.T., Adkison, M.G., Warren, W.S., and Bartness, T.J. (1998). Central nervous system origins of the sympathetic nervous system outflow to white adipose tissue. The American journal of physiology *275*, R291-299.
Barbano, F.M., Wang, H.-L., Morales, M., and Wise, R.A. (2016). Feeding and Reward Are Differentially Induced by Activating GABAergic Lateral Hypothalamic Projections to VTA. The Journal of Neuroscience *36*, 2975-2985.
Beck-Peccoz, P., Rodari, G., Giavoli, C., and Lania, A. (2017). Central hypothyroidism - a neglected thyroid disorder. Nature reviews Endocrinology *13*, 588-598.
Becker, E.E., and Kissileff, H.R. (1974). Inhibitory controls of feeding by the ventromedial hypothalamus. The American journal of physiology *226*, 383-396.
Beenken, A., and Mohammadi, M. (2009). The FGF family: biology, pathophysiology and therapy. Nature reviews Drug discovery *8*, 235-253.
Bellinger, L.L., and Bernardis, L.L. (2002). The dorsomedial hypothalamic nucleus and its role in ingestive behavior and body weight regulation: lessons learned from lesioning studies. Physiology & behavior *76*, 431-442.
Berglund, E.D., Vianna, C.R., Donato, J., Jr., Kim, M.H., Chuang, J.C., Lee, C.E., Lauzon, D.A., Lin, P., Brule, L.J., Scott, M.M.*, et al.* (2012). Direct leptin action on POMC neurons regulates glucose homeostasis and hepatic insulin sensitivity in mice. The Journal of clinical investigation *122*, 1000-1009.
Bernardis, L.L. (1970). Participation of the dorsomedial hypothalamic nucleus in the "feeding center" and water intake circuitry of the weanling rat. Journal of neuro-visceral relations *31*, 387-398.
Bernardis, L.L., Box, B.M., and Stevenson, J.A. (1963). Growth following hypothalamic lesions in the weanling rat. Endocrinology *72*, 684-692.
Bingham, N.C., Anderson, K.K., Reuter, A.L., Stallings, N.R., and Parker, K.L. (2008). Selective loss of leptin receptors in the ventromedial hypothalamic nucleus results in increased adiposity and a metabolic syndrome. Endocrinology *149*, 2138-2148.
Bingham, N.C., Verma-Kurvari, S., Parada, L.F., and Parker, K.L. (2006). Development of a steroidogenic factor 1/Cre transgenic mouse line. Genesis (New York, NY : 2000) *44*, 419-424.
Birrer, M.J., Johnson, M.E., Hao, K., Wong, K.K., Park, D.C., Bell, A., Welch, W.R., Berkowitz, R.S., and Mok, S.C. (2007). Whole genome oligonucleotide-based array comparative genomic hybridization analysis identified fibroblast growth factor 1 as a prognostic marker for advanced-stage serous ovarian adenocarcinomas. Journal of clinical oncology : official journal of the American Society of Clinical Oncology *25*, 2281-2287.
Bjursell, M., Gerdin, A.K., Ploj, K., Svensson, D., Svensson, L., Oscarsson, J., Snaith, M., Tornell, J., and Bohlooly, Y.M. (2006). Melanin-concentrating hormone receptor 1 deficiency increases

insulin sensitivity in obese leptin-deficient mice without affecting body weight. Diabetes *55*, 725-733.
Blackwell, J. (2004). Evaluation and treatment of hyperthyroidism and hypothyroidism. Journal of the American Academy of Nurse Practitioners *16*, 422-425.
Blake, N.G., Eckland, D.J., Foster, O.J., and Lightman, S.L. (1991). Inhibition of hypothalamic thyrotropin-releasing hormone messenger ribonucleic acid during food deprivation. Endocrinology *129*, 2714-2718.
Borg, W.P., Sherwin, R.S., During, M.J., Borg, M.A., and Shulman, G.I. (1995). Local ventromedial hypothalamus glucopenia triggers counterregulatory hormone release. Diabetes *44*, 180-184.
Borgland, S.L., Taha, S.A., Sarti, F., Fields, H.L., and Bonci, A. (2006). Orexin A in the VTA Is Critical for the Induction of Synaptic Plasticity and Behavioral Sensitization to Cocaine. Neuron *49*, 589-601.
Bouret, S.G., Draper, S.J., and Simerly, R.B. (2004). Formation of projection pathways from the arcuate nucleus of the hypothalamus to hypothalamic regions implicated in the neural control of feeding behavior in mice. The Journal of neuroscience : the official journal of the Society for Neuroscience *24*, 2797-2805.
Boutrel, B., Kenny, P.J., Specio, S.E., Martin-Fardon, R., Markou, A., Koob, G.F., and de Lecea, L. (2005). Role for hypocretin in mediating stress-induced reinstatement of cocaine-seeking behavior. Proceedings of the National Academy of Sciences of the United States of America *102*, 19168-19173.
Brady, L.S., Smith, M.A., Gold, P.W., and Herkenham, M. (1990). Altered expression of hypothalamic neuropeptide mRNAs in food-restricted and food-deprived rats. Neuroendocrinology *52*, 441-447.
Breen, D.M., Rasmussen, B.A., Cote, C.D., Jackson, V.M., and Lam, T.K. (2013). Nutrient-sensing mechanisms in the gut as therapeutic targets for diabetes. Diabetes *62*, 3005-3013.
Brobeck, J.R., Tepperman, J., and Long, C.N. (1943). Experimental Hypothalamic Hyperphagia in the Albino Rat. The Yale journal of biology and medicine *15*, 831-853.
Brooks, C.M., and Lambert, H.F. (1946). A study of the effect of limitation of food intake and the method of feeding on the rate of weight gain during hypothalamic obesity in the albino rat. The American journal of physiology *147*, 695-707.
Bruning, J.C., Gautam, D., Burks, D.J., Gillette, J., Schubert, M., Orban, P.C., Klein, R., Krone, W., Muller-Wieland, D., and Kahn, C.R. (2000). Role of brain insulin receptor in control of body weight and reproduction. Science (New York, NY) *289*, 2122-2125.
Butler, A.A., Kesterson, R.A., Khong, K., Cullen, M.J., Pelleymounter, M.A., Dekoning, J., Baetscher, M., and Cone, R.D. (2000). A unique metabolic syndrome causes obesity in the melanocortin-3 receptor-deficient mouse. Endocrinology *141*, 3518-3521.
Calton, M.A., Ersoy, B.A., Zhang, S., Kane, J.P., Malloy, M.J., Pullinger, C.R., Bromberg, Y., Pennacchio, L.A., Dent, R., McPherson, R.*, et al.* (2009). Association of functionally significant Melanocortin-4 but not Melanocortin-3 receptor mutations with severe adult obesity in a large North American case-control study. Human molecular genetics *18*, 1140-1147.
Campfield, L.A., Smith, F.J., Guisez, Y., Devos, R., and Burn, P. (1995). Recombinant mouse OB protein: evidence for a peripheral signal linking adiposity and central neural networks. Science (New York, NY) *269*, 546-549.
Castro, M.G., and Morrison, E. (1997). Post-translational processing of proopiomelanocortin in the pituitary and in the brain. Critical reviews in neurobiology *11*, 35-57.
Cerritelli, S., Hirschberg, S., Hill, R., Balthasar, N., and Pickering, A.E. (2016). Activation of Brainstem Pro-opiomelanocortin Neurons Produces Opioidergic Analgesia, Bradycardia and Bradypnoea. PLOS ONE *11*.

Chao, P.T., Yang, L., Aja, S., Moran, T.H., and Bi, S. (2011). Knockdown of NPY expression in the dorsomedial hypothalamus promotes development of brown adipocytes and prevents diet-induced obesity. Cell metabolism *13*, 573-583.
Chaudhri, O., Small, C., and Bloom, S. (2006). Gastrointestinal hormones regulating appetite. … of the Royal ….
Chhabra, K.H., Adams, J.M., Fagel, B., Lam, D.D., Qi, N., Rubinstein, M., and Low, M.J. (2016). Hypothalamic POMC Deficiency Improves Glucose Tolerance Despite Insulin Resistance by Increasing Glycosuria. Diabetes *65*, 660-672.
Chiang, J.Y. (2009). Bile acids: regulation of synthesis. Journal of lipid research *50*, 1955-1966.
Choudhury, A.I., Heffron, H., Smith, M.A., Al-Qassab, H., Xu, A.W., Selman, C., Simmgen, M., Clements, M., Claret, M., Maccoll, G.*, et al.* (2005). The role of insulin receptor substrate 2 in hypothalamic and beta cell function. The Journal of clinical investigation *115*, 940-950.
Claret, M., Smith, M.A., Batterham, R.L., Selman, C., Choudhury, A.I., Fryer, L.G., Clements, M., Al-Qassab, H., Heffron, H., Xu, A.W.*, et al.* (2007). AMPK is essential for energy homeostasis regulation and glucose sensing by POMC and AgRP neurons. The Journal of clinical investigation *117*, 2325-2336.
Clarke, G., Stilling, R.M., Kennedy, P.J., Stanton, C., Cryan, J.F., and Dinan, T.G. (2014). Minireview: Gut microbiota: the neglected endocrine organ. Molecular endocrinology (Baltimore, Md) *28*, 1221-1238.
Coll, A.P., Challis, B.G., Yeo, G.S., Snell, K., Piper, S.J., Halsall, D., Thresher, R.R., and O'Rahilly, S. (2004). The effects of proopiomelanocortin deficiency on murine adrenal development and responsiveness to adrenocorticotropin. Endocrinology *145*, 4721-4727.
Collin, M., Backberg, M., Ovesjo, M.L., Fisone, G., Edwards, R.H., Fujiyama, F., and Meister, B. (2003). Plasma membrane and vesicular glutamate transporter mRNAs/proteins in hypothalamic neurons that regulate body weight. The European journal of neuroscience *18*, 1265-1278.
Collins, S.M., Surette, M., and Bercik, P. (2012). The interplay between the intestinal microbiota and the brain. Nature reviews Microbiology *10*, 735-742.
Cone, R.D. (1999). The Central Melanocortin System and Energy Homeostasis. Trends in endocrinology and metabolism: TEM *10*, 211-216.
Cone, R.D. (2005). Anatomy and regulation of the central melanocortin system. Nature neuroscience *8*, 571-578.
Cool, D.R., Normant, E., Shen, F., Chen, H.C., Pannell, L., Zhang, Y., and Loh, Y.P. (1997). Carboxypeptidase E is a regulated secretory pathway sorting receptor: genetic obliteration leads to endocrine disorders in Cpe(fat) mice. Cell *88*, 73-83.
Coppari, R., Ichinose, M., Lee, C.E., Pullen, A.E., Kenny, C.D., McGovern, R.A., Tang, V., Liu, S.M., Ludwig, T., Chua, S.C., Jr.*, et al.* (2005). The hypothalamic arcuate nucleus: a key site for mediating leptin's effects on glucose homeostasis and locomotor activity. Cell metabolism *1*, 63-72.
Coppola, V., and Tessarollo, L. (2004). Control of hyperphagia prevents obesity in BDNF heterozygous mice. Neuroreport *15*, 2665-2668.
Coutinho, E.A., Okamoto, S., Ishikawa, A.W., Yokota, S., Wada, N., Hirabayashi, T., Saito, K., Sato, T., Takagi, K., Wang, C.C.*, et al.* (2017). Activation of SF1 Neurons in the Ventromedial Hypothalamus by DREADD Technology Increases Insulin Sensitivity in Peripheral Tissues. Diabetes *66*, 2372-2386.
Cowley, M.A., Smart, J.L., Rubinstein, M., Cerdan, M.G., Diano, S., Horvath, T.L., Cone, R.D., and Low, M.J. (2001). Leptin activates anorexigenic POMC neurons through a neural network in the arcuate nucleus. Nature *411*, 480-484.

Cummings, D.E., and Overduin, J. (2007). Gastrointestinal regulation of food intake. The Journal of clinical investigation *117*, 13-23.
David, L.A., Maurice, C.F., Carmody, R.N., Gootenberg, D.B., Button, J.E., Wolfe, B.E., Ling, A.V., Devlin, A.S., Varma, Y., Fischbach, M.A*., et al.* (2014). Diet rapidly and reproducibly alters the human gut microbiome. Nature *505*, 559-563.
Davis, A.M., Seney, M.L., Stallings, N.R., Zhao, L., Parker, K.L., and Tobet, S.A. (2004). Loss of steroidogenic factor 1 alters cellular topography in the mouse ventromedial nucleus of the hypothalamus. Journal of neurobiology *60*, 424-436.
Degirolamo, C., Sabba, C., and Moschetta, A. (2016). Therapeutic potential of the endocrine fibroblast growth factors FGF19, FGF21 and FGF23. Nature reviews Drug discovery *15*, 51-69.
Delgado, J.M., and Anand, B.K. (1953). Increase of food intake induced by electrical stimulation of the lateral hypothalamus. The American journal of physiology *172*, 162-168.
Demuro, A., Palma, E., Eusebi, F., and Miledi, R. (2001). Inhibition of nicotinic acetylcholine receptors by bicuculline. Neuropharmacology *41*, 854-861.
Dennison, C.S., King, C.M., Dicken, M.S., and Hentges, S.T. (2016). Age-dependent changes in amino acid phenotype and the role of glutamate release from hypothalamic proopiomelanocortin neurons. The Journal of comparative neurology *524*, 1222-1235.
Desbonnet, L., Clarke, G., Shanahan, F., Dinan, T.G., and Cryan, J.F. (2014). Microbiota is essential for social development in the mouse. Molecular psychiatry *19*, 146-148.
Dey, A., Xhu, X., Carroll, R., Turck, C.W., Stein, J., and Steiner, D.F. (2003). Biological processing of the cocaine and amphetamine-regulated transcript precursors by prohormone convertases, PC2 and PC1/3. The Journal of biological chemistry *278*, 15007-15014.
Dhillon, H., Zigman, J.M., Ye, C., Lee, C.E., McGovern, R.A., Tang, V., Kenny, C.D., Christiansen, L.M., White, R.D., Edelstein, E.A*., et al.* (2006). Leptin directly activates SF1 neurons in the VMH, and this action by leptin is required for normal body-weight homeostasis. Neuron *49*, 191-203.
Di Dalmazi, G., Pagotto, U., Pasquali, R., and Vicennati, V. (2012). Glucocorticoids and type 2 diabetes: from physiology to pathology. Journal of nutrition and metabolism *2012*, 525093.
Dietrich, M.O., Zimmer, M.R., Bober, J., and Horvath, T.L. (2015). Hypothalamic Agrp neurons drive stereotypic behaviors beyond feeding. Cell *160*, 1222-1232.
Dimitriadis, G., Leighton, B., Parry-Billings, M., Sasson, S., Young, M., Krause, U., Bevan, S., Piva, T., Wegener, G., and Newsholme, E.A. (1997). Effects of glucocorticoid excess on the sensitivity of glucose transport and metabolism to insulin in rat skeletal muscle. The Biochemical journal *321 (Pt 3)*, 707-712.
Dodd, G.T., Decherf, S., Loh, K., Simonds, S.E., Wiede, F., Balland, E., Merry, T.L., Munzberg, H., Zhang, Z.Y., Kahn, B.B*., et al.* (2015). Leptin and insulin act on POMC neurons to promote the browning of white fat. Cell *160*, 88-104.
Domingos, A.I., Sordillo, A., Dietrich, M.O., Liu, Z.-W.W., Tellez, L.A., Vaynshteyn, J., Ferreira, J.G., Ekstrand, M.I., Horvath, T.L., de Araujo, I.E*., et al.* (2013). Hypothalamic melanin concentrating hormone neurons communicate the nutrient value of sugar. eLife *2*.
Domingos, A.I., Vaynshteyn, J., Voss, H.U., Ren, X., Gradinaru, V., Zang, F., Deisseroth, K., de Araujo, I.E., and Friedman, J. (2011). Leptin regulates the reward value of nutrient. Nature Neuroscience *14*, 1562-1568.
Dominguez, G. (2006). The CART gene: structure and regulation. Peptides *27*, 1913-1918.
Douglass, J., and Daoud, S. (1996). Characterization of the human cDNA and genomic DNA encoding CART: a cocaine- and amphetamine-regulated transcript. Gene *169*, 241-245.
Douglass, J., McKinzie, A.A., and Couceyro, P. (1995). PCR differential display identifies a rat brain mRNA that is transcriptionally regulated by cocaine and amphetamine. The Journal of neuroscience : the official journal of the Society for Neuroscience *15*, 2471-2481.

Dunn-Meynell, A.A., Routh, V.H., Kang, L., Gaspers, L., and Levin, B.E. (2002). Glucokinase is the likely mediator of glucosensing in both glucose-excited and glucose-inhibited central neurons. Diabetes *51*, 2056-2065.
Elias, C.F., Lee, C., Kelly, J., Aschkenasi, C., Ahima, R.S., Couceyro, P.R., Kuhar, M.J., Saper, C.B., and Elmquist, J.K. (1998). Leptin activates hypothalamic CART neurons projecting to the spinal cord. Neuron *21*, 1375-1385.
Elias, C.F., Lee, C.E., Kelly, J.F., Ahima, R.S., Kuhar, M., Saper, C.B., and Elmquist, J.K. (2001). Characterization of CART neurons in the rat and human hypothalamus. The Journal of comparative neurology *432*, 1-19.
Elmquist, J.K., Bjorbaek, C., Ahima, R.S., Flier, J.S., and Saper, C.B. (1998). Distributions of leptin receptor mRNA isoforms in the rat brain. The Journal of comparative neurology *395*, 535-547.
Exton, J.H. (1979). Regulation of gluconeogenesis by glucocorticoids. Monographs on endocrinology *12*, 535-546.
Exton, J.H., Miller, T.B., Harper, S.C., and Park, C.R. (1976). Carbohydrate metabolism in perfused livers of adrenalectomized and steroid-replaced rats. The American journal of physiology *230*, 163-170.
Faith, J.J., Guruge, J.L., Charbonneau, M., Subramanian, S., Seedorf, H., Goodman, A.L., Clemente, J.C., Knight, R., Heath, A.C., Leibel, R.L.*, et al.* (2013). The long-term stability of the human gut microbiota. Science (New York, NY) *341*, 1237439.
Fan, W., Ellacott, K.L.J., Halatchev, I.G., Takahashi, K., Yu, P., and Cone, R.D. (2004). Cholecystokinin-mediated suppression of feeding involves the brainstem melanocortin system. Nature Neuroscience *7*, 335-336.
Fani, L., Bak, S., Delhanty, P., van Rossum, E.F., and van den Akker, E.L. (2014). The melanocortin-4 receptor as target for obesity treatment: a systematic review of emerging pharmacological therapeutic options. International journal of obesity (2005) *38*, 163-169.
Farooqi, I.S., Drop, S., Clements, A., Keogh, J.M., Biernacka, J., Lowenbein, S., Challis, B.G., and O'Rahilly, S. (2006). Heterozygosity for a POMC-null mutation and increased obesity risk in humans. Diabetes *55*, 2549-2553.
Fekete, C., Legradi, G., Mihaly, E., Huang, Q.H., Tatro, J.B., Rand, W.M., Emerson, C.H., and Lechan, R.M. (2000). alpha-Melanocyte-stimulating hormone is contained in nerve terminals innervating thyrotropin-releasing hormone-synthesizing neurons in the hypothalamic paraventricular nucleus and prevents fasting-induced suppression of prothyrotropin-releasing hormone gene expression. The Journal of neuroscience : the official journal of the Society for Neuroscience *20*, 1550-1558.
Fenselau, H., Campbell, J.N., Verstegen, A.M., Madara, J.C., Xu, J., Shah, B.P., Resch, J.M., Yang, Z., Mandelblat-Cerf, Y., Livneh, Y.*, et al.* (2017). A rapidly acting glutamatergic ARC-->PVH satiety circuit postsynaptically regulated by alpha-MSH. Nature neuroscience *20*, 42-51.
Ferguson, S.M., Eskenazi, D., Ishikawa, M., Wanat, M.J., Phillips, P.E., Dong, Y., Roth, B.L., and Neumaier, J.F. (2011). Transient neuronal inhibition reveals opposing roles of indirect and direct pathways in sensitization. Nature neuroscience *14*, 22-24.
Finak, G., Bertos, N., Pepin, F., Sadekova, S., Souleimanova, M., Zhao, H., Chen, H., Omeroglu, G., Meterissian, S., Omeroglu, A.*, et al.* (2008). Stromal gene expression predicts clinical outcome in breast cancer. Nature medicine *14*, 518-527.
Fioramonti, X., Contie, S., Song, Z., Routh, V.H., Lorsignol, A., and Penicaud, L. (2007). Characterization of glucosensing neuron subpopulations in the arcuate nucleus: integration in neuropeptide Y and pro-opio melanocortin networks? Diabetes *56*, 1219-1227.

Flak, J.N., Patterson, C.M., Garfield, A.S., D'Agostino, G., Goforth, P.B., Sutton, A.K., Malec, P.A., Wong, J.-M.T., Germani, M., Jones, J.C.*, et al.* (2014). Leptin-inhibited PBN neurons enhance responses to hypoglycemia in negative energy balance. Nature neuroscience *17*, 1744-1750.
Fu, L., John, L.M., Adams, S.H., Yu, X.X., Tomlinson, E., Renz, M., Williams, P.M., Soriano, R., Corpuz, R., Moffat, B.*, et al.* (2004). Fibroblast growth factor 19 increases metabolic rate and reverses dietary and leptin-deficient diabetes. Endocrinology *145*, 2594-2603.
Fuente-Martin, E., Garcia-Caceres, C., Granado, M., de Ceballos, M.L., Sanchez-Garrido, M.A., Sarman, B., Liu, Z.W., Dietrich, M.O., Tena-Sempere, M., Argente-Arizon, P.*, et al.* (2012). Leptin regulates glutamate and glucose transporters in hypothalamic astrocytes. The Journal of clinical investigation *122*, 3900-3913.
Fujikawa, T., Berglund, E.D., Patel, V.R., Ramadori, G., Vianna, C.R., Vong, L., Thorel, F., Chera, S., Herrera, P.L., Lowell, B.B.*, et al.* (2013). Leptin engages a hypothalamic neurocircuitry to permit survival in the absence of insulin. Cell metabolism *18*, 431-444.
Fujikawa, T., Chuang, J.C., Sakata, I., Ramadori, G., and Coppari, R. (2010). Leptin therapy improves insulin-deficient type 1 diabetes by CNS-dependent mechanisms in mice. Proc Natl Acad Sci U S A *107*, 17391-17396.
Fujikawa, T., and Coppari, R. (2015). Living without insulin: the role of leptin signaling in the hypothalamus. Frontiers in neuroscience *9*, 108.
Funato, H., Tsai, A.L., Willie, J.T., Kisanuki, Y., Williams, S.C., Sakurai, T., and Yanagisawa, M. (2009). Enhanced orexin receptor-2 signaling prevents diet-induced obesity and improves leptin sensitivity. Cell metabolism *9*, 64-76.
Furet, J.P., Kong, L.C., Tap, J., Poitou, C., Basdevant, A., Bouillot, J.L., Mariat, D., Corthier, G., Dore, J., Henegar, C.*, et al.* (2010). Differential adaptation of human gut microbiota to bariatric surgery-induced weight loss: links with metabolic and low-grade inflammation markers. Diabetes *59*, 3049-3057.
Furness, J.B. (2012). The enteric nervous system and neurogastroenterology. Nature reviews Gastroenterology & hepatology *9*, 286-294.
Galton, V.A., Wood, E.T., St Germain, E.A., Withrow, C.A., Aldrich, G., St Germain, G.M., Clark, A.S., and St Germain, D.L. (2007). Thyroid hormone homeostasis and action in the type 2 deiodinase-deficient rodent brain during development. Endocrinology *148*, 3080-3088.
Gao, Q., and Horvath, T.L. (2008). Neuronal control of energy homeostasis. FEBS letters *582*, 132-141.
Garfield, A.S., Lam, D.D., Marston, O.J., Przydzial, M.J., and Heisler, L.K. (2009). Role of central melanocortin pathways in energy homeostasis. Trends in endocrinology and metabolism: TEM *20*, 203-215.
Garfield, A.S., Li, C., Madara, J.C., Shah, B.P., Webber, E., Steger, J.S., Campbell, J.N., Gavrilova, O., Lee, C.E., Olson, D.P.*, et al.* (2015). A neural basis for melanocortin-4 receptor-regulated appetite. Nature neuroscience *18*, 863-871.
Garfield, A.S., Shah, B.P., Burgess, C.R., Li, M.M., Li, C., Steger, J.S., Madara, J.C., Campbell, J.N., Kroeger, D., Scammell, T.E.*, et al.* (2016). Dynamic GABAergic afferent modulation of AgRP neurons. Nature neuroscience *19*, 1628-1635.
Gautron, L., Elmquist, J.K., and Williams, K.W. (2015). Neural control of energy balance: translating circuits to therapies. Cell *161*, 133-145.
Gautvik, K.M., de Lecea, L., Gautvik, V.T., Danielson, P.E., Tranque, P., Dopazo, A., Bloom, F.E., and Sutcliffe, J.G. (1996). Overview of the most prevalent hypothalamus-specific mRNAs, as identified by directional tag PCR subtraction. Proceedings of the National Academy of Sciences of the United States of America *93*, 8733-8738.

Geerling, J.C., Shin, J.W., Chimenti, P.C., and Loewy, A.D. (2010). Paraventricular hypothalamic nucleus: axonal projections to the brainstem. The Journal of comparative neurology *518*, 1460-1499.
Geerling, J.J., Boon, M.R.R., Kooijman, S., Parlevliet, E.T., Havekes, L.M., Romijn, J.A., Meurs, I.M., and Rensen, P.C. (2014). Sympathetic nervous system control of triglyceride metabolism: novel concepts derived from recent studies. Journal of lipid research *55*, 180-189.
Ghamari-Langroudi, M., Vella, K.R., Srisai, D., Sugrue, M.L., Hollenberg, A.N., and Cone, R.D. (2010). Regulation of thyrotropin-releasing hormone-expressing neurons in paraventricular nucleus of the hypothalamus by signals of adiposity. Molecular endocrinology (Baltimore, Md) *24*, 2366-2381.
Goncalves, G.H., Li, W., Garcia, A.V., Figueiredo, M.S., and Bjorbaek, C. (2014). Hypothalamic agouti-related peptide neurons and the central melanocortin system are crucial mediators of leptin's antidiabetic actions. Cell reports *7*, 1093-1103.
Graessler, J., Qin, Y., Zhong, H., Zhang, J., Licinio, J., Wong, M.L., Xu, A., Chavakis, T., Bornstein, A.B., Ehrhart-Bornstein, M.*, et al.* (2013). Metagenomic sequencing of the human gut microbiome before and after bariatric surgery in obese patients with type 2 diabetes: correlation with inflammatory and metabolic parameters. The pharmacogenomics journal *13*, 514-522.
Graff, H., and Stellar, E. (1962). Hyperphagia, obesity, and finickiness. Journal of comparative and physiological psychology *55*, 418-424.
Grill, H.J., and Hayes, M.R. (2009). The nucleus tractus solitarius: a portal for visceral afferent signal processing, energy status assessment and integration of their combined effects on food intake. International Journal of Obesity *33*.
Grill, H.J., and Hayes, M.R. (2012). Hindbrain Neurons as an Essential Hub in the Neuroanatomically Distributed Control of Energy Balance. Cell Metabolism *16*, 296-309.
Gropp, E., Shanabrough, M., Borok, E., Xu, A.W., Janoschek, R., Buch, T., Plum, L., Balthasar, N., Hampel, B., Waisman, A.*, et al.* (2005). Agouti-related peptide-expressing neurons are mandatory for feeding. Nature neuroscience *8*, 1289-1291.
Grossman, S.P., Dacey, D., Halaris, A.E., Collier, T., and Routtenberg, A. (1978). Aphagia and adipsia after preferential destruction of nerve cell bodies in hypothalamus. Science (New York, NY) *202*, 537-539.
Grossman, S.P., and Grossman, L. (1982). Iontophoretic injections of kainic acid into the rat lateral hypothalamus: effects on ingestive behavior. Physiology & behavior *29*, 553-559.
Guan, X.M., Yu, H., Trumbauer, M., Frazier, E., Van der Ploeg, L.H., and Chen, H. (1998). Induction of neuropeptide Y expression in dorsomedial hypothalamus of diet-induced obese mice. Neuroreport *9*, 3415-3419.
Hagan, M.M., Rushing, P.A., Schwartz, M.W., Yagaloff, K.A., Burn, P., Woods, S.C., and Seeley, R.J. (1999). Role of the CNS melanocortin system in the response to overfeeding. The Journal of neuroscience : the official journal of the Society for Neuroscience *19*, 2362-2367.
Hall, F.S., Goeb, M., Li, X.F., Sora, I., and Uhl, G.R. (2004). mu-Opioid receptor knockout mice display reduced cocaine conditioned place preference but enhanced sensitization of cocaine-induced locomotion. Brain research Molecular brain research *121*, 123-130.
Haluzik, M., Sindelka, G., Widimsky, J., Jr., Prazny, M., Zelinka, T., and Skrha, J. (2002). Serum leptin levels in patients with primary hyperaldosteronism before and after treatment: relationships to insulin sensitivity. Journal of human hypertension *16*, 41-45.
Han, J.C., Liu, Q.R., Jones, M., Levinn, R.L., Menzie, C.M., Jefferson-George, K.S., Adler-Wailes, D.C., Sanford, E.L., Lacbawan, F.L., Uhl, G.R.*, et al.* (2008). Brain-derived neurotrophic factor and obesity in the WAGR syndrome. The New England journal of medicine *359*, 918-927.

Hara, J., Yanagisawa, M., and Sakurai, T. (2005). Difference in obesity phenotype between orexin-knockout mice and orexin neuron-deficient mice with same genetic background and environmental conditions. Neuroscience letters *380*, 239-242.
Harlan, S.M., Morgan, D.A., Agassandian, K., Guo, D.F., Cassell, M.D., Sigmund, C.D., Mark, A.L., and Rahmouni, K. (2011). Ablation of the leptin receptor in the hypothalamic arcuate nucleus abrogates leptin-induced sympathetic activation. Circulation research *108*, 808-812.
Harris, G.C., Wimmer, M., and Aston-Jones, G. (2005). A role for lateral hypothalamic orexin neurons in reward seeking. Nature *437*, 556-559.
Hatoum, I.J., Stylopoulos, N., Vanhoose, A.M., Boyd, K.L., Yin, D.P., Ellacott, K.L., Ma, L.L., Blaszczyk, K., Keogh, J.M., Cone, R.D*., et al.* (2012). Melanocortin-4 receptor signaling is required for weight loss after gastric bypass surgery. The Journal of clinical endocrinology and metabolism *97*, E1023-1031.
Haynes, W.G., Morgan, D.A., Djalali, A., Sivitz, W.I., and Mark, A.L. (1999). Interactions between the melanocortin system and leptin in control of sympathetic nerve traffic. Hypertension (Dallas, Tex : 1979) *33*, 542-547.
Hennessy, J.W., and Grossman, S.P. (1976). Overeating and obesity produced by interruption of the caudal connections of the hypothalamus: evidence of hormonal and metabolic disruption. Physiology & behavior *17*, 103-109.
Hervey, G.R. (1959). The effects of lesions in the hypothalamus in parabiotic rats. The Journal of physiology *145*, 336-352.
Hess, W.R., and Akert, K. (1955). Experimental data on role of hypothalamus in mechanism of emotional behavior. AMA archives of neurology and psychiatry *73*, 127-129.
Hill, J., Duckworth, M., Murdock, P., Rennie, G., Sabido-David, C., Ames, R.S., Szekeres, P., Wilson, S., Bergsma, D.J., Gloger, I.S*., et al.* (2001). Molecular cloning and functional characterization of MCH2, a novel human MCH receptor. The Journal of biological chemistry *276*, 20125-20129.
Hill, J.W. (2012). PVN pathways controlling energy homeostasis. Indian journal of endocrinology and metabolism *16*, S627-636.
Hill, J.W., Elias, C.F., Fukuda, M., Williams, K.W., Berglund, E.D., Holland, W.L., Cho, Y.R., Chuang, J.C., Xu, Y., Choi, M*., et al.* (2010). Direct insulin and leptin action on pro-opiomelanocortin neurons is required for normal glucose homeostasis and fertility. Cell metabolism *11*, 286-297.
Hochgeschwender, U., Costa, J.L., Reed, P., Bui, S., and Brennan, M.B. (2003). Altered glucose homeostasis in proopiomelanocortin-null mouse mutants lacking central and peripheral melanocortin. Endocrinology *144*, 5194-5202.
Hoermann, R., Midgley, J.E., Larisch, R., and Dietrich, J.W. (2015). Homeostatic Control of the Thyroid-Pituitary Axis: Perspectives for Diagnosis and Treatment. Frontiers in endocrinology *6*, 177.
Hommel, J.D., Trinko, R., Sears, R.M., Georgescu, D., Liu, Z.-W., Gao, X.-B., Thurmon, J.J., Marinelli, M., and DiLeone, R.J. (2006). Leptin Receptor Signaling in Midbrain Dopamine Neurons Regulates Feeding. Neuron *51*.
Hsu, P.D., Lander, E.S., and Zhang, F. (2014). Development and applications of CRISPR-Cas9 for genome engineering. Cell *157*, 1262-1278.
Hubert, G.W., Jones, D.C., Moffett, M.C., Rogge, G., and Kuhar, M.J. (2008). CART peptides as modulators of dopamine and psychostimulants and interactions with the mesolimbic dopaminergic system. Biochemical pharmacology *75*, 57-62.
Hunt, P., and Clements-Jewery, S. (1981). A steroid derivative, R 5135, antagonizes the GABA/benzodiazepine receptor interaction. Neuropharmacology *20*, 357-361.

Huo, L., Gamber, K., Greeley, S., Silva, J., Huntoon, N., Leng, X.H., and Bjorbaek, C. (2009). Leptin-dependent control of glucose balance and locomotor activity by POMC neurons. Cell metabolism *9*, 537-547.
Huszar, D., Lynch, C.A., Fairchild-Huntress, V., Dunmore, J.H., Fang, Q., Berkemeier, L.R., Gu, W., Kesterson, R.A., Boston, B.A., Cone, R.D*., et al.* (1997). Targeted disruption of the melanocortin-4 receptor results in obesity in mice. Cell *88*, 131-141.
Hwa, J.J., Ghibaudi, L., Compton, D., Fawzi, A.B., and Strader, C.D. (1996). Intracerebroventricular injection of leptin increases thermogenesis and mobilizes fat metabolism in ob/ob mice. Hormone and metabolic research = Hormon- und Stoffwechselforschung = Hormones et metabolisme *28*, 659-663.
Ibrahim, N., Bosch, M.A., Smart, J.L., Qiu, J., Rubinstein, M., Ronnekleiv, O.K., Low, M.J., and Kelly, M.J. (2003). Hypothalamic proopiomelanocortin neurons are glucose responsive and express K(ATP) channels. Endocrinology *144*, 1331-1340.
Insel, T.R. (2010). The challenge of translation in social neuroscience: a review of oxytocin, vasopressin, and affiliative behavior. Neuron *65*, 768-779.
Ishikawa, T., Yang, H., and Tache, Y. (1988). Medullary sites of action of the TRH analogue, RX 77368, for stimulation of gastric acid secretion in the rat. Gastroenterology *95*, 1470-1476.
Jamieson, P.M., Li, C., Kukura, C., Vaughan, J., and Vale, W. (2006). Urocortin 3 modulates the neuroendocrine stress response and is regulated in rat amygdala and hypothalamus by stress and glucocorticoids. Endocrinology *147*, 4578-4588.
Jansen, A.S., Hoffman, J.L., and Loewy, A.D. (1997). CNS sites involved in sympathetic and parasympathetic control of the pancreas: a viral tracing study. Brain research *766*, 29-38.
Jennings, J.H., Rizzi, G., Stamatakis, A.M., Ung, R.L., and Stuber, G.D. (2013). The inhibitory circuit architecture of the lateral hypothalamus orchestrates feeding. Science (New York, NY) *341*, 1517-1521.
Jennings, J.H., Ung, R.L., Resendez, S.L., Stamatakis, A.M., Taylor, J.G., Huang, J., Veleta, K., Kantak, P.A., Aita, M., Shilling-Scrivo, K*., et al.* (2015). Visualizing Hypothalamic Network Dynamics for Appetitive and Consummatory Behaviors. Cell *160*, 516-527.
Johansson, A. (2011). Recent progress in the discovery of melanin-concentrating hormone 1-receptor antagonists. Expert opinion on therapeutic patents *21*, 905-925.
Johnston, G.A. (2013). Advantages of an antagonist: bicuculline and other GABA antagonists. British journal of pharmacology *169*, 328-336.
Kamohara, S., Burcelin, R., Halaas, J.L., Friedman, J.M., and Charron, M.J. (1997). Acute stimulation of glucose metabolism in mice by leptin treatment. Nature *389*, 374-377.
Kan, S.H., Elanko, N., Johnson, D., Cornejo-Roldan, L., Cook, J., Reich, E.W., Tomkins, S., Verloes, A., Twigg, S.R., Rannan-Eliya, S*., et al.* (2002). Genomic screening of fibroblast growth-factor receptor 2 reveals a wide spectrum of mutations in patients with syndromic craniosynostosis. American journal of human genetics *70*, 472-486.
Kang, J., Heart, E., and Sung, C.K. (2001). Effects of cellular ATP depletion on glucose transport and insulin signaling in 3T3-L1 adipocytes. American journal of physiology Endocrinology and metabolism *280*, E428-435.
Kang, Y., Leung, Y.M., Manning-Fox, J.E., Xia, F., Xie, H., Sheu, L., Tsushima, R.G., Light, P.E., and Gaisano, H.Y. (2004). Syntaxin-1A inhibits cardiac KATP channels by its actions on nucleotide binding folds 1 and 2 of sulfonylurea receptor 2A. The Journal of biological chemistry *279*, 47125-47131.
Kasahara, Y., Takayanagi, Y., Kawada, T., Itoi, K., and Nishimori, K. (2007). Impaired thermoregulatory ability of oxytocin-deficient mice during cold-exposure. Bioscience, biotechnology, and biochemistry *71*, 3122-3126.

Keating, G.L., Kuhar, M.J., and Rye, D.B. (2008). High dose CART peptide induces abnormal EEG activity and behavioral seizures. Neuropeptides *42*, 199-204.
Kempadoo, K.A., Tourino, C., Cho, S.L., Magnani, F., Leinninger, G.-M., Stuber, G.D., Zhang, F., Myers, M.G., Deisseroth, K., de Lecea, L*., et al.* (2013). Hypothalamic Neurotensin Projections Promote Reward by Enhancing Glutamate Transmission in the VTA. The Journal of Neuroscience *33*, 7618-7626.
Kennedy, G.C. (1950). The hypothalamic control of food intake in rats. Proceedings of the Royal Society of London Series B, Biological sciences *137*, 535-549.
Kennedy, G.C. (1953). The role of depot fat in the hypothalamic control of food intake in the rat. Proceedings of the Royal Society of London Series B, Biological sciences *140*, 578-596.
Kievit, P., Halem, H., Marks, D.L., Dong, J.Z., Glavas, M.M., Sinnayah, P., Pranger, L., Cowley, M.A., Grove, K.L., and Culler, M.D. (2013). Chronic treatment with a melanocortin-4 receptor agonist causes weight loss, reduces insulin resistance, and improves cardiovascular function in diet-induced obese rhesus macaques. Diabetes *62*, 490-497.
Kim, J.G., Suyama, S., Koch, M., Jin, S., Argente-Arizon, P., Argente, J., Liu, Z.W., Zimmer, M.R., Jeong, J.K., Szigeti-Buck, K*., et al.* (2014). Leptin signaling in astrocytes regulates hypothalamic neuronal circuits and feeding. Nature neuroscience *17*, 908-910.
Kim, K.W., Donato, J., Jr., Berglund, E.D., Choi, Y.H., Kohno, D., Elias, C.F., Depinho, R.A., and Elmquist, J.K. (2012). FOXO1 in the ventromedial hypothalamus regulates energy balance. The Journal of clinical investigation *122*, 2578-2589.
Kim, K.W., Jo, Y.H., Zhao, L., Stallings, N.R., Chua, S.C., Jr., and Parker, K.L. (2008). Steroidogenic factor 1 regulates expression of the cannabinoid receptor 1 in the ventromedial hypothalamic nucleus. Molecular endocrinology (Baltimore, Md) *22*, 1950-1961.
Kim, K.W., Li, S., Zhao, H., Peng, B., Tobet, S.A., Elmquist, J.K., Parker, K.L., and Zhao, L. (2010). CNS-specific ablation of steroidogenic factor 1 results in impaired female reproductive function. Molecular endocrinology (Baltimore, Md) *24*, 1240-1250.
King, B.M., and Gaston, M.G. (1977). Reappearance of dynamic hyperphagia during the static phase in medial hypothalamic lesioned rats. Physiology & behavior *18*, 945-950.
Kir, S., Beddow, S.A., Samuel, V.T., Miller, P., Previs, S.F., Suino-Powell, K., Xu, H.E., Shulman, G.I., Kliewer, S.A., and Mangelsdorf, D.J. (2011). FGF19 as a postprandial, insulin-independent activator of hepatic protein and glycogen synthesis. Science (New York, NY) *331*, 1621-1624.
Klieverik, L.P., Janssen, S.F., van Riel, A., Foppen, E., Bisschop, P.H., Serlie, M.J., Boelen, A., Ackermans, M.T., Sauerwein, H.P., Fliers, E*., et al.* (2009). Thyroid hormone modulates glucose production via a sympathetic pathway from the hypothalamic paraventricular nucleus to the liver. Proceedings of the National Academy of Sciences of the United States of America *106*, 5966-5971.
Klockener, T., Hess, S., Belgardt, B.F., Paeger, L., Verhagen, L.A., Husch, A., Sohn, J.W., Hampel, B., Dhillon, H., Zigman, J.M*., et al.* (2011). High-fat feeding promotes obesity via insulin receptor/PI3K-dependent inhibition of SF-1 VMH neurons. Nature neuroscience *14*, 911-918.
Kokkotou, E., Jeon, J.Y., Wang, X., Marino, F.E., Carlson, M., Trombly, D.J., and Maratos-Flier, E. (2005). Mice with MCH ablation resist diet-induced obesity through strain-specific mechanisms. American journal of physiology Regulatory, integrative and comparative physiology *289*, R117-124.
Kong, D., Dagon, Y., Campbell, J.N., Guo, Y., Yang, Z., Yi, X., Aryal, P., Wellenstein, K., Kahn, B.B., Sabatini, B.L*., et al.* (2016). A Postsynaptic AMPK-->p21-Activated Kinase Pathway Drives Fasting-Induced Synaptic Plasticity in AgRP Neurons. Neuron *91*, 25-33.

Kong, D., Tong, Q., Ye, C., Koda, S., Fuller, P.M., Krashes, M.J., Vong, L., Ray, R.S., Olson, D.P., and Lowell, B.B. (2012). GABAergic RIP-Cre neurons in the arcuate nucleus selectively regulate energy expenditure. Cell *151*, 645-657.
Kong, D., Vong, L., Parton, L.E., Ye, C., Tong, Q., Hu, X., Choi, B., Bruning, J.C., and Lowell, B.B. (2010). Glucose stimulation of hypothalamic MCH neurons involves K(ATP) channels, is modulated by UCP2, and regulates peripheral glucose homeostasis. Cell Metab *12*, 545-552.
Kong, L.C., Tap, J., Aron-Wisnewsky, J., Pelloux, V., Basdevant, A., Bouillot, J.L., Zucker, J.D., Dore, J., and Clement, K. (2013). Gut microbiota after gastric bypass in human obesity: increased richness and associations of bacterial genera with adipose tissue genes. The American journal of clinical nutrition *98*, 16-24.
Kong, W., Stanley, S., Gardiner, J., Abbott, C., Murphy, K., Seth, A., Connoley, I., Ghatei, M., Stephens, D., and Bloom, S. (2003). A role for arcuate cocaine and amphetamine-regulated transcript in hyperphagia, thermogenesis, and cold adaptation. FASEB journal : official publication of the Federation of American Societies for Experimental Biology *17*, 1688-1690.
Konner, A.C., Janoschek, R., Plum, L., Jordan, S.D., Rother, E., Ma, X., Xu, C., Enriori, P., Hampel, B., Barsh, G.S*., et al.* (2007). Insulin action in AgRP-expressing neurons is required for suppression of hepatic glucose production. Cell metabolism *5*, 438-449.
Koob, G.F. (1992). Drugs of abuse: anatomy, pharmacology and function of reward pathways. Trends in pharmacological sciences *13*, 177-184.
Krashes, M.J., Koda, S., Ye, C., Rogan, S.C., Adams, A.C., Cusher, D.S., Maratos-Flier, E., Roth, B.L., and Lowell, B.B. (2011). Rapid, reversible activation of AgRP neurons drives feeding behavior in mice. The Journal of clinical investigation *121*, 1424-1428.
Krashes, M.J., Lowell, B.B., and Garfield, A.S. (2016). Melanocortin-4 receptor-regulated energy homeostasis. Nature neuroscience *19*, 206-219.
Kraus-Friedmann, N. (1984). Hormonal regulation of hepatic gluconeogenesis. Physiological reviews *64*, 170-259.
Kristensen, P., Judge, M.E., Thim, L., Ribel, U., Christjansen, K.N., Wulff, B.S., Clausen, J.T., Jensen, P.B., Madsen, O.D., Vrang, N*., et al.* (1998). Hypothalamic CART is a new anorectic peptide regulated by leptin. Nature *393*, 72-76.
Krude, H., Biebermann, H., and Gruters, A. (2003). Mutations in the human proopiomelanocortin gene. Annals of the New York Academy of Sciences *994*, 233-239.
Krude, H., Biebermann, H., Luck, W., Horn, R., Brabant, G., and Gruters, A. (1998). Severe early-onset obesity, adrenal insufficiency and red hair pigmentation caused by POMC mutations in humans. Nature genetics *19*, 155-157.
Kuo, T., Harris, C.A., and Wang, J.C. (2013). Metabolic functions of glucocorticoid receptor in skeletal muscle. Molecular and cellular endocrinology *380*, 79-88.
Lakatos, A., Prinster, S., Vicentic, A., Hall, R.A., and Kuhar, M.J. (2005). Cocaine- and amphetamine-regulated transcript (CART) peptide activates the extracellular signal-regulated kinase (ERK) pathway in AtT20 cells via putative G-protein coupled receptors. Neuroscience letters *384*, 198-202.
Lambert, P.D., Couceyro, P.R., McGirr, K.M., Dall Vechia, S.E., Smith, Y., and Kuhar, M.J. (1998). CART peptides in the central control of feeding and interactions with neuropeptide Y. Synapse (New York, NY) *29*, 293-298.
Lapchak, P.A., and Hefti, F. (1992). BDNF and NGF treatment in lesioned rats: effects on cholinergic function and weight gain. Neuroreport *3*, 405-408.
Laque, A., Zhang, Y., Gettys, S., Nguyen, T.A., Bui, K., Morrison, C.D., and Munzberg, H. (2013). Leptin receptor neurons in the mouse hypothalamus are colocalized with the neuropeptide

galanin and mediate anorexigenic leptin action. American journal of physiology Endocrinology and metabolism *304*, E999-1011.
Larsen, P.J., Hay-Schmidt, A., and Mikkelsen, J.D. (1994). Efferent connections from the lateral hypothalamic region and the lateral preoptic area to the hypothalamic paraventricular nucleus of the rat. The Journal of comparative neurology *342*, 299-319.
Larsen, P.J., Vrang, N., Petersen, P.C., and Kristensen, P. (2000). Chronic intracerebroventricular administration of recombinant CART(42-89) peptide inhibits and causes weight loss in lean and obese Zucker (fa/fa) rats. Obesity research *8*, 590-596.
Lau, J., and Herzog, H. (2014). CART in the regulation of appetite and energy homeostasis. Frontiers in neuroscience *8*, 313.
le Roux, C.W., and Bloom, S.R. (2005). Why do patients lose weight after Roux-en-Y gastric bypass? The Journal of clinical endocrinology and metabolism *90*, 591-592.
Lee, D.K., Jeong, J.H., Chun, S.K., Chua, S., Jr., and Jo, Y.H. (2015). Interplay between glucose and leptin signalling determines the strength of GABAergic synapses at POMC neurons. Nature communications *6*, 6618.
Ley, R.E., Backhed, F., Turnbaugh, P., Lozupone, C.A., Knight, R.D., and Gordon, J.I. (2005). Obesity alters gut microbial ecology. Proceedings of the National Academy of Sciences of the United States of America *102*, 11070-11075.
Li, W.D., Joo, E.J., Furlong, E.B., Galvin, M., Abel, K., Bell, C.J., and Price, R.A. (2000). Melanocortin 3 receptor (MC3R) gene variants in extremely obese women. International journal of obesity and related metabolic disorders : journal of the International Association for the Study of Obesity *24*, 206-210.
Lin, H.V., Plum, L., Ono, H., Gutierrez-Juarez, R., Shanabrough, M., Borok, E., Horvath, T.L., Rossetti, L., and Accili, D. (2010). Divergent regulation of energy expenditure and hepatic glucose production by insulin receptor in agouti-related protein and POMC neurons. Diabetes *59*, 337-346.
Lin, Y., Hall, R.A., and Kuhar, M.J. (2011). CART peptide stimulation of G protein-mediated signaling in differentiated PC12 cells: identification of PACAP 6-38 as a CART receptor antagonist. Neuropeptides *45*, 351-358.
Liu, H., Kishi, T., Roseberry, A.G., Cai, X., Lee, C.E., Montez, J.M., Friedman, J.M., and Elmquist, J.K. (2003). Transgenic mice expressing green fluorescent protein under the control of the melanocortin-4 receptor promoter. The Journal of neuroscience : the official journal of the Society for Neuroscience *23*, 7143-7154.
Lopez, M., Alvarez, C.V., Nogueiras, R., and Dieguez, C. (2013). Energy balance regulation by thyroid hormones at central level. Trends in molecular medicine *19*, 418-427.
Ludwig, D.S., Tritos, N.A., Mastaitis, J.W., Kulkarni, R., Kokkotou, E., Elmquist, J., Lowell, B., Flier, J.S., and Maratos-Flier, E. (2001). Melanin-concentrating hormone overexpression in transgenic mice leads to obesity and insulin resistance. The Journal of clinical investigation *107*, 379-386.
Luquet, S., Perez, F.A., Hnasko, T.S., and Palmiter, R.D. (2005). NPY/AgRP neurons are essential for feeding in adult mice but can be ablated in neonates. Science (New York, NY) *310*, 683-685.
Lyons, W.E., Mamounas, L.A., Ricaurte, G.A., Coppola, V., Reid, S.W., Bora, S.H., Wihler, C., Koliatsos, V.E., and Tessarollo, L. (1999). Brain-derived neurotrophic factor-deficient mice develop aggressiveness and hyperphagia in conjunction with brain serotonergic abnormalities. Proceedings of the National Academy of Sciences of the United States of America *96*, 15239-15244.
Maffei, M., Halaas, J., Ravussin, E., Pratley, R.E., Lee, G.H., Zhang, Y., Fei, H., Kim, S., Lallone, R., Ranganathan, S*., et al.* (1995). Leptin levels in human and rodent: measurement of plasma leptin and ob RNA in obese and weight-reduced subjects. Nature medicine *1*, 1155-1161.

Majdic, G., Young, M., Gomez-Sanchez, E., Anderson, P., Szczepaniak, L.S., Dobbins, R.L., McGarry, J.D., and Parker, K.L. (2002). Knockout mice lacking steroidogenic factor 1 are a novel genetic model of hypothalamic obesity. Endocrinology *143*, 607-614.
Maletinska, L., Maixnerova, J., Matyskova, R., Haugvicova, R., Sloncova, E., Elbert, T., Slaninova, J., and Zelezna, B. (2007). Cocaine- and amphetamine-regulated transcript (CART) peptide specific binding in pheochromocytoma cells PC12. European journal of pharmacology *559*, 109-114.
Malik, S., McGlone, F., Bedrossian, D., and Dagher, A. (2008). Ghrelin Modulates Brain Activity in Areas that Control Appetitive Behavior. Cell Metabolism *7*, 400-409.
Marcelin, G., Jo, Y.H., Li, X., Schwartz, G.J., Zhang, Y., Dun, N.J., Lyu, R.M., Blouet, C., Chang, J.K., and Chua, S., Jr. (2014). Central action of FGF19 reduces hypothalamic AGRP/NPY neuron activity and improves glucose metabolism. Molecular metabolism *3*, 19-28.
Marcus, J.N., Aschkenasi, C.J., Lee, C.E., Chemelli, R.M., Saper, C.B., Yanagisawa, M., and Elmquist, J.K. (2001). Differential expression of orexin receptors 1 and 2 in the rat brain. The Journal of comparative neurology *435*, 6-25.
Marino, J.S., Xu, Y., and Hill, J.W. (2011). Central insulin and leptin-mediated autonomic control of glucose homeostasis. Trends in endocrinology and metabolism: TEM *22*, 275-285.
Matschinsky, F.M. (1996). Banting Lecture 1995. A lesson in metabolic regulation inspired by the glucokinase glucose sensor paradigm. Diabetes *45*, 223-241.
Maynard, C.L., Elson, C.O., Hatton, R.D., and Weaver, C.T. (2012). Reciprocal interactions of the intestinal microbiota and immune system. Nature *489*, 231-241.
McClellan, K.M., Parker, K.L., and Tobet, S. (2006). Development of the ventromedial nucleus of the hypothalamus. Frontiers in neuroendocrinology *27*, 193-209.
Meister, B. (2007). Neurotransmitters in key neurons of the hypothalamus that regulate feeding behavior and body weight. Physiology & behavior *92*, 263-271.
Mencarelli, M., Dubern, B., Alili, R., Maestrini, S., Benajiba, L., Tagliaferri, M., Galan, P., Rinaldi, M., Simon, C., Tounian, P.*, et al.* (2011). Rare melanocortin-3 receptor mutations with in vitro functional consequences are associated with human obesity. Human molecular genetics *20*, 392-399.
Miki, T., Liss, B., Minami, K., Shiuchi, T., Saraya, A., Kashima, Y., Horiuchi, M., Ashcroft, F., Minokoshi, Y., Roeper, J.*, et al.* (2001). ATP-sensitive K+ channels in the hypothalamus are essential for the maintenance of glucose homeostasis. Nature neuroscience *4*, 507-512.
Mikkelsen, K.H., Knop, F.K., Frost, M., Hallas, J., and Pottegard, A. (2015). Use of Antibiotics and Risk of Type 2 Diabetes: A Population-Based Case-Control Study. The Journal of clinical endocrinology and metabolism *100*, 3633-3640.
Mingrone, G., Panunzi, S., De Gaetano, A., Guidone, C., Iaconelli, A., Leccesi, L., Nanni, G., Pomp, A., Castagneto, M., Ghirlanda, G.*, et al.* (2012). Bariatric surgery versus conventional medical therapy for type 2 diabetes. The New England journal of medicine *366*, 1577-1585.
Minokoshi, Y., Haque, M.S., and Shimazu, T. (1999). Microinjection of leptin into the ventromedial hypothalamus increases glucose uptake in peripheral tissues in rats. Diabetes *48*, 287-291.
Miras, A.D., and le Roux, C.W. (2013). Mechanisms underlying weight loss after bariatric surgery. Nature reviews Gastroenterology & hepatology *10*, 575-584.
Mizuno, T.M., Kleopoulos, S.P., Bergen, H.T., Roberts, J.L., Priest, C.A., and Mobbs, C.V. (1998). Hypothalamic pro-opiomelanocortin mRNA is reduced by fasting and [corrected] in ob/ob and db/db mice, but is stimulated by leptin. Diabetes *47*, 294-297.

Moffett, M., Stanek, L., Harley, J., Rogge, G., Asnicar, M., Hsiung, H., and Kuhar, M. (2006). Studies of cocaine- and amphetamine-regulated transcript (CART) knockout mice. Peptides *27*, 2037-2045.
Montemurro, D.G., and Stevenson, J.A. (1957). Adipsia produced by hypothalamic lesions in the rat. Canadian journal of biochemistry and physiology *35*, 31-37.
Morrison, C.D., and Munzberg, H. (2012). Capricious Cre: the devil is in the details. Endocrinology *153*, 1005-1007.
Morrison, S.F., Madden, C.J., and Tupone, D. (2012). Central control of brown adipose tissue thermogenesis. Frontiers in endocrinology *3*.
Morton, G.J., Matsen, M.E., Bracy, D.P., Meek, T.H., Nguyen, H.T., Stefanovski, D., Bergman, R.N., Wasserman, D.H., and Schwartz, M.W. (2013). FGF19 action in the brain induces insulin-independent glucose lowering. The Journal of clinical investigation *123*, 4799-4808.
Mountjoy, K.G., Caron, A., Hubbard, K., Shome, A., Grey, A.C., Sun, B., Bould, S., Middleditch, M., Pontre, B., McGregor, A*., et al.* (2017). Desacetyl-alpha-melanocyte stimulating hormone and alpha-melanocyte stimulating hormone are required to regulate energy balance. Molecular metabolism.
Mountjoy, K.G., Mortrud, M.T., Low, M.J., Simerly, R.B., and Cone, R.D. (1994). Localization of the melanocortin-4 receptor (MC4-R) in neuroendocrine and autonomic control circuits in the brain. Molecular endocrinology (Baltimore, Md) *8*, 1298-1308.
Murphy, B.A., Fakira, K.A., Song, Z., Beuve, A., and Routh, V.H. (2009). AMP-activated protein kinase and nitric oxide regulate the glucose sensitivity of ventromedial hypothalamic glucose-inhibited neurons. American journal of physiology Cell physiology *297*, C750-758.
Musatov, S., Chen, W., Pfaff, D.W., Mobbs, C.V., Yang, X.J., Clegg, D.J., Kaplitt, M.G., and Ogawa, S. (2007). Silencing of estrogen receptor alpha in the ventromedial nucleus of hypothalamus leads to metabolic syndrome. Proceedings of the National Academy of Sciences of the United States of America *104*, 2501-2506.
Myers, M.G., Cowley, M.A., and Munzberg, H. (2008). Mechanisms of leptin action and leptin resistance. Annual review of physiology *70*, 537-556.
Myers, M.G., Jr., and Olson, D.P. (2012). Central nervous system control of metabolism. Nature *491*, 357-363.
Nakamura, Y., Darnieder, L.M., Deeb, T.Z., and Moss, S.J. (2015). Regulation of GABAARs by phosphorylation. Advances in pharmacology (San Diego, Calif) *72*, 97-146.
Naleid, A.M., Grace, M.K., Cummings, D.E., and Levine, A.S. (2005). Ghrelin induces feeding in the mesolimbic reward pathway between the ventral tegmental area and the nucleus accumbens. Peptides *26*, 2274-2279.
Nicholes, K., Guillet, S., Tomlinson, E., Hillan, K., Wright, B., Frantz, G.D., Pham, T.A., Dillard-Telm, L., Tsai, S.P., Stephan, J.P*., et al.* (2002). A mouse model of hepatocellular carcinoma: ectopic expression of fibroblast growth factor 19 in skeletal muscle of transgenic mice. The American journal of pathology *160*, 2295-2307.
Nieh, E.H., Kim, S.-Y., Namburi, P., and Tye, K.M. (2013). Optogenetic dissection of neural circuits underlying emotional valence and motivated behaviors. Brain Research *1511*, 73-92.
Nieh, E.H., Vander Weele, C.M., Matthews, G.A., Presbrey, K.N., Wichmann, R., Leppla, C.A., Izadmehr, E.M., and Tye, K.M. (2016). Inhibitory Input from the Lateral Hypothalamus to the Ventral Tegmental Area Disinhibits Dopamine Neurons and Promotes Behavioral Activation. Neuron *90*, 1286-1298.
Oldfield, B.J., Giles, M.E., Watson, A., Anderson, C., Colvill, L.M., and McKinley, M.J. (2002). The neurochemical characterisation of hypothalamic pathways projecting polysynaptically to brown adipose tissue in the rat. Neuroscience *110*, 515-526.

Olds, J., and Milner, P. (1954). Positive reinforcement produced by electrical stimulation of septal area and other regions of rat brain. Journal of comparative and physiological psychology *47*, 419-427.
Ollmann, M.M., Wilson, B.D., Yang, Y.K., Kerns, J.A., Chen, Y., Gantz, I., and Barsh, G.S. (1997). Antagonism of central melanocortin receptors in vitro and in vivo by agouti-related protein. Science (New York, NY) *278*, 135-138.
Olson, B.R., Drutarosky, M.D., Stricker, E.M., and Verbalis, J.G. (1991). Brain oxytocin receptor antagonism blunts the effects of anorexigenic treatments in rats: evidence for central oxytocin inhibition of food intake. Endocrinology *129*, 785-791.
Opland, D., Sutton, A., Woodworth, H., Brown, J., Bugescu, R., Garcia, A., Christensen, L., Rhodes, C., Myers, M., and Leinninger, G. (2013). Loss of neurotensin receptor-1 disrupts the control of the mesolimbic dopamine system by leptin and promotes hedonic feeding and obesity. Molecular Metabolism *2*, 423-434.
Ornitz, D.M., and Itoh, N. (2015). The Fibroblast Growth Factor signaling pathway. Wiley interdisciplinary reviews Developmental biology *4*, 215-266.
Padilla, S.L., Carmody, J.S., and Zeltser, L.M. (2010). Pomc-expressing progenitors give rise to antagonistic neuronal populations in hypothalamic feeding circuits. Nature medicine *16*, 403-405.
Padilla, S.L., Reef, D., and Zeltser, L.M. (2012). Defining POMC neurons using transgenic reagents: impact of transient Pomc expression in diverse immature neuronal populations. Endocrinology *153*, 1219-1231.
Paranjape, S.A., Chan, O., Zhu, W., Horblitt, A.M., Grillo, C.A., Wilson, S., Reagan, L., and Sherwin, R.S. (2011). Chronic reduction of insulin receptors in the ventromedial hypothalamus produces glucose intolerance and islet dysfunction in the absence of weight gain. American journal of physiology Endocrinology and metabolism *301*, E978-983.
Parton, L.E., Ye, C.P., Coppari, R., Enriori, P.J., Choi, B., Zhang, C.-Y., Xu, C., Vianna, C.R., Balthasar, N., and Lee, C.E. (2007a). Glucose sensing by POMC neurons regulates glucose homeostasis and is impaired in obesity. Nature *449*, 228-232.
Parton, L.E., Ye, C.P., Coppari, R., Enriori, P.J., Choi, B., Zhang, C.Y., Xu, C., Vianna, C.R., Balthasar, N., Lee, C.E*., et al.* (2007b). Glucose sensing by POMC neurons regulates glucose homeostasis and is impaired in obesity. Nature *449*, 228-232.
Patapoutian, A., and Reichardt, L.F. (2001). Trk receptors: mediators of neurotrophin action. Current opinion in neurobiology *11*, 272-280.
Pellerin, L., and Magistretti, P.J. (1994). Glutamate uptake into astrocytes stimulates aerobic glycolysis: a mechanism coupling neuronal activity to glucose utilization. Proceedings of the National Academy of Sciences of the United States of America *91*, 10625-10629.
Pelleymounter, M.A., Cullen, M.J., Baker, M.B., Hecht, R., Winters, D., Boone, T., and Collins, F. (1995a). Effects of the obese gene product on body weight regulation in ob/ob mice. Science (New York, NY) *269*, 540-543.
Pelleymounter, M.A., Cullen, M.J., and Wellman, C.L. (1995b). Characteristics of BDNF-induced weight loss. Experimental neurology *131*, 229-238.
Perry, R.J., Lee, S., Ma, L., Zhang, D., Schlessinger, J., and Shulman, G.I. (2015). FGF1 and FGF19 reverse diabetes by suppression of the hypothalamic-pituitary-adrenal axis. Nature communications *6*, 6980.
Perry, R.J., Zhang, X.M., Zhang, D., Kumashiro, N., Camporez, J.P., Cline, G.W., Rothman, D.L., and Shulman, G.I. (2014). Leptin reverses diabetes by suppression of the hypothalamic-pituitary-adrenal axis. Nature medicine *20*, 759-763.

Platt, R.J., Chen, S., Zhou, Y., Yim, M.J., Swiech, L., Kempton, H.R., Dahlman, J.E., Parnas, O., Eisenhaure, T.M., and Jovanovic, M. (2014a). CRISPR-Cas9 knockin mice for genome editing and cancer modeling. Cell *159*, 440-455.
Platt, R.J., Chen, S., Zhou, Y., Yim, M.J., Swiech, L., Kempton, H.R., Dahlman, J.E., Parnas, O., Eisenhaure, T.M., Jovanovic, M.*, et al.* (2014b). CRISPR-Cas9 knockin mice for genome editing and cancer modeling. Cell *159*, 440-455.
Prasad-Reddy, L., and Isaacs, D. (2015). A clinical review of GLP-1 receptor agonists: efficacy and safety in diabetes and beyond. Drugs in context *4*, 212283.
Pritchard, L.E., Turnbull, A.V., and White, A. (2002). Pro-opiomelanocortin processing in the hypothalamus: impact on melanocortin signalling and obesity. The Journal of endocrinology *172*, 411-421.
Qian, S., Chen, H., Weingarth, D., Trumbauer, M.E., Novi, D.E., Guan, X., Yu, H., Shen, Z., Feng, Y., Frazier, E.*, et al.* (2002). Neither agouti-related protein nor neuropeptide Y is critically required for the regulation of energy homeostasis in mice. Molecular and cellular biology *22*, 5027-5035.
Radziejewski, C., Robinson, R.C., DiStefano, P.S., and Taylor, J.W. (1992). Dimeric structure and conformational stability of brain-derived neurotrophic factor and neurotrophin-3. Biochemistry *31*, 4431-4436.
Rau, A.R., and Hentges, S.T. (2017). The Relevance of AgRP Neuron-Derived GABA Inputs to POMC Neurons Differs for Spontaneous and Evoked Release. The Journal of neuroscience : the official journal of the Society for Neuroscience *37*, 7362-7372.
Reichardt, L.F. (2006). Neurotrophin-regulated signalling pathways. Philosophical transactions of the Royal Society of London Series B, Biological sciences *361*, 1545-1564.
Reul, J.M., and de Kloet, E.R. (1985). Two receptor systems for corticosterone in rat brain: microdistribution and differential occupation. Endocrinology *117*, 2505-2511.
Rhee, S.H., Pothoulakis, C., and Mayer, E.A. (2009). Principles and clinical implications of the brain-gut-enteric microbiota axis. Nature reviews Gastroenterology & hepatology *6*, 306-314.
Rinaman, L. (2007). Visceral sensory inputs to the endocrine hypothalamus. Frontiers in neuroendocrinology *28*, 50-60.
Rios, M., Fan, G., Fekete, C., Kelly, J., Bates, B., Kuehn, R., Lechan, R.M., and Jaenisch, R. (2001). Conditional deletion of brain-derived neurotrophic factor in the postnatal brain leads to obesity and hyperactivity. Molecular endocrinology (Baltimore, Md) *15*, 1748-1757.
Rogge, G., Jones, D., Hubert, G.W., Lin, Y., and Kuhar, M.J. (2008). CART peptides: regulators of body weight, reward and other functions. Nature reviews Neuroscience *9*, 747-758.
Roman, C.W., Derkach, V.A., and Palmiter, R.D. (2016). Genetically and functionally defined NTS to PBN brain circuits mediating anorexia. Nature Communications *7*, 11905.
Rosin, D.L., Weston, M.C., Sevigny, C.P., Stornetta, R.L., and Guyenet, P.G. (2003). Hypothalamic orexin (hypocretin) neurons express vesicular glutamate transporters VGLUT1 or VGLUT2. The Journal of comparative neurology *465*, 593-603.
Rubinstein, M., Mogil, J.S., Japon, M., Chan, E.C., Allen, R.G., and Low, M.J. (1996). Absence of opioid stress-induced analgesia in mice lacking beta-endorphin by site-directed mutagenesis. Proceedings of the National Academy of Sciences of the United States of America *93*, 3995-4000.
Ruffin, M., and Nicolaidis, S. (1999). Electrical stimulation of the ventromedial hypothalamus enhances both fat utilization and metabolic rate that precede and parallel the inhibition of feeding behavior. Brain research *846*, 23-29.
Ryan, K.K., Kohli, R., Gutierrez-Aguilar, R., Gaitonde, S.G., Woods, S.C., and Seeley, R.J. (2013). Fibroblast growth factor-19 action in the brain reduces food intake and body weight and improves glucose tolerance in male rats. Endocrinology *154*, 9-15.

Sakaguchi, T., and Bray, G.A. (1987a). The effect of intrahypothalamic injections of glucose on sympathetic efferent firing rate. Brain research bulletin *18*, 591-595.
Sakaguchi, T., and Bray, G.A. (1987b). Intrahypothalamic injection of insulin decreases firing rate of sympathetic nerves. Proceedings of the National Academy of Sciences of the United States of America *84*, 2012-2014.
Sandoval, D.A., Bagnol, D., Woods, S.C., D'Alessio, D.A., and Seeley, R.J. (2008). Arcuate glucagon-like peptide 1 receptors regulate glucose homeostasis but not food intake. Diabetes *57*, 2046-2054.
Santulli, G. (2015). Adrenal Glands: From Pathophysiology to Clinical Evidence (Nova Science Publishers, Incorporated).
Sawchenko, P.E. (1987). Evidence for a local site of action for glucocorticoids in inhibiting CRF and vasopressin expression in the paraventricular nucleus. Brain research *403*, 213-223.
Scarlett, J.M., Rojas, J.M., Matsen, M.E., Kaiyala, K.J., Stefanovski, D., Bergman, R.N., Nguyen, H.T., Dorfman, M.D., Lantier, L., Wasserman, D.H.*, et al.* (2016). Central injection of fibroblast growth factor 1 induces sustained remission of diabetic hyperglycemia in rodents. Nature medicine *22*, 800-806.
Schauer, P.R., Bhatt, D.L., Kirwan, J.P., Wolski, K., Brethauer, S.A., Navaneethan, S.D., Aminian, A., Pothier, C.E., Kim, E.S., Nissen, S.E.*, et al.* (2014). Bariatric surgery versus intensive medical therapy for diabetes--3-year outcomes. The New England journal of medicine *370*, 2002-2013.
Schuld, A., Hebebrand, J., Geller, F., and Pollmacher, T. (2000). Increased body-mass index in patients with narcolepsy. Lancet (London, England) *355*, 1274-1275.
Schwartz, M.W., Seeley, R.J., Woods, S.C., Weigle, D.S., Campfield, L.A., Burn, P., and Baskin, D.G. (1997). Leptin increases hypothalamic pro-opiomelanocortin mRNA expression in the rostral arcuate nucleus. Diabetes *46*, 2119-2123.
Scott, M.M., Lachey, J.L., Sternson, S.M., Lee, C.E., Elias, C.F., Friedman, J.M., and Elmquist, J.K. (2009). Leptin targets in the mouse brain. The Journal of comparative neurology *514*, 518-532.
Sears, R.M., Fink, A.E., Wigestrand, M.B., Farb, C.R., de Lecea, L., and Ledoux, J.E. (2013). Orexin/hypocretin system modulates amygdala-dependent threat learning through the locus coeruleus. Proceedings of the National Academy of Sciences of the United States of America *110*, 20260-20265.
Segal, J.P., Stallings, N.R., Lee, C.E., Zhao, L., Socci, N., Viale, A., Harris, T.M., Soares, M.B., Childs, G., Elmquist, J.K.*, et al.* (2005). Use of laser-capture microdissection for the identification of marker genes for the ventromedial hypothalamic nucleus. The Journal of neuroscience : the official journal of the Society for Neuroscience *25*, 4181-4188.
Shimada, M., Tritos, N.A., Lowell, B.B., Flier, J.S., and Maratos-Flier, E. (1998). Mice lacking melanin-concentrating hormone are hypophagic and lean. Nature *396*, 670-674.
Shiuchi, T., Haque, M.S., Okamoto, S., Inoue, T., Kageyama, H., Lee, S., Toda, C., Suzuki, A., Bachman, E.S., Kim, Y.B.*, et al.* (2009). Hypothalamic orexin stimulates feeding-associated glucose utilization in skeletal muscle via sympathetic nervous system. Cell metabolism *10*, 466-480.
Simmonds, M.A., and Turner, J.P. (1985). Antagonism of inhibitory amino acids by the steroid derivative RU5135. British journal of pharmacology *84*, 631-635.
Sisley, S., Gutierrez-Aguilar, R., Scott, M., D'Alessio, D.A., Sandoval, D.A., and Seeley, R.J. (2014). Neuronal GLP1R mediates liraglutide's anorectic but not glucose-lowering effect. The Journal of clinical investigation *124*, 2456-2463.
Sistare, F.D., and Haynes, R.C., Jr. (1985). Acute stimulation by glucocorticoids of gluconeogenesis from lactate/pyruvate in isolated hepatocytes from normal and adrenalectomized rats. The Journal of biological chemistry *260*, 12754-12760.

Sjostrom, L., Narbro, K., Sjostrom, C.D., Karason, K., Larsson, B., Wedel, H., Lystig, T., Sullivan, M., Bouchard, C., Carlsson, B.*, et al.* (2007). Effects of bariatric surgery on mortality in Swedish obese subjects. The New England journal of medicine *357*, 741-752.
Smart, J.L., Tolle, V., and Low, M.J. (2006). Glucocorticoids exacerbate obesity and insulin resistance in neuron-specific proopiomelanocortin-deficient mice. The Journal of clinical investigation *116*, 495-505.
Song, C.K., Vaughan, C.H., Keen-Rhinehart, E., Harris, R.B., Richard, D., and Bartness, T.J. (2008). Melanocortin-4 receptor mRNA expressed in sympathetic outflow neurons to brown adipose tissue: neuroanatomical and functional evidence. American journal of physiology Regulatory, integrative and comparative physiology *295*, R417-428.
Song, K.H., Li, T., Owsley, E., Strom, S., and Chiang, J.Y. (2009). Bile acids activate fibroblast growth factor 19 signaling in human hepatocytes to inhibit cholesterol 7alpha-hydroxylase gene expression. Hepatology (Baltimore, Md) *49*, 297-305.
Song, Z., and Routh, V.H. (2005). Differential effects of glucose and lactate on glucosensing neurons in the ventromedial hypothalamic nucleus. Diabetes *54*, 15-22.
Spanagel, R., Herz, A., Bals-Kubik, R., and Shippenberg, T.S. (1991). Beta-endorphin-induced locomotor stimulation and reinforcement are associated with an increase in dopamine release in the nucleus accumbens. Psychopharmacology *104*, 51-56.
Speliotes, E.K., Willer, C.J., Berndt, S.I., Monda, K.L., Thorleifsson, G., Jackson, A.U., Lango Allen, H., Lindgren, C.M., Luan, J., Magi, R.*, et al.* (2010). Association analyses of 249,796 individuals reveal 18 new loci associated with body mass index. Nature genetics *42*, 937-948.
Spiess, J., Villarreal, J., and Vale, W. (1981). Isolation and sequence analysis of a somatostatin-like polypeptide from ovine hypothalamus. Biochemistry *20*, 1982-1988.
Sprouse-Blum, A.S., Smith, G., Sugai, D., and Parsa, F.D. (2010). Understanding endorphins and their importance in pain management. Hawaii medical journal *69*, 70-71.
Stamatakis, A.M., Van Swieten, M., Basiri, M.L., Blair, G.A., Kantak, P., and Stuber, G.D. (2016). Lateral Hypothalamic Area Glutamatergic Neurons and Their Projections to the Lateral Habenula Regulate Feeding and Reward. The Journal of neuroscience : the official journal of the Society for Neuroscience *36*, 302-311.
Stanley, S., Pinto, S., Segal, J., Perez, C.A., Viale, A., DeFalco, J., Cai, X., Heisler, L.K., and Friedman, J.M. (2010). Identification of neuronal subpopulations that project from hypothalamus to both liver and adipose tissue polysynaptically. Proceedings of the National Academy of Sciences of the United States of America *107*, 7024-7029.
Steculorum, S.M., Ruud, J., Karakasilioti, I., Backes, H., Engstrom Ruud, L., Timper, K., Hess, M.E., Tsaousidou, E., Mauer, J., Vogt, M.C.*, et al.* (2016). AgRP Neurons Control Systemic Insulin Sensitivity via Myostatin Expression in Brown Adipose Tissue. Cell *165*, 125-138.
Steinfelder, H.J., Hauser, P., Nakayama, Y., Radovick, S., McClaskey, J.H., Taylor, T., Weintraub, B.D., and Wondisford, F.E. (1991). Thyrotropin-releasing hormone regulation of human TSHB expression: role of a pituitary-specific transcription factor (Pit-1/GHF-1) and potential interaction with a thyroid hormone-inhibitory element. Proceedings of the National Academy of Sciences of the United States of America *88*, 3130-3134.
Stricker, E.M., Swerdloff, A.F., and Zigmond, M.J. (1978). Intrahypothalamic injections of kainic acid produce feeding and drinking deficits in rats. Brain research *158*, 470-473.
Suez, J., Korem, T., Zeevi, D., Zilberman-Schapira, G., Thaiss, C.A., Maza, O., Israeli, D., Zmora, N., Gilad, S., Weinberger, A.*, et al.* (2014). Artificial sweeteners induce glucose intolerance by altering the gut microbiota. Nature *514*, 181-186.

Suh, J.M., Jonker, J.W., Ahmadian, M., Goetz, R., Lackey, D., Osborn, O., Huang, Z., Liu, W., Yoshihara, E., van Dijk, T.H.*, et al.* (2014). Endocrinization of FGF1 produces a neomorphic and potent insulin sensitizer. Nature *513*, 436-439.
Sutton, G.M., Duos, B., Patterson, L.M., and Berthoud, H.-R. (2005). Melanocortinergic modulation of cholecystokinin-induced suppression of feeding through extracellular signal-regulated kinase signaling in rat solitary nucleus. Endocrinology *146*, 3739-3747.
Sutton, G.M., Trevaskis, J.L., Hulver, M.W., McMillan, R.P., Markward, N.J., Babin, M.J., Meyer, E.A., and Butler, A.A. (2006). Diet-genotype interactions in the development of the obese, insulin-resistant phenotype of C57BL/6J mice lacking melanocortin-3 or -4 receptors. Endocrinology *147*, 2183-2196.
Takayanagi, Y., Kasahara, Y., Onaka, T., Takahashi, N., Kawada, T., and Nishimori, K. (2008). Oxytocin receptor-deficient mice developed late-onset obesity. Neuroreport *19*, 951-955.
Tervo, D.G., Hwang, B.Y., Viswanathan, S., Gaj, T., Lavzin, M., Ritola, K.D., Lindo, S., Michael, S., Kuleshova, E., Ojala, D.*, et al.* (2016). A Designer AAV Variant Permits Efficient Retrograde Access to Projection Neurons. Neuron *92*, 372-382.
Thorens, B. (2014). Neural regulation of pancreatic islet cell mass and function. Diabetes.
Tian, D.R., Li, X.D., Shi, Y.S., Wan, Y., Wang, X.M., Chang, J.K., Yang, J., and Han, J.S. (2004). Changes of hypothalamic alpha-MSH and CART peptide expression in diet-induced obese rats. Peptides *25*, 2147-2153.
Toda, C., Santoro, A., Kim, J.D., and Diano, S. (2017). POMC Neurons: From Birth to Death. Annual review of physiology *79*, 209-236.
Tomlinson, E., Fu, L., John, L., Hultgren, B., Huang, X., Renz, M., Stephan, J.P., Tsai, S.P., Powell-Braxton, L., French, D.*, et al.* (2002). Transgenic mice expressing human fibroblast growth factor-19 display increased metabolic rate and decreased adiposity. Endocrinology *143*, 1741-1747.
Tong, Q., Ye, C.P., Jones, J.E., Elmquist, J.K., and Lowell, B.B. (2008). Synaptic release of GABA by AgRP neurons is required for normal regulation of energy balance. Nat Neurosci *11*, 998-1000.
Tounian, P., Schneiter, P., Henry, S., Delarue, J., and Tappy, L. (1997). Effects of dexamethasone on hepatic glucose production and fructose metabolism in healthy humans. The American journal of physiology *273*, E315-320.
Tremaroli, V., Karlsson, F., Werling, M., Stahlman, M., Kovatcheva-Datchary, P., Olbers, T., Fandriks, L., le Roux, C.W., Nielsen, J., and Backhed, F. (2015). Roux-en-Y Gastric Bypass and Vertical Banded Gastroplasty Induce Long-Term Changes on the Human Gut Microbiome Contributing to Fat Mass Regulation. Cell metabolism *22*, 228-238.
Trevaskis, J.L., Gawronska-Kozak, B., Sutton, G.M., McNeil, M., Stephens, J.M., Smith, S.R., and Butler, A.A. (2007). Role of adiponectin and inflammation in insulin resistance of Mc3r and Mc4r knockout mice. Obesity (Silver Spring, Md) *15*, 2664-2672.
Turnbaugh, P.J., Backhed, F., Fulton, L., and Gordon, J.I. (2008). Diet-induced obesity is linked to marked but reversible alterations in the mouse distal gut microbiome. Cell host & microbe *3*, 213-223.
Turnbaugh, P.J., Ley, R.E., Mahowald, M.A., Magrini, V., Mardis, E.R., and Gordon, J.I. (2006). An obesity-associated gut microbiome with increased capacity for energy harvest. Nature *444*, 1027-1031.
Turner, N., and Grose, R. (2010). Fibroblast growth factor signalling: from development to cancer. Nature reviews Cancer *10*, 116-129.
Uchida, I., Cestari, I.N., and Yang, J. (1996). The differential antagonism by bicuculline and SR95531 of pentobarbitone-induced currents in cultured hippocampal neurons. European journal of pharmacology *307*, 89-96.

Unger, T.J., Calderon, G.A., Bradley, L.C., Sena-Esteves, M., and Rios, M. (2007). Selective deletion of Bdnf in the ventromedial and dorsomedial hypothalamus of adult mice results in hyperphagic behavior and obesity. The Journal of neuroscience : the official journal of the Society for Neuroscience *27*, 14265-14274.
Vaisse, C., Clement, K., Guy-Grand, B., and Froguel, P. (1998). A frameshift mutation in human MC4R is associated with a dominant form of obesity. Nature genetics *20*, 113-114.
van de Wall, E., Leshan, R., Xu, A.W., Balthasar, N., Coppari, R., Liu, S.M., Jo, Y.H., MacKenzie, R.G., Allison, D.B., Dun, N.J*., et al.* (2008). Collective and individual functions of leptin receptor modulated neurons controlling metabolism and ingestion. Endocrinology *149*, 1773-1785.
van den Pol, A.N., Yao, Y., Fu, L.-Y., Foo, K., Huang, H., Coppari, R., Lowell, B.B., and Broberger, C. (2009). Neuromedin B and gastrin-releasing peptide excite arcuate nucleus neuropeptide Y neurons in a novel transgenic mouse expressing strong Renilla green fluorescent protein in NPY neurons. The Journal of Neuroscience *29*, 4622-4639.
Vaughan, J.M., Fischer, W.H., Hoeger, C., Rivier, J., and Vale, W. (1989). Characterization of melanin-concentrating hormone from rat hypothalamus. Endocrinology *125*, 1660-1665.
Veening, J.G., and Barendregt, H.P. (2015). The effects of beta-endorphin: state change modification. Fluids and barriers of the CNS *12*, 3.
Vella, K.R., Ramadoss, P., Lam, F.S., Harris, J.C., Ye, F.D., Same, P.D., O'Neill, N.F., Maratos-Flier, E., and Hollenberg, A.N. (2011). NPY and MC4R signaling regulate thyroid hormone levels during fasting through both central and peripheral pathways. Cell metabolism *14*, 780-790.
Verty, A.N., Allen, A.M., and Oldfield, B.J. (2010). The endogenous actions of hypothalamic peptides on brown adipose tissue thermogenesis in the rat. Endocrinology *151*, 4236-4246.
Vicentic, A., and Jones, D.C. (2007). The CART (cocaine- and amphetamine-regulated transcript) system in appetite and drug addiction. The Journal of pharmacology and experimental therapeutics *320*, 499-506.
Vicentic, A., Lakatos, A., and Jones, D. (2006). The CART receptors: background and recent advances. Peptides *27*, 1934-1937.
Vicentic, A., Lakatos, A., and Kuhar, M.J. (2005). CART (cocaine- and amphetamine-regulated transcript) peptide receptors: specific binding in AtT20 cells. European journal of pharmacology *528*, 188-189.
Vong, L., Ye, C., Yang, Z., Choi, B., Chua, S., Jr., and Lowell, B.B. (2011). Leptin action on GABAergic neurons prevents obesity and reduces inhibitory tone to POMC neurons. Neuron *71*, 142-154.
Vrang, N., Larsen, P.J., Clausen, J.T., and Kristensen, P. (1999). Neurochemical characterization of hypothalamic cocaine- amphetamine-regulated transcript neurons. The Journal of neuroscience : the official journal of the Society for Neuroscience *19*, Rc5.
Vrieze, A., Van Nood, E., Holleman, F., Salojarvi, J., Kootte, R.S., Bartelsman, J.F., Dallinga-Thie, G.M., Ackermans, M.T., Serlie, M.J., Oozeer, R*., et al.* (2012). Transfer of intestinal microbiota from lean donors increases insulin sensitivity in individuals with metabolic syndrome. Gastroenterology *143*, 913-916.e917.
Wang, C., Bomberg, E., Levine, A., Billington, C., and Kotz, C.M. (2007). Brain-derived neurotrophic factor in the ventromedial nucleus of the hypothalamus reduces energy intake. American journal of physiology Regulatory, integrative and comparative physiology *293*, R1037-1045.
Wang, D., He, X., Zhao, Z., Feng, Q., Lin, R., Sun, Y., Ding, T., Xu, F., Luo, M., and Zhan, C. (2015). Whole-brain mapping of the direct inputs and axonal projections of POMC and AgRP neurons. Frontiers in neuroanatomy *9*, 40.

Wang, M.Y., Chen, L., Clark, G.O., Lee, Y., Stevens, R.D., Ilkayeva, O.R., Wenner, B.R., Bain, J.R., Charron, M.J., Newgard, C.B.*, et al.* (2010). Leptin therapy in insulin-deficient type I diabetes. Proceedings of the National Academy of Sciences of the United States of America *107*, 4813-4819.
Watts, A.G. (2005). Glucocorticoid regulation of peptide genes in neuroendocrine CRH neurons: a complexity beyond negative feedback. Frontiers in neuroendocrinology *26*, 109-130.
Weinstein, S.P., Wilson, C.M., Pritsker, A., and Cushman, S.W. (1998). Dexamethasone inhibits insulin-stimulated recruitment of GLUT4 to the cell surface in rat skeletal muscle. Metabolism: clinical and experimental *47*, 3-6.
Werling, M., Fandriks, L., Bjorklund, P., Maleckas, A., Brandberg, J., Lonroth, H., le Roux, C.W., and Olbers, T. (2013). Long-term results of a randomized clinical trial comparing Roux-en-Y gastric bypass with vertical banded gastroplasty. The British journal of surgery *100*, 222-230.
Whiddon, B.B., and Palmiter, R.D. (2013). Ablation of neurons expressing melanin-concentrating hormone (MCH) in adult mice improves glucose tolerance independent of MCH signaling. The Journal of neuroscience : the official journal of the Society for Neuroscience *33*, 2009-2016.
White, A., and Gibson, S. (1998). ACTH precursors: biological significance and clinical relevance. Clinical endocrinology *48*, 251-255.
Wierup, N., Richards, W.G., Bannon, A.W., Kuhar, M.J., Ahren, B., and Sundler, F. (2005). CART knock out mice have impaired insulin secretion and glucose intolerance, altered beta cell morphology and increased body weight. Regulatory peptides *129*, 203-211.
Williams, K.W., Margatho, L.O., Lee, C.E., Choi, M., Lee, S., Scott, M.M., Elias, C.F., and Elmquist, J.K. (2010). Segregation of acute leptin and insulin effects in distinct populations of arcuate proopiomelanocortin neurons. The Journal of neuroscience : the official journal of the Society for Neuroscience *30*, 2472-2479.
Willie, J.T., Chemelli, R.M., Sinton, C.M., and Yanagisawa, M. (2001). To eat or to sleep? Orexin in the regulation of feeding and wakefulness. Annual review of neuroscience *24*, 429-458.
Willie, J.T., Sinton, C.M., Maratos-Flier, E., and Yanagisawa, M. (2008). Abnormal response of melanin-concentrating hormone deficient mice to fasting: hyperactivity and rapid eye movement sleep suppression. Neuroscience *156*, 819-829.
Wittmann, G., Hrabovszky, E., and Lechan, R.M. (2013). Distinct glutamatergic and GABAergic subsets of hypothalamic pro-opiomelanocortin neurons revealed by in situ hybridization in male rats and mice. The Journal of comparative neurology *521*, 3287-3302.
Wu, A.L., Coulter, S., Liddle, C., Wong, A., Eastham-Anderson, J., French, D.M., Peterson, A.S., and Sonoda, J. (2011a). FGF19 regulates cell proliferation, glucose and bile acid metabolism via FGFR4-dependent and independent pathways. PloS one *6*, e17868.
Wu, A.L., Kolumam, G., Stawicki, S., Chen, Y., Li, J., Zavala-Solorio, J., Phamluong, K., Feng, B., Li, L., Marsters, S.*, et al.* (2011b). Amelioration of type 2 diabetes by antibody-mediated activation of fibroblast growth factor receptor 1. Science translational medicine *3*, 113ra126.
Wu, X., Ge, H., Lemon, B., Vonderfecht, S., Baribault, H., Weiszmann, J., Gupte, J., Gardner, J., Lindberg, R., Wang, Z.*, et al.* (2010a). Separating mitogenic and metabolic activities of fibroblast growth factor 19 (FGF19). Proceedings of the National Academy of Sciences of the United States of America *107*, 14158-14163.
Wu, Z., Yang, H., and Colosi, P. (2010b). Effect of genome size on AAV vector packaging. Molecular therapy : the journal of the American Society of Gene Therapy *18*, 80-86.
Xin, X., Storlien, L.H., and Huang, X.F. (2000). Hypothalamic c-fos-like immunoreactivity in high-fat diet-induced obese and resistant mice. Brain research bulletin *52*, 235-242.

Xu, B., Goulding, E.H., Zang, K., Cepoi, D., Cone, R.D., Jones, K.R., Tecott, L.H., and Reichardt, L.F. (2003). Brain-derived neurotrophic factor regulates energy balance downstream of melanocortin-4 receptor. Nature neuroscience *6*, 736-742.
Xu, Y., Chang, J.T., Myers, M.G., Jr., Xu, Y., and Tong, Q. (2016). Euglycemia Restoration by Central Leptin in Type 1 Diabetes Requires STAT3 Signaling but Not Fast-Acting Neurotransmitter Release. Diabetes *65*, 1040-1049.
Xu, Y., Hill, J.W., Fukuda, M., Gautron, L., Sohn, J.W., Kim, K.W., Lee, C.E., Choi, M.J., Lauzon, D.A., Dhillon, H.*, et al.* (2010). PI3K signaling in the ventromedial hypothalamic nucleus is required for normal energy homeostasis. Cell metabolism *12*, 88-95.
Yang, C., Jin, C., Li, X., Wang, F., McKeehan, W.L., and Luo, Y. (2012). Differential specificity of endocrine FGF19 and FGF21 to FGFR1 and FGFR4 in complex with KLB. PloS one *7*, e33870.
Yang, L., Scott, K.A., Hyun, J., Tamashiro, K.L., Tray, N., Moran, T.H., and Bi, S. (2009). Role of dorsomedial hypothalamic neuropeptide Y in modulating food intake and energy balance. The Journal of neuroscience : the official journal of the Society for Neuroscience *29*, 179-190.
Yang, X.J., Kow, L.M., Funabashi, T., and Mobbs, C.V. (1999). Hypothalamic glucose sensor: similarities to and differences from pancreatic beta-cell mechanisms. Diabetes *48*, 1763-1772.
Yaswen, L., Diehl, N., Brennan, M.B., and Hochgeschwender, U. (1999). Obesity in the mouse model of pro-opiomelanocortin deficiency responds to peripheral melanocortin. Nature medicine *5*, 1066-1070.
Yatsunenko, T., Rey, F.E., Manary, M.J., Trehan, I., Dominguez-Bello, M.G., Contreras, M., Magris, M., Hidalgo, G., Baldassano, R.N., Anokhin, A.P.*, et al.* (2012). Human gut microbiome viewed across age and geography. Nature *486*, 222-227.
Yen, P.M. (2001). Physiological and molecular basis of thyroid hormone action. Physiological reviews *81*, 1097-1142.
Yeo, G.S., Farooqi, I.S., Aminian, S., Halsall, D.J., Stanhope, R.G., and O'Rahilly, S. (1998). A frameshift mutation in MC4R associated with dominantly inherited human obesity. Nature genetics *20*, 111-112.
Yu, C., Wang, F., Kan, M., Jin, C., Jones, R.B., Weinstein, M., Deng, C.X., and McKeehan, W.L. (2000). Elevated cholesterol metabolism and bile acid synthesis in mice lacking membrane tyrosine kinase receptor FGFR4. The Journal of biological chemistry *275*, 15482-15489.
Yu, X., Park, B.H., Wang, M.Y., Wang, Z.V., and Unger, R.H. (2008). Making insulin-deficient type 1 diabetic rodents thrive without insulin. Proceedings of the National Academy of Sciences of the United States of America *105*, 14070-14075.
Zechner, J.F., Mirshahi, U.L., Satapati, S., Berglund, E.D., Rossi, J., Scott, M.M., Still, C.D., Gerhard, G.S., Burgess, S.C., Mirshahi, T.*, et al.* (2013). Weight-independent effects of roux-en-Y gastric bypass on glucose homeostasis via melanocortin-4 receptors in mice and humans. Gastroenterology *144*, 580-590.e587.
Zhan, C., Zhou, J., Feng, Q., Zhang, J.E., Lin, S., Bao, J., Wu, P., and Luo, M. (2013). Acute and long-term suppression of feeding behavior by POMC neurons in the brainstem and hypothalamus, respectively. The Journal of neuroscience : the official journal of the Society for Neuroscience *33*, 3624-3632.
Zhang, G., Bai, H., Zhang, H., Dean, C., Wu, Q., Li, J., Guariglia, S., Meng, Q., and Cai, D. (2011). Neuropeptide exocytosis involving synaptotagmin-4 and oxytocin in hypothalamic programming of body weight and energy balance. Neuron *69*, 523-535.
Zhang, J., Xue, F., and Chang, Y. (2008). Structural determinants for antagonist pharmacology that distinguish the rho1 GABAC receptor from GABAA receptors. Molecular pharmacology *74*, 941-951.

Zhang, Y., Proenca, R., Maffei, M., Barone, M., Leopold, L., and Friedman, J.M. (1994). Positional cloning of the mouse obese gene and its human homologue. Nature *372*, 425-432.